Quantifying and hedging wrong-way risk in interest rate swaps using copulas

by

Mats Draijer

to obtain the degree of Master of Science
at the Delft University of Technology,
to be defended publicly on Friday July 17, 2020 at 16:00 PM.

Student number:	4298829	
Project duration:	October 1, 2019 – July 17, 2020	
Thesis committee:	Dr. P. Cirillo,	TU Delft, supervisor
	Prof. dr. ir. C. W. Oosterlee,	TU Delft
	B. Arendshorst MSc.,	KPMG, supervisor

Abstract

Wrong-way risk (WWR), which is the dependence between the probability of default (PD) and the exposure at default of a counterparty, is an aspect of credit risk that can lead to high losses. This thesis aims firstly to quantify WWR in interest rate swaps (IRSs) using a copula model, where a copula is used to couple the PD implied by credit default swap (CDS) spreads and the 10 year swap rates. Specific attention is given to choosing and fitting a copula. For datasets obtained from periods of regular economic conditions and periods of financial crisis, the t copula is found to be the best fit. In general, negative dependence between the log-returns of the implied PDs and the log-returns of the swap rates is observed, especially in the tails of high PD log-returns and low swap rate log-returns during regular periods. This means that the general demand for loans is lower during a worsening economy. During crisis periods however, the dependence is weaker than in regular periods; implying that loans are in higher demand in these times, e.g. because companies need loans to survive.

The second purpose of this thesis is the introduction of a novel product aimed at hedging WWR in IRSs. This product, named an IRS partial insurance contract (IPI), introduces an upper bound to the credit losses on an IRS. If this bound is exceeded, the amount by which the losses exceed the bound is paid out by the IPI seller to the IPI buyer. An analytical expression for the no-arbitrage price of an IPI is obtained, using a copula model for WWR. This expression shows that an IPI can be replicated by a portfolio of swaptions and CDSs.

Preface

When I first started looking for a subject for my thesis, it was my supervising professor Pasquale Cirillo who suggested the development of a new financial product. I was immediately enthusiastic about this, and combined with the subject of wrong-way risk, it became the topic of this thesis. The research combined the fields of financial derivatives, credit risk and statistics, which interest me a great deal, and so it is with pleasure that I have been researching these topics for the past nine months.

This thesis has been submitted for the degree of Master of Science in Applied Mathematics at Delft University of Technology, with a specialisation in Financial Engineering. Academic supervision was provided by dr. Pasquale Cirillo. The work has been carried out at KPMG under the supervision of Bart Arendshorst, in the department Financial Risk Management, which is part of the suite Risk & Regulatory.

I would like to thank dr. Cirillo for his excellent supervision and the great feedback he has provided. Our meetings have always motivated me to expand my scope and inspired me to be thorough. The supervision of Bart has also been invaluable, as his expertise in applied credit risk helped me connect the theory behind this thesis to the financial industry, especially where regulations were concerned. Furthermore, I express my thanks to KPMG for giving me an inspiring place to write this thesis. The colleagues at Financial Risk Management were always happy to give me advice or be a sparring partner. I also appreciate the opportunity they gave me to work with them on several client projects, which was an instructive experience. Additionally, my thanks go to Hugo Lambriex and Laurens Poppezijn, without whom the data collection would not have been possible. Finally, I'm grateful to my family and friends for their support over the past months.

Mats Draijer
Delft, July 2020

Acronyms

AIC Akaike information criterion

CDF Cumulative distribution function

CDS Credit default swap

CIR Cox-Ingersoll-Ross

CVA Credit valuation adjustment

EAD Exposure at default

EL Expected losses

IPI Interest rate swap partial insurance contract

IRS Interest rate swap

LGD Loss given default

LIBOR London Inter-bank Offered Rate

MLE Maximum likelihood estimation

OLS Ordinary least squares

OTC Over the counter

PD Probability of default

RWR Right-way risk

WWR Wrong-way risk

Contents

1 Introduction

The concept of credit risk, which deals with the risk of the counterparty of a financial transaction not being able to pay the due amounts fully and in a timely manner,[1] is often associated with mortgages and other fixed income products. But credit risk is also present for derivative products, of which many exist in the current financial landscape. For these products, the concept of wrong-way risk (WWR) may arise: positive dependence between the exposure of a financial product to one counterparty and the probability of default (PD) of the other counterparty. The case of negative dependence is known as right-way risk.[2]

Within the class of derivatives, WWR and credit risk in general are most meaningful for over-the-counter (OTC) traded, unsecured products. The interest rate swap (IRS) market is by far the largest of the global OTC derivatives markets; according to the Bank for International Settlements (2019), the global notional amount outstanding for IRSs at the end of June 2019 was $368 trillion, accounting for 58% of the OTC derivatives markets. Furthermore, IRSs are mainly used for hedging and similar purposes, such as changing the duration of a fixed income portfolio. Any form of risk, including WWR, is generally less desirable for products used for hedging than for those used for speculation. Mainly for these two reasons, this thesis focuses on WWR for IRSs. This also provides an easy extension to other interest rate contracts; the notional amount outstanding for all interest rate derivativew was $524 trillion, or 82% of the OTC derivatives markets.

Research on WWR has been performed since 2003 (Cherubini and Luciano; 2003), but advanced modelling of WWR has not yet fully found its way into the Basel framework by the Basel Committee on Banking Supervision (2019), the worlds leading capital standards setter. The Basel IV standards state that banks need to identify cases of high exposures to WWR. For products that depend on a single third-party company, such as options and credit default swaps, banks are required to make changes to their calculations. The exposure at default (EAD) needs to be calculated conditional on default of the counterparty, since the EAD and the default are no longer independent, and an assumption must be made that the LGD is equal to 1. The assumption of LGD = 1 typically means that the product gets the treatment of an unsecured exposure, even if the product is secured. For products such as IRSs however, there are no such clear rules. The only directives for all exposures subject to large amounts of WWR are that they must be taken out of any potential netting sets, and that regulators may require banks to increase a factor in the calculation of the EAD. The question of whether this factor is increased, and by how much, is left up to the individual market regulators, such as central banks and national market authorities. This lack of a centralised directive shows that there is no clear consensus on how to deal with WWR in regulations; more research into WWR can help a best practice for the modelling of it to emerge.

Therefore, the first of the two main goals of this thesis is the quantification of WWR in interest rate swaps. The quantification is done through a copula approach. Research on copula models for IRSs has been performed by e.g. Cherubini (2013) and Černý and Witzany (2018), giving useful results for the CVA of interest rate swaps. The issue of path inconsistency, and possible solutions, are pointed out by Böcker and

[1] Among other types of risk.

[2] Although this thesis focuses on wrong-way risk, the case of right-way risk is analogous and can be analysed in mostly the same way.

Brunnbauer (2014). Calibration is performed by e.g. Hofer (2016), Pan (2018) and Rosen and Saunders (2012), although they all only use a Gaussian copula; the choice of which copula to use is not considered. These papers find that the receiver position in an IRS is subject to WWR; this observation is expected to be confirmed by the results in this thesis. Incorporating WWR in other quantities than CVA is also explored little throughout the literature. The quantification performed in this study contributes to the existing literature by considering the choice of copula by means of a quantitative goodness of fit comparison. Hence, a sub-goal to aid in quantifying WWR is finding the optimal copula to describe a dataset of PDs and swap rates. Another sub-goal is assessing the impact of different economic conditions on WWR. The hypothesis is that the behaviour during crisis periods is similar to the lower (with respect to PD) tail behaviour in regular periods. This tail is expected to contain strong WWR, since when many defaults occur, all movements on financial markets tend to be driven in a specific direction (downward for most variables).

Besides regulatory relevance, the quantification of WWR is also useful for institutions exposed to it, giving them greater insight into expected or potential future cash flows. After quantifying WWR, an institution may decide to simply accept the risk, but many institutions prefer to hedge their risks. As there are currently few methods to mitigate WWR, research into reducing one's exposure to it is relevant.

Furthermore, if hedging products for WWR are developed, regulators can incentivise institutions to cover their WWR by allowing them to hold less capital if their positions subject to WWR are hedged. The Basel IV framework currently does not allow this, which may be partly due to the lack of available hedging methods for WWR. However, new regulations could allow newly developed hedging products to be used as credit risk mitigants (CRMs).[3] This would also help regulators achieve their goal of financial stability, especially since WWR manifests itself mostly during downturn periods, as shown in this thesis.

The two points above show the relevance of the second main goal of this thesis: developing a new financial product for hedging WWR in IRSs. The expectation is that this product will be a (partial) hedge for credit risk in general, since isolating WWR for the purposes of determining the cash flows of a product requires the two counterparties to agree on one model for WWR. A product with such a requirement seems unlikely to be traded in practice. A sub-goal of developing the novel product is determining its no-arbitrage price in terms of the no-arbitrage values of other financial products. This allows the price of an IPI to be calculated easily if pricing methods for these other financial products are in place.

The thesis develops as follows. In Chapter 2, the concept of WWR is described in detail and the benefits and drawbacks of the main classes of existing models are explored, being the copula approach, a functional relationship, and correlated dynamics. Then the methodology of choosing and calibrating copula is detailed in Chapter 3. The approach employs copulas to couple the counterparty's PD and the swap rate. This methodology is tested on artificial data. The real-world data from regular economic situations and from periods of financial downturn is described in Chapter 4; data for the counterparty's PD is implied from CDS spreads. The dependence between the counterparty's PD and the swap rate is analysed using the copula model and several other methods. In Chapter 5, the new product (i.e. the IPI) is introduced and its cash flows are defined. A different copula model for WWR is used in this part, since the model coupling the counterparty's PD and the swap rate cannot describe a default event effectively. Therefore the copula model described by Cherubini (2013) and Černý and Witzany (2018) is used in this chapter, which couples the time of default and the swap rate. An analytical expression for the no-arbitrage price of an IPI is determined using this model. Finally, Chapter 6 concludes and gives potential subjects for future research.

[3] The capital requirements for a certain exposure are lowered if an institution also has positions in credit risk mitigants for that exposure.

2
Fundamentals of Wrong-Way Risk Modelling

The expected loss on a credit exposure is commonly calculated by multiplying three variables: the probability of default (PD), the loss given default (LGD) and the exposure at default (EAD). The product of these three variables equals the expected loss (EL) of a certain exposure. Regulators require banks to calculate these three variables, either through models provided by the regulator (standardised approach, SA) or by letting banks build their own models (internal rating-based approach, IRB). Banks are required to hold provisions for expected losses and capital reserves for unexpected losses due to defaults of their counterparties. While the PD, LGD and EAD are often modelled separately, independence between them cannot be assumed in general. Since the capital reserves held depend on the result of the IRB models, errors in these models may result in banks holding too little capital, and as a consequence banks are less resilient in times of crisis. Research into dependence between PD and LGD has been performed by e.g. Cheng and Cirillo (2019) and Fischer et al. (2016). This thesis focuses on dependence between PD and EAD; although the term wrong-way risk is sometimes interpreted as dependence between PD and either EAD or LGD, in this thesis it refers only to dependence between PD and EAD.

In this chapter, the notion of wrong-way risk (WWR) is clarified first in Section 2.1. Several situations where WWR appears are described, among others interest rate swaps, the main product in this thesis. Then the existing literature for modelling WWR is highlighted in Section 2.2. The copula approach is described first, being the main methodology used in this thesis; then the other approaches for WWR models are sketched to give the reader a complete overview of the current state of the art. Finally, the benefits and drawbacks for each of the approaches are given in Section 2.3.

2.1. Basic principles of wrong-way risk

WWR is the positive dependence between the PD and the EAD of a given counterparty. To illustrate the concept, first consider the following example.

Example 2.1 (Line of Credit)**.** A line of credit is a loan-related product, also known as a revolving credit facility for consumers and SME or a committed credit line for large corporates. Banks sometimes extend lines of credit to borrowers, where borrowers initially only borrow a small sum or nothing at all, but can borrow more (up to a cap) as they need it. Suppose bank A extends a line of credit to borrower B. When B is in financial distress, its PD rises and it may need more funds to fulfill its financial obligations. Therefore B is more likely to draw extra loans from the line of credit than it is to pay back (part of) its loan. This raises the exposure for A, while the full borrowed amount is less likely to be paid back. It is clear that this increase in exposure and the increase in PD are dependent; this is WWR. One occurrence of this is Shell taking out large sums of cash out of committed credit lines during the 2020 corona crisis, which hit the oil and gas sector particularly hard (van Dijk; 2020).

In general, say counterparty A has an exposure to counterparty B. Suppose there is one case where the credit quality of B worsens during the next year, and one case where it stays the same; the exposure of A to B

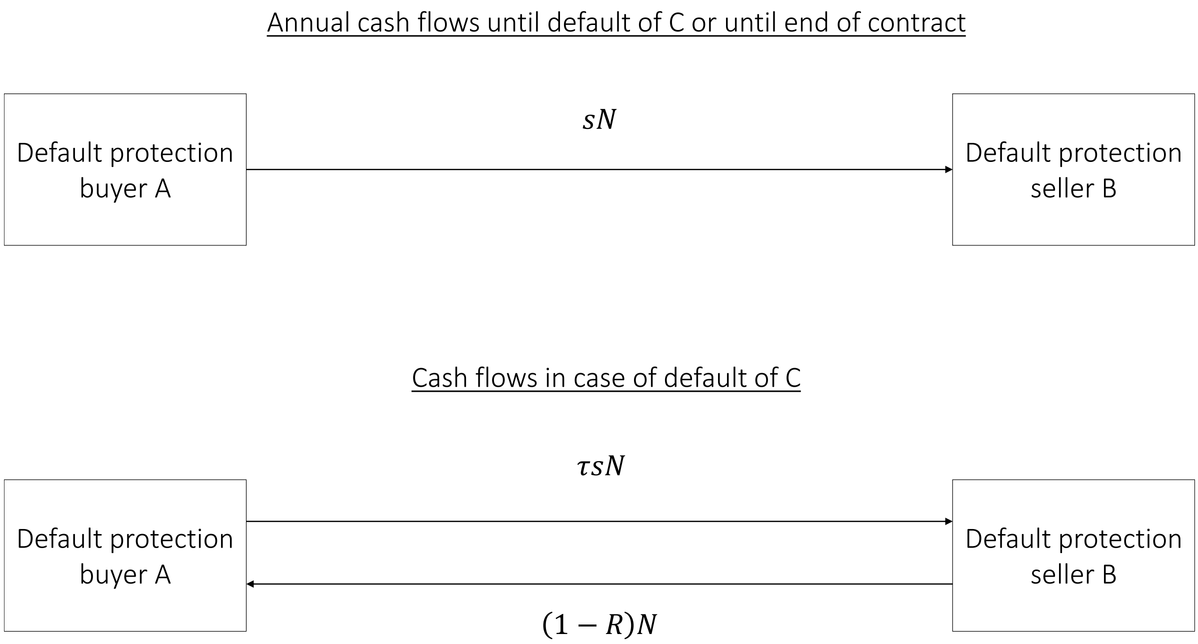

Figure 2.1: Schematic overview of the cash flows in a CDS contract. s os the CDS spread as a percentage of the notional amount, N is the notional amount, τ is the time that has passed since the last payment date as a fraction of one year, and R is the recovery rate (i.e. $(1-R)$ is the loss given default). Note that contracts where payments are made more often than once a year are also possible.

in one year has a tendency to be higher in the first case. As PD and EAD both increase, the EL of A to counterparty B increases compared to circumstances at origination. Whenever B defaults, there is a tendency for the exposure to have increased, meaning a larger loss for A than in the case of no WWR. This increases credit risk for A with respect to the case of independence between the PD of B and the EAD, which implies that any credit risk model that assumes independence between PD and EAD likely underestimates credit risk. The opposite of WWR is right-way risk: the tendency for the exposure of A to B to be low whenever B defaults, meaning lower credit risk for A than in the case of independence (Hull and White; 2012).

WWR is an aspect of credit risk leading to potentially high losses. Whenever WWR is present, the default event is exacerbated with higher losses. But even when there is no default, but only the counterparty's credit rating deteriorating, WWR may negatively affect an investor. When the counterparty's credit rating deteriorates, the probability of the default-free value of the portfolio rising increases. With the increased PD and EAD of the counterparty, the Basel framework requires more capital to be held. Furthermore, market participants are hesitant to bear the increased credit risk, which negatively affects the market value of the portfolio. As with all forms of credit risk, WWR is most relevant for uncollateralised financial products that are traded over-the-counter, without losses being mitigated due to clearing houses.

As one might expect, the presence and severity of WWR depends on the portfolio and on the counterparty. A certain portfolio P with exposure to counterparty A may be subject to WWR, while a different portfolio Q with exposure to counterparty A, or the same portfolio P with exposure to a different counterparty B, may constitute right-way risk. Below two more examples are given to help one's understanding of WWR.

Example 2.2 (Credit Default Swap)**.** A derivative that can contain WWR is a CDS (Credit Default Swap). The point of view of protection buyer A is taken, who enters into a CDS with protection seller B on reference entity C. Recall that a CDS works as follows (see also Figure 2.1): A pays B a periodic payment, and if a predetermined credit event[1] occurs, B pays A a predefined amount called the notional amount, multiplied by one minus the recovery rate. At the same time, a final periodic payment from A to B is made and the swap is terminated. WWR for A occurs when the default events of B and C are positively dependent; and this is often the case, since

[1] Usually defined as the default of C, or another event involving the credit quality of C.

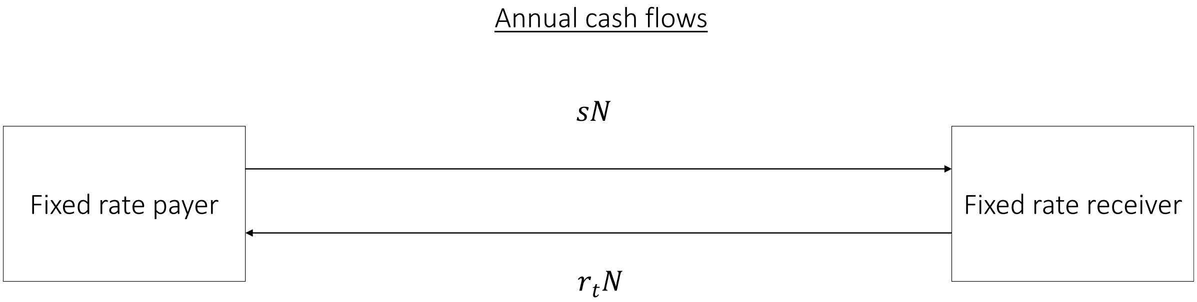

Figure 2.2: A schematic overview of the cash flows of an interest rate swaps. s is the fixed swap rate, r_t is the floating rate, and N is the notional amount. Contracts with payments more than once a year are also possible.

both companies are affected by macroeconomic variables.[2] The dependence is even stronger if B and C are in the same industry. (This could happen in the financial industry, since protection seller B is usually a bank or an insurance company.) To see why this implies WWR, consider the event that both B and C default. In this case, A should receive a large payment from B through the CDS. However, this amount is largely lost, since B has defaulted. WWR manifests itself throughout the whole lifetime of the swap through the probability of this double default. If the PD of C increases, the exposure of A to B increases: this exposure is equal to the present value of expected payments, including the payment made by B to A in case C defaults. But if the PD of C increases, the PD of B is likely to increase as well. So the exposure and the counterparty's PD increase together, i.e. there is WWR.

Example 2.3 (WWR in interest rate swaps)**.** WWR in interest rate swaps is the focal point for this thesis. Possible WWR in fixed-for-floating interest rate swaps can be caused by dependence between the counterparty's PD and the floating rate, which is usually a benchmark interest rate such as the 6 month LIBOR rate. See Figure 2.2 for an overview of the cash flows in an interest rate swap. If there is positive dependence, an increase in the counterparty's PD would mean a higher floating rate and thus an increase in value of the swap for the payer position. This means WWR for the swap payer, since their exposure rises along with the counterparty's PD. But negative dependence between the counterparty's PD and the floating rate also constitutes WWR, this time for the swap receiver. For the receiver, a decreasing floating rate increases the value of the swap and with that his exposure to the counterparty, whose PD increases at the same time in the negative dependence case. Historical market data provides evidence of negative dependence between interest rates and default rates of financial companies (see for example Ben-Abdallah et al.; 2019). Similar results are found by Harris et al. (2015) for financials as well as for a small portfolio of non-financials. This shows WWR in interest rate swaps is indeed present in reality for the fixed rate receiver.

2.2. Models for WWR

The modelling of WWR is a specific kind of dependence modelling, for which there are several different statistical tools available. Most methodologies in the current literature can be divided into three main schools of thought. As mentioned, the focus in this thesis is on the copula approach (number 1 below). The reasoning behind choosing this approach over the other approaches is explained in Section 2.3. The three schools of thought are as follows.

1. Using copulas is the most explored approach. Cherubini (2013) was one of the first to use this approach, employing it to obtain analytic expressions for the CVA of both interest rate swaps and credit default swaps. Many other scholars have also provided valuable insights, such as Böcker and Brunnbauer (2014), who brought the issue of path inconsistency to attention.

2. Another approach is defining a functional relationship between the portfolio value and a variable indicating counterparty credit quality. This was the subject of one of the first papers on WWR, written by Hull and White (2012). A more general version of this approach was chosen as the most preferable out of several methods by Ruiz et al. (2015).

[2] Not always; the default of one of the two companies might happen because of non-macroeconomic reasons, such as the loss of a large client or a natural disaster. The PD of the other company may not be affected in this case.

3. WWR can also be modelled by means of stochastic processes for the relevant variables, e.g. the interest rate and the hazard rate when considering interest rate swaps. Dependence between these variables is introduced by correlating the Brownian motions underlying these variables. Ben-Abdallah et al. (2019) are among those who explored this approach for interest rate swaps and swaptions.

These approaches and their uses in the literature are discussed below.

2.2.1. First school of thought: Copula models

Before describing the existing copula models for WWR, the definition of copulas and some fundamental theory are given. For more information on copulas, see Appendix A or Nelsen (2006).

A vector of random variables is defined by its joint distribution, while the individual random variables can be considered by looking at their marginals. An intuitive point of view is that the *copula* of a random vector is the function that remains when the effect the marginals have on the joint distribution is removed.[3] The formal definition of a copula is given below.

Definition 2.4. A d-dimensional copula $C(\cdot)$ is a distribution function on $[0,1]^d$ with standard uniform marginals.

While copulas can be defined for any dimension $d \geq 2$, $d \in \mathbb{N}$, this thesis only considers two-dimensional copulas. This is because there are two random variables of interest, i.e. the probability of default and the interest rate.

The intuitive interpretation above is confirmed by Sklar's theorem (Sklar; 1959). This important theorem shows that a copula can be obtained from all multivariate distribution functions, and that copulas can be used together with univariate CDFs to construct multivariate CDFs.

Theorem 2.5 (Sklar 1959)**.** Let F be a bivariate joint distribution with marginals F_1, F_2. Then there exists a copula $C : [0,1]\times[0,1] \to [0,1]$ such that, for all $x_1, x_2 \in \overline{\mathbb{R}} = [-\infty, \infty]$,

$$F(x_1, x_2) = C(F_1(x_1), F_2(x_2)). \tag{2.1}$$

If the marginals are continuous, then $C(\cdot,\cdot)$ is unique; otherwise $C(\cdot,\cdot)$ is uniquely determined on $\operatorname{Ran} F_1 \times \operatorname{Ran} F_2$, where $\operatorname{Ran} F_i = F_i(\mathbb{R})$ denotes the range of $F_i(\cdot)$ for $i = 1,2$. Conversely, if $C(\cdot,\cdot)$ is a copula and $F_1(\cdot)$ and $F_2(\cdot)$ are univariate distribution functions, then the function $F(\cdot)$ defined in (2.1) is a joint distribution function with marginals $F_1(\cdot)$ and $F_2(\cdot)$.

Proof. See Schweizer and Sklar (1983). □

Corollary 2.6. The copula $C(\cdot,\cdot)$ can be obtained from the multivariate CDF and the marginals as

$$C(u_1, u_2) = F(F_1^{\leftarrow}(u_1), F_2^{\leftarrow}(u_2)), \quad u_1, u_2 \in [0,1], \tag{2.2}$$

where $F_1^{\leftarrow}(\cdot)$ and $F_2^{\leftarrow}(\cdot)$ denote the generalised inverses of $F_1(\cdot)$ and $F_2(\cdot)$ respectively.

In the above framework, $C(\cdot,\cdot)$ may be referred to as the *copula of* F, or as the *copula of* X if X is a bivariate random variable with multivariate CDF $F(\cdot,\cdot)$ and marginals $F_1(\cdot), F_2(\cdot)$.

One common type of copula that is considered in this thesis is the class of elliptical copulas. These are the copulas of elliptical distributions, such as the normal distribution and the t distribution. Both of these are copulas that are implied by a multivariate distribution. This means the copula is defined as the copula of the corresponding multivariate distribution through (2.2). As such, there is no closed form expression for these copulas.

The other main copula class considered in this thesis is that of Archimedean copulas. An Archimedean copula is of the form

$$C(u_1, u_2) = \phi^{[-1]}(\phi(u_1) + \phi(u_2)), \quad u_1, u_2 \in [0,1], \tag{2.3}$$

[3] There has been discussion about the question of whether the copula completely describes the dependence structure of a multivariate distribution. This has largely to do with one's interpretation of the term 'dependence structure'. There are many, such as Genest and Rémillard (2006), who define a dependence structure as a margin-free concept. However, some dependence concepts from extreme value theory require marginals to be known, as described in section 8.2 of the paper by Mikosch (2006). See also Section 2.3.

where $\phi : [0,1] \to [0,\infty]$ is a convex, continuous, strictly decreasing function with $\phi(1) = 0$ and $\phi(0) \leqslant \infty$, known as the generator of the copula, and $\phi^{[-1]}(\cdot)$ is the pseudo-inverse of $\phi(\cdot)$, defined as

$$\phi^{[-1]}(t) = \begin{cases} \phi^{-1}(t), & 0 \leqslant t \leqslant \phi(0), \\ 0, & \phi(0) < t \leqslant \infty. \end{cases} \tag{2.4}$$

The pseudo-inverse $\phi^{[-1]}(\cdot)$ has domain $[0,\infty]$. The definitions of the specific copulas mentioned in this thesis can be found in Appendix A.

Umberto Cherubini was one of the first to use copulas to model WWR in credit default swaps, writing about this in 2003 (Cherubini and Luciano; 2003), before the term wrong-way risk was in use. Additionally, the first version of his 2013 paper (Cherubini; 2013) was already written in 2004.[4] In both papers, the focus is on rewriting CVA in terms of prices of other financial products, which are assumed to be known. The early paper (Cherubini and Luciano; 2003) describes the price of a bivariate digital put option, which pays out if the stock values of two different companies are below two respective strike prices. The price D of this option is given by

$$\frac{D\left(S_A < K_A, S_Z < K_Z\right)}{B} = C\left(\ddot{D}_A, \ddot{D}_Z\right), \tag{2.5}$$

where $S_A \geq 0$ and $S_Z \geq 0$ are the stock values of companies A and Z respectively, $K_A \geq 0$ and $K_Z \geq 0$ are the respective strike prices, $B > 0$ is the value of a risk-free asset, C is the copula of the two stock values, and $\ddot{D}_A$ and $\ddot{D}_Z$ are the discounted values of single digital put options on S_A and S_Z with strike prices K_A and K_Z respectively.

Using a structural model of default (i.e. a company goes into default if its stock value is below its debt at some time $T > 0$, which is usually the maturity of a product), a double default scenario can be described by the above formula. The payoffs of two kinds of credit derivatives are then described, considering each scenario of a combination of default and no default of two companies. Combining the payoff in each scenario with the probability of that scenario occurring then yields general copula-based formulas for the price of a defaultable CDS and the price of a two-name credit switch. A credit switch is a multi-name credit derivative closely related to a multi-name CDS. The Fréchet bound copulas are used in the obtained formula as well as a mixture copula linearly interpolating between the perfect positive dependence, independence and perfect negative dependence cases. A closed-form expression is obtained for the price of both products in all of these dependence cases.

In the later paper by Cherubini (2013), a similar approach is taken for CVA for interest rate swaps. The copula model used is

$$\mathbb{Q}\left(\mathrm{sr}\left(t_j, t_n\right) > u, t_{j-1} \leq \tau \leq t_j\right) = \tilde{C}\left(1 - G(u), S\left(t_{j-1}\right) - S\left(t_j\right)\right), \tag{2.6}$$

where $\mathbb{Q}$ is the risk-neutral probability measure, $0 \leq t_{j-1} < t_j < t_n$ are points in time, $\mathrm{sr}\left(t_j, t_n\right) \in \mathbb{R}$ is the swap rate at time t_j for an IRS with maturity t_n, $\tau \geq 0$ is the time of default of the counterparty, $\tilde{C}$ is the copula of $\mathrm{sr}\left(t_j, t_n\right)$ and τ, which is assumed to be constant over time, G is the CDF of $\mathrm{sr}\left(t_j, t_n\right)$ and S is the survival function the counterparty. Note that default is no longer modelled by structural models (as it was in Cherubini and Luciano; 2003), but instead as the time of default being before maturity of the contract. This allows taking into account the timing of the default event and the level of the swap rate at the time of default.

A general formula for CVA for interest rate swaps is developed using the above formula. The comonotonicity and countermonotonicity copulas are used in the formula, which constitute WWR for the payer and receiver positions respectively. An extension is provided by the mixture copula interpolating linearly between the independence and comonotonicity copulas. It is shown that in all cases, the CVA formula can be written as a linear combination of CDS positions and positions in a default-free swaptions. Numerical simulations are used to show the impact of WWR on the CVA of an IRS.

[4] There are no differences in content between the 2004 and 2013 versions; the only updates were to the terminology.

A modified version of the approach by Cherubini (2013) for interest rate swaps is given by Černý and Witzany (2018). They point out a flaw in (2.6), noting that according to the copula definition,

$$\mathbb{Q}\left(\operatorname{sr}\left(t_{i+1}, t_n\right) > u, \tau \leqslant t\right) = \tilde{C}(1 - G(u), S(t)) \tag{2.7}$$

for all t, and so

$$\mathbb{Q}\left(\operatorname{sr}\left(t_{i+1}, t_n\right) > u, t_i \leq \tau \leq t_{i+1}\right) = \tilde{C}(1 - G(u), S(t_i)) - \tilde{C}(1 - G(u), S(t_{i+1})). \tag{2.8}$$

Using this modified copula model, and the same mixture copula as Cherubini (2013), new expressions for the CVA for interest rate swaps in terms of swaptions and credit default swaps are found. Finally, IRS prices including CVA are calculated for several WWR models and different levels of WWR.

A copula approach for portfolios in general is given by Böcker and Brunnbauer (2014). Here the copula model is as follows:

$$\mathbb{Q}(\tilde{V}(s) \leqslant \tilde{v}, \tau \leqslant t) = C_s\left(G_s(\tilde{v}), F(t)\right) \quad \tilde{v} \in \mathbb{R}, t > 0, \tag{2.9}$$

where $\tilde{V}(s)$ is the discounted portfolio value at time $s > 0$ with CDF $G_s(\cdot)$, $F(\cdot)$ is the CDF of τ, and C_s is the copula of $\tilde{V}(s)$ and τ. Now let Ω be the path space of market variables. The paper then considers the cumulated default probability over the interval $[0, T]$ along a path $t \mapsto \tilde{V}(t, \omega), \omega \in \Omega$, of the portfolio value, which is given by:

$$\mathbb{Q}(\tau(\omega) \leqslant T) = \int_0^T \phi_t\left(G_t(\tilde{V}(t, \omega)), F(t)\right) f(t) \mathrm{d}t \tag{2.10}$$

where ϕ_t is the copula density of C_t and in the discrete-time setting $G_t(\tilde{V}(t, \omega))$ can be estimated by the relative rank of the portfolio value of path ω at time t. Since this rank is in general not independent from t, the integral in (2.10) does not calculate to 1 when $T \to \infty$, leading to an inconsistent pathwise default probability. This is a consequence of modelling dependence between a spatial variable (portfolio value) and a temporal value (time of default) using a copula. Another consequence of this is that tail dependence works differently than expected, since the portfolio value around the time of default is not affected by tail dependence if the time of default is not in the tail of its distribution. A solution for the path inconsistency is proposed by not using the portfolio value at the current point in time in the copula, but a time-independent variable such as the portfolio value at a fixed point in time or the average portfolio value up to a fixed point in time.

Another combination of copulas and structural models of default is explored by Hofer (2016). He uses the structural approach of assuming that a counterparty defaults when its equity drops below a certain barrier level. Then the distribution of the counterparty's equity value is coupled with the portfolio value through

$$\mathbb{Q}(V_{t_j} \leq v, S_{t_j} \leq s) = C_j\left(G_{t_j}(v), F_{S_{t_j}}(s)\right), \tag{2.11}$$

where $V_{t_j} \in \mathbb{R}$ is the portfolio value at time $t_j > 0$ with CDF $G_{t_j}(\cdot)$, $S_{t_j} \in \mathbb{R}$ is the counterparty's equity value at time t_j with CDF $F_{S_{t_j}}(\cdot)$, and C_j is their copula. The calculations are done in a discretised, path-wise fashion, making the approach path-consistent in terms of Böcker and Brunnbauer (2014). An advantage of this approach is that calibration of the copula can be done using past data for the portfolio constituents and the equity of the counterparty.

A similar approach is given by Pan (2018), who analyzes CVA for commodity futures using a Gaussian copula one-factor model. Here the counterparty asset value is described by

$$A_t = \beta Y + \sqrt{1 - \beta^2} \varepsilon_t, \tag{2.12}$$

where $Y > 0$ is a systemic factor called the credit deterioration indicator, $\beta < 0$ is the correlation coefficient between the asset value A_t and the risk factor Y, and $\varepsilon_t \in \mathbb{R}$ is an idiosyncratic factor. Default of the counterparty before time t is modelled as the event $A_t < C_t$, where C_t is a credit criterion given by

$$C_t = \phi^{-1}\left(\mathrm{PD}_t\right), \tag{2.13}$$

with $\phi^{-1}(\cdot)$ denoting the inverse of the standard normal CDF and PD_t being obtained from transition probabilities published by rating agencies such as S&P. The commodity price is given by a formula containing a standard normally distributed market factor X, which is related to credit factor Y through

$$X = \rho Y + \sqrt{1-\rho^2}\omega, \tag{2.14}$$

where $\rho \in [-1,1]$ is the Pearson correlation coefficient between the market factor and the credit factor, and ω is a standard normally distributed random variable independent from Y. This is used to obtain an analytical expression for CVA on commodity futures.

Similarly, Rosen and Saunders (2012) also use a credit risk factor and a market factor. The credit risk factor Z is a standard normally distributed variable given by

$$Z = \beta Y + \sqrt{1-\beta^2}\varepsilon, \tag{2.15}$$

where Y and ε are both standard normally distributed variables representing systemic and idiosyncratic risk respectively. This is similar to (2.12), with the difference being that here the credit risk factor does not change over time and it is a latent, standard normally distributed random variable rather than representing asset value. Default occurs when

$$Z = \phi^{-1}(F(t)), \tag{2.16}$$

where $\phi^{-1}(\cdot)$ is the inverse of the standard normal CDF and $F(\cdot)$ is the CDF of the default time of the counterparty. For the exposure modelling, it is assumed that there are $M \in \mathbb{N}$ possible scenarios simulated using Monte Carlo. These scenarios are denoted with ω_m, with $m = 1,\dots,M$. The exposure scenario that is realised is called ω, and is determined as follows:

$$\omega = \omega_m \Leftrightarrow C_{m-1} < X \leq C_m, \quad m = 1,\dots,M, \tag{2.17}$$

where X is a standard normally distributed market factor, and the thresholds C_m are given by

$$C_m = \begin{cases} -\infty & m = 0, \\ \phi^{-1}(Q_m) & m = 1,\dots,M-1, \\ \infty & m = M, \end{cases} \tag{2.18}$$

with

$$Q_m = \sum_{j=1}^{m} q_m, \quad m = 1,\dots,M, \tag{2.19}$$

and where

$$q_m = P(\omega = \omega_m), \quad m = 1,\dots,M \tag{2.20}$$

is the probability of the exposure scenario ω_m being attained. A bivariate normal distribution is used for the systemic credit factor Y and the market factor X. This naturally implies that a Gaussian copula connects the two factors, as in Pan (2018).

2.2.2. Second school of thought: Functional relationship

A famous paper that is often cited in other research into WWR (by e.g. Ben-Abdallah et al.; 2019; Černý and Witzany; 2018) is due to Hull and White (2012). Their approach is to model a relationship between the counterparty's hazard rate h and the portfolio value w. This relationship is given by the function

$$h(t) = \exp[a(t) + bw(t) + \sigma\varepsilon], \tag{2.21}$$

where $a : [0,\infty) \to \mathbb{R}$ is a function of time, $b \in \mathbb{R}$ is a constant measuring the amount of right or wrong-way risk, $\sigma > 0$ is a constant measuring the amount of noise in the relationship, and ε is a random variable with a standard normal distribution. However, the noise term is neglected based on its low impact on the results in practice. Hence, the model becomes

$$h(t) = \exp[a(t) + bw(t)], \tag{2.22}$$

implying that some shift in the hazard rate corresponds deterministically to a shift in the portfolio value, and vice versa. For this reason the model has been regarded as non-probabilistic (Böcker and Brunnbauer; 2014).

A modified version of this approach is given by Ruiz et al. (2015). Rather than the full portfolio value, a single market variable x is used which is related to PD rather than hazard rate. The market variable x can be e.g. the equity price for corporates or the FX rate of the currency for sovereigns. The relation is described as

$$PD = g(x) + \sigma\varepsilon, \tag{2.23}$$

where $g : \mathbb{R} \to \mathbb{R}$ is the function describing the dependence structure, $\sigma > 0$ is a constant measuring the amount of noise in the relationship, and ε is a random variable with a standard normal distribution. Four different forms for g are tested against market data to see which performs best in terms of best fit and smallest noise. These forms are power, exponential, logarithmic and linear:

$$\begin{aligned} g_1 &= A_1 x^{B_1}, \\ g_2 &= A_2 e^{B_2 x}, \\ g_3 &= A_3 + B_3 \ln(x), \\ g_4 &= A_4 + B_4 x. \end{aligned} \tag{2.24}$$

The best performance is found for the power function, while the exponential function, which is the function also used by Hull and White (2012), works second best.

2.2.3. Third school of thought: Correlated dynamics

This is the approach considered by e.g. Ben-Abdallah et al. (2019). Interest rate is described by a CCG model (Casassus et al.; 2005), which assumes stochastic interest rates as well as stochastic interest rate volatility. The CCG model is given by

$$\begin{aligned} dr_t &= \xi_r(\theta_{rt} - r_t)\,dt + \sqrt{V_t}\,dZ_{1t}, \\ d\theta_{rt} &= \left(\gamma(t) - 2\xi_r\theta_{rt} + \frac{V_t}{\xi_r}\right)dt, \\ dV_t &= \xi_V(\theta_V - V_t)\,dt + \nu_V\sqrt{V_t}\left(\rho_{rV}\,dZ_{1t} + \sqrt{1-\rho_{rV}^2}\,dZ_{2t}\right), \end{aligned} \tag{2.25}$$

where the instantaneous spot rate r_t, the long-run interest rate θ_{rt} and the interest rate variance V_t are stochastic processes. The spot rate follows a mean-reverting process with speed of adjustment $\xi_r > 0$. The variance process is a square root process with speed of adjustment $\xi_V > 0$, long-run variance level θ_V and volatility of variance parameter ν_V. $\gamma(t)$ is a deterministic function of time, and Z_{1t} and Z_{2t} are two independent standard Brownian motions. The parameter $\rho_{rV} \in [-1, 1]$ is the Pearson correlation coefficient between the Brownian components of r_t and V_t.

For the default intensity λ_t a CIR model (Cox et al.; 1985) is used, given by

$$d\lambda_t = \xi_\lambda(\theta_\lambda - \lambda_t)\,dt + \nu_\lambda\sqrt{\lambda_t}\left(\rho_{r\lambda}\,dZ_{1t} + \frac{\rho_{V\lambda} - \rho_{rV}\rho_{r\lambda}}{\sqrt{1-\rho_{rV}^2}}\,dZ_{2t} + \sqrt{1 - \rho_{r\lambda}^2 - \frac{(\rho_{V\lambda} - \rho_{rV}\rho_{r\lambda})^2}{1-\rho_{rV}^2}}\,dZ_{3t}\right), \tag{2.26}$$

where λ_t is a mean-reverting stochastic process with speed of adjustment $\xi_\lambda > 0$, long-run default intensity θ_λ, and volatility ν_λ. Z_{3t} is a standard Brownian motion independent of Z_{1t} and Z_{2t}, $\rho_{r\lambda} \in [-1, 1]$ is the Pearson correlation coefficient between the Brownian components of r_t and λ_t, and $\rho_{V\lambda} \in [-1, 1]$ is the Pearson correlation coefficient between the Brownian components of V_t and λ_t. This expression can be used to calculate the probability of a company defaulting between two points in time, by which the time of default can be simulated. The parameters are estimated using historical market data, and the impact of WWR on CVA for interest rate swaps and interest rate swaptions is assessed. This is done by comparing the cases of different combinations of zero and nonzero $\rho_{r\lambda}$ and $\rho_{V\lambda}$. The findings are that the calibrated negative values of $\rho_{r\lambda}$ have the expected effect of WWR for receiver positions, while the effect of nonzero $\rho_{V\lambda}$ is minimal for the CVA of both swaps and swaptions.

Harris et al. (2015) use a very similar method. Their model for the instantaneous forward rate $f(t,T)$ is given by

$$\begin{aligned} df_{t,T} &= \mu^f_{t,T}dt + \sum_{i=1}^{N} \sigma^{f,i}_{t,T}\sqrt{v^i_t}dZ^i_{1t} \\ dv^i_t &= k^i\left(\theta^i - v^i_t\right)dt + \sigma^i\sqrt{v^i_t}\left(\rho^i dZ^i_{1t} + \sqrt{1-\rho^{i2}}dZ^i_{2t}\right), \quad i = 1,\dots,N, \end{aligned} \tag{2.27}$$

where $f_{t,T}$ is a stochastic process describing the instantaneous forward rate observed at time $t \geq 0$ for the rate taking effect at time $T \geq t$, and v^i_t is a CIR-process describing the variance of the i-th random driver of $f_{t,T}$. $\mu^f_{t,T}$ and $\sigma^{f,i}_{t,T}$ are deterministic functions mapping from $[0,T]\times\mathbb{R}$ to $\mathbb{R}$. $k^i > 0$ denotes the speed of adjustment of v^i_t, $\theta^i > 0$ denotes the long-run variance and σ^i denotes the volatility of variance. Z^i_{1t} and Z^i_{2t} are independent standard Brownian motions with respect to the risk-neutral measure. $\rho^i \in [-1,1]$ is the Pearson correlation coefficient between the i-th Brownian component of $f_{t,T}$ and the Brownian component of v^i_t.

The hazard rate λ_t is also given by a CIR process:

$$d\lambda_t = \xi_\lambda(\theta_\lambda - \lambda_t)dt + \nu_\lambda\sqrt{\lambda_t}dW_t, \tag{2.28}$$

where the parameters are as in (2.26) and W_t is a standard Brownian motion correlated with the Brownian components of the v^i_t. Default between times t and $t+dt$ is modelled by the event

$$\omega \leq \lambda_t dt, \tag{2.29}$$

where ω is a standard uniform random variable and $\lambda_t dt$ is the probability of default between times t and $t+dt$ conditional on no earlier default. The model is calibrated and numerical results are obtained on the impact of correlation between the hazard rate and the interest rate variance on the credit risk of collateralised interest rate derivatives.

The approaches by Ben-Abdallah et al. (2019) and Harris et al. (2015) correspond roughly to using a Gaussian copula, since increments of standard Brownian motions are normally distributed and the dependence is modelled through a single correlation parameter.

A somewhat different approach, but one that is also based on correlated dynamics, is given by Brigo et al. (2018). They consider CVA for options, hence dynamics for the default intensity and the option prices are given. The option prices are based on the underlying stock S_t following a geometric Brownian motion, i.e. under the risk-neutral measure,

$$dS_t = rS_t dt + \sigma S_t dW^S_t, \tag{2.30}$$

where $r \in \mathbb{R}$ is the risk-free rate, $\sigma > 0$ is the volatility of the stock, and W^S_t is a standard Brownian motion. Once again, default intensity is modelled through a CIR process, given by

$$d\lambda_t = \xi_\lambda(\theta_\lambda - \lambda_t)dt + \nu_\lambda\sqrt{\lambda_t}dW^\lambda_t, \tag{2.31}$$

with parameters as in (2.26) and W^λ_t a standard Brownian motion with correlation $\rho \in [-1,1]$ with W^S_t. A change of measure is applied to account for WWR. For two proxies of the change of measure, analytic expressions are obtained for expected positive exposure and CVA.

2.3. Benefits and drawbacks of the models

As mentioned before, copulas are the approach to modelling WWR in this thesis. To substantiate the choice for this methodology, the benefits and drawbacks of all three models are explored here. A critical view on copulas as a statistical tool is given by Mikosch (2006), as a response to the surge in popularity of copulas in the early 2000s. Although his paper was itself criticised by Genest and Rémillard (2006), he describes several points which are good to take into account when using copulas. Below, the main benefits of copulas are detailed, after which the three main points of attention are described. Then the benefits and drawbacks of the functional relationship and correlated dynamics are given, as well as the reasoning for not using these models.

First of all, a great benefit of copulas is their flexibility. A large amount of copula families are explored in the literature, and mixtures or other adaptations of copulas can be created as well. Many different combinations of tail dependence, radial symmetry, exchangeability, positive or negative dependence and other properties can be found in existing copulas.

Furthermore, the splitting of a multivariate distribution into marginals and a copula allows for specifying a copula independently from the marginals. For example, a multivariate distribution with normal marginals and a t copula may be created. This also provides a way to specify a dependence structure between two random variables with different marginals. These two points are an advantage over using a standard multivariate distribution such as the multivariate beta distribution, while all standard multivariate distributions can also be constructed using marginals and a copula.

Another benefit is that copulas can be extracted from any multivariate distribution through Theorem 2.5. In this way, a copula can be created corresponding to any dependence structure described by a multivariate distribution function. In addition, since researchers have been studying copulas for a long time (see for example Sklar; 1959), much is known about copulas and there is a lot of literature available. Finally, copulas are intuitive objects in statistics, since they are themselves multivariate distribution functions.

The first point of attention for copulas is that the marginals must not be disregarded when a complete view of dependence is to be obtained. While copulas give a lot of useful information on the dependence structure, there are dependence measures which cannot be calculated with only the information the copula gives. When one is only interested in information that is contained in the copula, such as the ordering of data, the marginals do not need to be taken into account. Otherwise, the copula can be used together with the marginals, which together completely define the multivariate distribution through Theorem 2.5. This is an avoidable pitfall rather than a drawback, however.

Another point of attention is fitting copulas to data. When fitting a multivariate distribution to multivariate data, observations directly from the copula itself are generally not available. This means one first needs to fit marginals to the data, after which the data can be transformed to virtual data points to which a copula can be fitted. This process is described in detail in Section 3.1 (see also McNeil et al.; 2005). Since two fitting processes are carried out, one needs to keep in mind that the fit could be worse than if a multivariate distribution would have been directly fitted.

Finally, a general point on mathematical tools is that they are intended for specific uses, and they perform worse when used for other purposes. This point also applies to copulas. They work best when modelling dependence between two spatial variables, and there might be issues when one tries to model space-time dependence with them. Some of these issues are described by Böcker and Brunnbauer (2014).

The main benefits of the functional relationship approach are described by Ruiz et al. (2015), being the simplicity of the mathematical framework and the robustness of its calibration to empirical data. However, the model has been regarded as non-probabilistic (Böcker and Brunnbauer; 2014). Indeed, the only stochastic part is a noise term in the otherwise deterministic function describing the dependence structure. This is the main reason this approach is not used in this thesis.

A key advantage of the correlated dynamics approach is that numerical tools are well-suited to model stochastic processes such as forward dynamics. Introducing the dependence through correlation in the underlying Brownian motion maintains simplicity. The reason this model is not used, however, is that it is restricted to a single type of dependence structure. For example, it cannot be altered to account for more upper tail dependence while keeping the same level of lower tail dependence, or to account for the presence or absence of radial symmetry.

In conclusion, the copula approach is used mainly because of its flexibility and because it allows for any combination of copula and marginals. There are several pitfalls, being that marginals must not be disregarded, the indirect fitting process may affect the quality of the fit, and issues may arise when attempting to model space-time dependence with copulas. Although these pitfalls are important to keep in mind, they can be navigated around by using copulas with care.

3

Modelling dependence between probability of default and interest rate

As described in Section 2.3, copulas are useful tools for dependence modelling, but they are not without their complications. One of the pitfalls in the use of copulas is fitting them to data. As true observations from a copula are generally not available, an estimate of the marginals is required to be able to estimate the copula corresponding to the distribution generating the data. This estimate for the marginals introduces more inaccuracy in the resulting estimate. Furthermore, as different copulas can give comparable results, such as the t and Gaussian copulas, it may be difficult to distinguish which copula underlies the data. A careful approach to copula fitting is therefore required.

One methodology of checking the robustness of a fitting method is to use a dataset where the underlying distribution is known. For a copula approach, this implies knowing both the marginals and the copula of the dataset. To that end, a dataset of probabilities of default and interest rates is simulated in this chapter. Fitting estimates for the marginals as well as an estimate for the copula to this known dataset yields valuable insights with regard to the performance of the fitting process. Furthermore, useful information is obtained about which copulas show similar results when fitting them to data and which copulas show different results.

The chapter starts by detailing a modified version of maximum likelihood estimation to be applied to copulas in Section 3.1. Next, the methodology is applied to artificial data: the process of generating the dataset of artificial data is described in Section 3.2.1; then in Section 3.2.2, the fitting process is applied to the generated dataset. The chapter concludes by analysing these results and drawing conclusions from them.

3.1. Copula fitting method

The method used to fit copulas to the data is maximum likelihood estimation (MLE). Fitting a copula to a dataset with MLE is not as straightforward as fitting a multivariate distribution, however; the dataset can be viewed as a set of observations from a multivariate distribution, while direct observations from the copula are generally unavailable. However, the copula and the multivariate distribution are related through Theorem 2.5. This theorem shows that the marginals F_1 and F_2 are needed to move from the multivariate distribution to the copula; similarly, the marginals can be used to transform the dataset into a so-called *pseudo-sample* of observations from the copula. The empirical marginals $\hat{F}_1$ and $\hat{F}_2$ are used as estimates for the marginals. The pseudo-sample then consists of the vectors $\hat{\mathbf{U}}_1, \ldots, \hat{\mathbf{U}}_n$ given by

$$\hat{\mathbf{U}}_i = (\hat{U}_{i,1},\ \hat{U}_{i,2}) = (\hat{F}_1^{-1}(X_{i,1}),\ \hat{F}_2^{-1}(X_{i,2})), \quad i = 1, \ldots, n, \tag{3.1}$$

where $(X_{i,1}, X_{i,2})$, $i = 1, \ldots, n$ are the original observations and $\hat{F}_1^{-1}$ and $\hat{F}_2^{-1}$ denote the inverses of $\hat{F}_1$ and $\hat{F}_2$. Then this pseudo-sample is used as if it were a sample from the copula and use MLE to estimate the copula parameters. This means

$$\ln L(\theta; \hat{\mathbf{U}}_1, \ldots, \hat{\mathbf{U}}_n) = \sum_{i=1}^{n} \ln c_\theta(\hat{\mathbf{U}}_i) \tag{3.2}$$

is maximised with respect to parameter θ, where c_θ is the copula density as in (A.22) of a parametric copula C_θ. Copula parameters can be estimated in several ways (Nelsen; 2006). In this thesis MLE is mainly used, because of its immediate use and the attractive properties, such as asymptotic consistency and efficiency (Newey and McFadden; 1994). Furthermore, several goodness-of-fit test statistics, such as the Akaike Information Criterion (AIC), take the (log-)likelihood as an input, so it is a small step to calculate these statistics after performing MLE.

3.2. Application to artificial data

Before looking at real-world data, a model to simulate artificial data is built. This artificial data aids in understanding the process of fitting a copula to market data. It is used to see if the fitting model returns the same copula used to simulate the artificial data. Additionally, the differences between fitting different copulas can be observed.

Daily data is simulated for instantaneous interest rates and hazard rates; these instantaneous interest rates are used to calculate implied swap rates. As is common practice in the field of finance, the log-returns of the data are considered. The benefit of using log-returns or returns over raw data is normalisation; while the data may originate from different price levels, the (log-)returns are comparable. As daily data is simulated, the returns are small, which means the approximation $\log(1+r) \approx r$, $|r| \ll 1$ can be used, ensuring that log-returns are close to actual returns. The main benefit of using log-returns over returns is time-additivity; the log-return over $n \in \mathbb{N}$ days can be described by the sum of single-day log-returns, while the raw return over n days equals the product of single-day returns.

For this simulation, the marginals for instantaneous interest rates and hazard rates need to be defined, as well as a copula. The copula choice is left open for now, to allow for checking the effects of using different copulas.

3.2.1. Generating artificial data

For the marginal of instantaneous interest rates $r_t \in \mathbb{R}$, $t \geq 0$, it is assumed that r_t follows a Cox-Ingersoll-Ross (CIR) process (Cox et al.; 1985). This is a mean-reverting process given by

$$dr_t = a(b - r_t)dt + \sigma_r \sqrt{r_t} dW_t^r, \tag{3.3}$$

where W_t^r is a standard Brownian motion, $b \in \mathbb{R}$ is the mean, $a > 0$ is the speed of mean reversion and $\sigma \geq 0$ is the volatility. This process is well-known to be a good model for instantaneous interest rates, although it only models positive rates. To estimate the parameters of the process, the formula for the T-year swap rate $\mathrm{sr}_T : [0,\infty) \to \mathbb{R}$ at time t is used, given by

$$\mathrm{sr}_T(t) = \frac{1}{T}\int_t^{t+T} r(s)ds, \quad T > 0. \tag{3.4}$$

Using the fundamental theorem of calculus, this can be rewritten to

$$\frac{d}{dt}\mathrm{sr}_T(t) = \frac{r(t+T) - r(t)}{T}. \tag{3.5}$$

For $T \to 0$, the right side is equivalent to the definition of the derivative of $r(t)$, meaning that sr_T approximates r for T small enough. Therefore, the overnight London Interbank Offered Rate (LIBOR) is used as an approximation for realised instantaneous interest rate.[1] The CIR process can be discretised as

$$\frac{r_{t+\Delta t} - r_t}{\sqrt{r}_t} = \frac{ab\Delta t}{\sqrt{r}_t} - a\sqrt{r}_t\Delta t + \sigma\sqrt{\Delta t}\varepsilon_t, \tag{3.6}$$

where the ε_t are i.i.d. standard normally distributed random variables. Through this equation, ordinary least squares (OLS) and overnight LIBOR data obtained from Quandl are used to estimate the parameters of the CIR process. r_t is calculated as a percentage, i.e. $r_t = 1$ means the overnight rate is 1%. This scaling has no

[1] The LIBOR is chosen because it is a benchmark interest rate frequently used as a basis for the floating leg of an interest rate swap. Even though LIBOR is not a swap rate, the approximation in (3.5) still holds.

r_0	0.4345	λ_0	0.0152
a	0.7199	α	1.6085
b	0.2136	β	0.0269
σ_r	0.3377	σ_λ	0.1799

Table 3.1: Parameters for the CIR processes detailing the marginals of the instantaneous interest rate (parameters on the left) and the hazard rate (right). r_0 is the USD overnight LIBOR on November 7, 2016. r_t is calculated as a percentage, i.e. $r_t = 1$ means the overnight rate is 1%.

effect on the log-returns.

For the marginal of hazard rates $\lambda_t \geq 0$, the approach by Ben-Abdallah et al. (2019) is followed for the purposes of generating artificial data. This means the hazard rates follow a CIR process as well:

$$d\lambda_t = \alpha(\beta - \lambda_t)\,dt + \sigma_\lambda\sqrt{\lambda_t}\,dW_t^\lambda, \tag{3.7}$$

with standard Brownian motion W_t^λ, mean $b \in \mathbb{R}$, speed of mean reversion $a > 0$ and volatility $\sigma \geq 0$. As the purpose of this process is only to generate realistic data, the parameters used are those found for JP Morgan in the calibration by Ben-Abdallah et al. (2019). The parameters for the marginals of both the instantaneous interest rate and the hazard rate are shown in Table 3.1. Note that the calibration method uses data from during the 2008 credit crisis, so hazard rate levels and volatility are higher compared to stable periods.

The method used to obtain a sample from the copula is as follows. The goal is to obtain a sample of swap rate log-returns and hazard rate log-returns with marginals F_1, F_2 such that the swap rate and the hazard rate both follow a CIR process. Then if some copula C is the copula underlying the sample, $C(F_1(x_1), F_2(x_2))$ is the joint distribution function underlying the sample due to Theorem 2.5 (Sklar).

The first step is to obtain a sample from the copula itself, i.e. from the joint distribution with CDF C. For copulas derived from well-known distributions such as the t and Gaussian copulas, obtaining such a sample is simple; for other copulas such as Archimedean copulas, this is slightly more involved. The sampling processes for the t, Gaussian and Clayton copulas are shown in the examples below.

Example 3.1 (Sampling from a Gaussian or t copula)**.** Suppose $F : \mathbb{R}^2 \to [0,1]$ is the bivariate normal distribution for some set of parameters and $F_1, F_2 : \mathbb{R} \to [0,1]$ are its marginals. If $\mathbf{X} = (X_1, X_2)$ is a realisation from F, then one simply needs to transform each component with its marginal to obtain $\mathbf{U} = (U_1, U_2) = (F_1(X_1), F_2(X_2))$, which has the Gaussian copula as its joint distribution function. If instead F is the bivariate t distribution with marginals F_1 and F_2, the above method yields a realisation from the t copula.

Example 3.2 (Sampling from a Clayton copula)**.** Suppose $\hat{V}$ is a realisation of the gamma distributed random variable $V \sim \mathrm{Ga}(1/\theta, 1)$ with $\theta > 0$. The CDF of V has Laplace-Stieltjes transform[2] $\hat{G}(t) = (1+t)^{-1/\theta}$, with inverse $\hat{G}^{-1}(t) = t^{-\theta} - 1$. Note that $\hat{G}^{-1}(t)$ is equal to the generator $\left(t^{-\theta} - 1\right)/\theta$ of the Clayton copula up to the constant $1/\theta$. Now if $\hat{X}_1, \hat{X}_2$ are two independent realisations from a standard uniform distribution, then $\hat{\mathbf{U}} = \left(\hat{G}\left(-\ln(\hat{X}_1)/V\right), \hat{G}\left(-\ln(\hat{X}_2)/V\right)\right)$ has the Clayton copula as its joint distribution function. Samples from other Archimedean copulas can be obtained in a similar way, obtaining realisations from a random variable V such that the Laplace-Stieltjes transform of the CDF of V is the inverse of the generator of the copula.

Suppose $\hat{\mathbf{U}}_1, \ldots, \hat{\mathbf{U}}_n = (\hat{U}_{1,1}, \hat{U}_{1,2}), \ldots, (\hat{U_{n,1}}, \hat{U_{n,2}})$ is a sample of the desired copula. Now the quantile transformation can be used to obtain $\hat{\mathbf{X}}_1, \ldots, \hat{\mathbf{X}}_n$, where

$$\hat{\mathbf{X}}_i = (\hat{X}_{i,1}, \hat{X}_{i,2}) = (F_1^{-1}(\hat{U}_{1,i}), F_2^{-1}(\hat{U}_{2,i})), \quad i = 1, \ldots, n. \tag{3.8}$$

Then $\hat{\mathbf{X}}_1, \ldots, \hat{\mathbf{X}}_n$ is a sample from a multivariate distribution with the desired marginals F_1 and F_2 and the desired joint distribution function $C(F_1(x_1), F_2(x_2))$. The marginals are such that the swap rate and the hazard rate follow a CIR process; these marginals, however, cannot be obtained explicitly in a straightforward

[2] The Laplace-Stieltjes transform of a CDF $G : [0,\infty) \to [0,1]$ is

$$\hat{G}(t) = \int_0^\infty e^{-tx}\,\mathrm{d}G(x), \quad t \geq 0.$$

manner. Therefore, the CIR processes for the swap rate and hazard rate as defined earlier in this section are simulated, and log-returns are calculated from the results. The empirical distributions $\hat{F}_1$ and $\hat{F}_2$ based on these results for the log-returns are used as estimates for the marginals F_1 and F_2 in (3.8) to obtain the desired sample.

3.2.2. Fitting copulas to artificial data

The procedure described in Section 3.1 is now used to fit several different copulas to the artificial data. The t, Gaussian, Frank, Clayton, Gumbel and Joecopulas are considered. The reason for this choice is that these copulas are most likely to be a good fit to the data, as described in Section 4.6.

All of these copulas are first used in the simulation for artificial data. All copula parameters are chosen such that the Kendall's τ correlation is equal to 0.4, in order to have comparable results. The t copula used for the simulation has 4 degrees of freedom. All of the copulas which exhibit tail dependence in one of the two tails do so in the upper tail, except for the Clayton copula. Therefore, the rotated Clayton copula is used; this is the copula of the bivariate random variable $\mathbf{U}$ when the copula of $1-\mathbf{U}$ is the Clayton copula, i.e. the rotated Clayton copula is the survival copula of the Clayton copula.

Several different copulas are now fitted to the artificial data. The results are shown in Table 3.2. The goodness-of-fit test based on the test statistic $S_N^{(B)}$ as described by Genest et al. (2009) is performed. The null hypothesis is $H_0 : C \in \mathscr{C}_0$, where C is the copula associated with the bivariate distribution underlying the data, and $\mathscr{C}_0$ is a certain parametric family of copulas. The test statistic is defined as

$$S_n^{(B)} = n\int_{[0,1]^2} \{D_n(\mathbf{u}) - C_\perp(\mathbf{u})\}^2 \,\mathrm{d}\mathbf{u}, \tag{3.9}$$

where $n \in \mathbb{N}$ is the size of the dataset, $C_\perp$ is the independence copula, $\mathbf{u} = (u_1, u_2) \in [0,1]^2$, and

$$D_n(\mathbf{u}) = \frac{1}{n}\sum_{i=1}^{n} \mathbb{1}\{\hat{\mathbf{U}}_i \leq \mathbf{u}\} \tag{3.10}$$

is the empirical distribution associated with pseudo-observations $\hat{\mathbf{U}}_i \in [0,1]^2$, with indicator function $\mathbb{1}\{\cdot\}$. There is no explicit expression for the distribution of $S_N^{(B)}$, so the standard deviation of the test statistic cannot be obtained. The p-values, however, are obtained by means of a bootstrap procedure.

The results in Table 3.2 show that for most sets of data, the best fitting copula is the true copula used to generate the data. For the data generated by the t, Frank, rotated Clayton and Gumbel copulas, the lowest AIC and highest p-value are found for the true copula. For data generated by the t and Frank copulas, there is no other copula that fits the data well. In addition, the contour plots of copula densities in Figure 3.1 match well with the superimposed scatterplots of the pseudo-observations of the data generated by the true copulas.

According to the test, the t copula is a better fit for the data generated by the Gaussian copula than the Gaussian copula itself. This is as expected, since the t copula approaches the Gaussian copula as the amount of degrees of freedom tends to infinity. The number of fitted degrees of freedom for the t copula is indeed large (6175.64). Since the t copula has an extra parameter, the Gaussian copula does perform better in terms of the AIC. The data generated by the Gaussian copula is also described moderately well by the Frank and Gumbel copulas.

A remarkable observation is that according to the test, the rotated Clayton copula is a better fit for the data generated by the Joe copula than the Joe copula itself, reporting a significantly higher p-value. The AIC for this dataset is lower (implying a better fit) for the Joe copula, but only slightly. Similarly, for the dataset generated by the rotated Clayton copula, the Joe copula has a lower AIC than the rotated Clayton copula, but the rotated Clayton copula has a slightly higher p-value. For each of the other fitted copulas, the results for the rotated Clayton and Joe copulas as true copulas are close to each other. This indicates that the pseudo-observations of the data generated by these two copulas are very similar. The contour plots in Figure 3.1 show that the densities of these two copulas are indeed very similar. Conversely, note the fitting results of the rotated Clayton and Joe copulas for data generated by the other copulas. For every single dataset, the rotated

Clayton copula is a better fit than the Joe copula.

Something that stands out in the contour plots is that the copula density has peaks in the extreme tails, in the corners of the graphs. This is because most copula densities contain terms which diverge as their arguments tend to 0 or 1, such as the inverses $t^{-1}(\cdot)$ and $\Phi^{-1}(\cdot)$ of the univariate t and Gaussian distributions respectively for the t and Gaussian copulas. This phenomenon is mostly present in those tails where there is tail dependence, although not exclusively. It is also observed for the Gaussian copula, but for the copulas with tail dependence in only one tail, i.e. the Gumbel, Joe and rotated Clayton copulas, this phenomenon is barely present in the tails where these copulas do not have tail dependence. Also note that these density peaks in the extreme tails are far higher than the the highest boundary in the contour plots, but scaling is such that the main parts of the plots are most informative. Therefore some information about the extremal behaviour of the copula densities, in the plot areas within the highest contour lines (darkest red part), is not visible in the contour plots.

In conclusion, the goodness-of-fit test combined with the AIC can generally identify the true copula associated with the data. This provides evidence for good discriminatory power of the fitting process. Several useful observations can be made, such as the datasets generated by the rotated Clayton and Joe copulas being similar, while the rotated Clayton copula is a better fit than the Joe copula for all datasets not generated by the rotated Clayton or Joe copulas. These observations are good to take into account when fitting copulas to real-world data.

True copula		Fitted copula C^t	C^{Ga}	C^{Fr}	$C^{\text{R-Cl}}$	C^{Gu}	C^{Joe}
C^t	Parameter(s)	**0.63, 2.88**	0.63	4.67	1.14	1.75	1.98
	LL	**114.58**	100.25	89.50	84.23	102.49	82.21
	$S_N^{(B)}$	**0.041**	0.053	0.048	0.098	0.064	0.171
	p-value	**0.355**	0.109	0.107	0.040	0.028	0.000
	AIC	**-225.16**	-198.50	-176.99	-166.47	-202.97	-162.42
C^{Ga}	Parameter(s)	0.65, 6175.64	**0.65**	4.86	1.06	1.70	1.92
	LL	105.64	**105.64**	100.97	81.11	94.55	74.60
	$S_N^{(B)}$	0.034	**0.034**	0.038	0.088	0.043	0.215
	p-value	0.420	**0.412**	0.293	0.071	0.228	0.000
	AIC	-207.28	**-209.28**	-199.95	-160.21	-187.10	-147.21
C^{Fr}	Parameter(s)	0.53, 22418.48	0.53	**3.88**	0.67	1.47	1.57
	LL	63.33	63.33	**68.60**	39.76	49.84	32.67
	$S_N^{(B)}$	0.050	0.050	**0.017**	0.132	0.097	0.295
	p-value	0.087	0.114	**0.963**	0.010	0.000	0.000
	AIC	-122.67	-124.67	**-135.20**	-77.53	-97.69	-63.33
$C^{\text{R-Cl}}$	Parameter(s)	0.61, 3.96	0.59	4.48	**1.57**	1.81	2.38
	LL	96.30	83.89	84.38	**127.98**	118.16	129.04
	$S_N^{(B)}$	0.103	0.069	0.081	**0.028**	0.050	0.024
	p-value	0.004	0.022	0.006	**0.850**	0.130	0.757
	AIC	-188.60	-165.78	-166.76	**-253.96**	-234.33	-256.08
C^{Gu}	Parameter(s)	0.62, 10.64	0.62	4.62	1.17	**1.72**	2.02
	LL	94.77	93.20	90.19	88.80	**98.05**	86.28
	$S_N^{(B)}$	0.049	0.048	0.051	0.053	**0.035**	0.111
	p-value	0.134	0.138	0.086	0.321	**0.356**	0.001
	AIC	-185.55	-184.41	-178.38	-175.60	**-194.10**	-170.55
C^{Joe}	Parameter(s)	0.61, 5.38	0.61	4.50	1.49	1.80	**2.30**
	LL	94.57	89.97	85.85	120.72	115.31	**120.83**
	$S_N^{(B)}$	0.096	0.073	0.084	0.023	0.049	**0.035**
	p-value	0.008	0.014	0.003	0.939	0.134	**0.346**
	AIC	-185.13	-177.93	-169.69	-239.44	-228.63	**-239.65**

Table 3.2: Results of fitting the t, Gaussian, Frank, rotated Clayton, Gumbel and Joe copulas to artificial data generated by these copulas. 'Parameter(s)' denotes the fitted estimates of ρ and the degrees of freedom respectively for the t copula, ρ for the Gaussian copula, and θ for the Frank, rotated Clayton, Gumbel and Joe copulas. The t, Gaussian, Frank and Gumbel copulas are recognised as the true copula by the fitting process, while the goodness of fit statistics do not distinguish well between the rotated Clayton and Joe copulas. For a description of the test and further interpretation see Section 3.2.2.

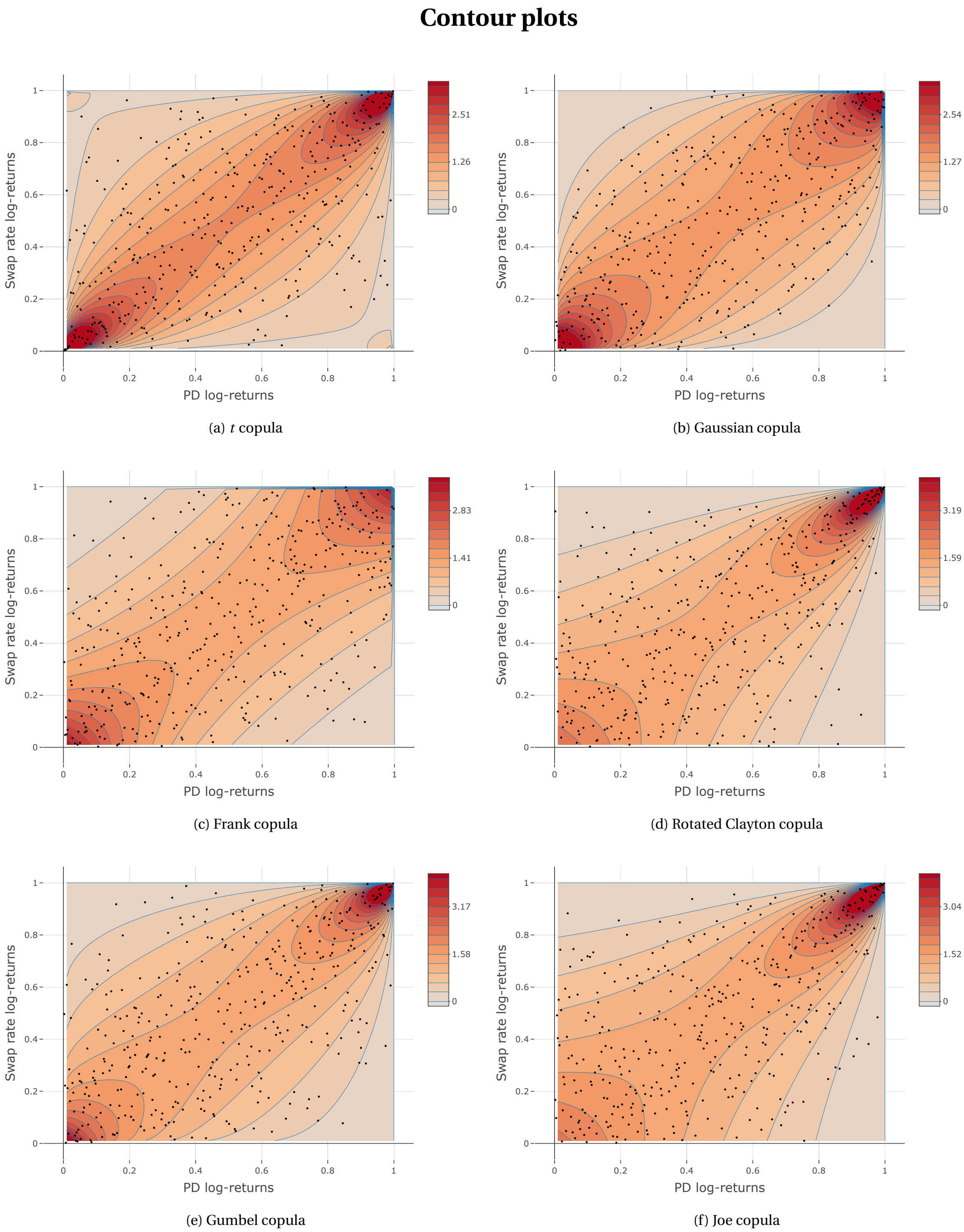

(a) t copula

(b) Gaussian copula

(c) Frank copula

(d) Rotated Clayton copula

(e) Gumbel copula

(f) Joe copula

Figure 3.1: Contour plots of the densities of the t, Gaussian, Frank, rotated Clayton, Gumbel and Joe copulas, superimposed with scatterplots of the pseudo-observations of the artificial data generated by these respective copulas. Note that the scales for the contour plots are different for each copula. The scatterplots and the contour plots fit each other well, while the similarity between the densities of the rotated Clayton and Joe copulas is clear.

4

Data & Results

When dealing with defaults, an issue is often the lack of historical data or the poor quality of the data. Especially for companies with a high credit rating, very few similar companies have defaulted in the past. Furthermore, past defaults have usually occurred in periods of economic downturn. This gives rise to another issue when dependence between defaults and market conditions such as interest rates is considered; it is especially difficult to obtain enough meaningful data on defaults for periods with few defaults and on their behaviour with respect to interest rates. As is further discussed in this chapter, a solution for this is to use market-implied PDs rather than historical default data. These implied PDs can be recovered from CDS spread data, since these spreads depend on the PD of the reference entity.

First, Section 4.1 details this method of extracting implied PD data from observed CDS spread data. The data on CDS spreads and swap rates is then discussed in Section 4.2 and Section 4.3 respectively. The dependence between swap rates and implied PDs is explored in Section 4.4. The collection and the analysis of data from downturn periods is described in Section 4.5. Finally, several copulas are fit to both the non-downturn data and the downturn data in Section 4.6 and the results are discussed. More summary statistics describing the data are provided in Appendix C.

4.1. Market-implied PD

The product under consideration is a fixed for floating interest rate swap, where on a predefined set of payment dates, the fixed rate payer pays fixed rate s times an agreed upon notional amount N to the fixed rate receiver. In return, the receiver pays floating rate r_t times the notional amount N to the payer, where r_t changes over time. Usually, r_t is a benchmark interest rate such as the 6 month LIBOR. The relevant PD is the probability that a company defaults on its interest rate swaps, i.e. the IRS PD. It would be safe to assume that when a company goes into default, it defaults on its interest rate swaps as well. However, as described at the beginning of this chapter, historical data on defaults is unavailable in large enough quantities and in a sufficient number of different market conditions. A more widely available alternative is data on CDS spreads. Recall that in a CDS, counterparty A pays counterparty B a fixed spread, and in return B pays A a fixed amount when the reference entity goes into default. The default event in a CDS is generally defined as the reference entity being unable to repay its debt. The assumption is made that the PD on debt, i.e. the CDS-implied PD, is equal to the IRS PD. This is a conservative choice, since the CDS-implied PD is a probability under the risk-neutral measure, since it is used for pricing. This risk-neutral PD is lower than the real world PD, which is estimated in this chapter.

The assumption that the CDS-implied PD is equal to the IRS PD is motivated as follows. The assumption is that a company defaults when it cannot fulfill at least one of its financial obligations; this event is equivalent to both defaulting on bonds and defaulting on IRS, when the NPV (net present value) of the IRS is negative for the company going into default. The amount lost due to default can be different for the two instruments, depending on the seniority of the instruments, i.e. the order in which creditors are paid back[1]. It is also pos-

[1] Derivatives such as interest rate swaps generally have higher seniority than debt instruments (bonds), so the LGD is higher for bonds (Bolton and Oehmke; 2014).

Time (years)	Default probability	Survival probability	Expected payment	Discount factor	PV of expected payment
1	λ	$1-\lambda$	$s(1-\lambda)$	e^{-r_1}	$s(1-\lambda)e^{-r_1}$
2	$\lambda(1-\lambda)$	$(1-\lambda)^2$	$s(1-\lambda)^2$	e^{-2r_2}	$s(1-\lambda)^2e^{-2r_2}$
3	$\lambda(1-\lambda)^2$	$(1-\lambda)^3$	$s(1-\lambda)^3$	e^{-3r_3}	$s(1-\lambda)^3e^{-3r_3}$
$\vdots$	$\vdots$	$\vdots$	$\vdots$	$\vdots$	$\vdots$
9	$\lambda(1-\lambda)^8$	$(1-\lambda)^9$	$s(1-\lambda)^9$	e^{-9r_9}	$s(1-\lambda)^9e^{-9r_9}$
10	$\lambda(1-\lambda)^9$	$(1-\lambda)^{10}$	$s(1-\lambda)^{10}$	$e^{-10r_{10}}$	$s(1-\lambda)^{10}e^{-10r_{10}}$
Total					$s\sum_{i=1}^{10}(1-\lambda)^i e^{-ir_i}$

Table 4.1: Calculation of the present value of expected payments. $s>0$ is the CDS spread as a percentage of the notional amount, $\lambda\in[0,1]$ is the one-year probability of default conditional on no earlier default, and $r_i\in\mathbb{R}$ is the discount rate for cash flows taking place in i years from the current time. The notional amount is 1.

Time (years)	Default probability	Expected accrual payment	Expected payoff	Discount factor	PV of expected accrual payment	PV of expected payoff
0.5	λ	$0.5s\lambda$	(1 - RR) λ	$e^{-0.5r_{0.5}}$	$0.5s\lambda e^{-0.5r_{0.5}}$	(1 - RR) $\lambda e^{-0.5r_{0.5}}$
1.5	$\lambda(1-\lambda)$	$0.5s\lambda(1-\lambda)$	(1 - RR) $\lambda(1-\lambda)$	$e^{-1.5r_{1.5}}$	$0.5s\lambda(1-\lambda)e^{-1.5r_{1.5}}$	(1 - RR) $\lambda(1-\lambda)e^{-1.5r_{1.5}}$
2.5	$\lambda(1-\lambda)^2$	$0.5s\lambda(1-\lambda)^2$	(1 - RR) $\lambda(1-\lambda)^2$	$e^{-2.5r_{2.5}}$	$0.5s\lambda(1-\lambda)^2e^{-2.5r_{2.5}}$	(1 - RR) $\lambda(1-\lambda)^2e^{-2.5r_{2.5}}$
$\vdots$	$\vdots$	$\vdots$	$\vdots$	$\vdots$	$\vdots$	$\vdots$
8.5	$\lambda(1-\lambda)^8$	$0.5s\lambda(1-\lambda)^8$	(1 - RR) $\lambda(1-\lambda)^8$	$e^{-8.5r_{8.5}}$	$0.5s\lambda(1-\lambda)^8e^{-8.5r_{8.5}}$	(1 - RR) $\lambda(1-\lambda)^8e^{-8.5r_{8.5}}$
9.5	$\lambda(1-\lambda)^9$	$0.5s\lambda(1-\lambda)^9$	(1 - RR) $\lambda(1-\lambda)^9$	$e^{-9.5r_{9.5}}$	$0.5s\lambda(1-\lambda)^9e^{-9.5r_{9.5}}$	(1 - RR) $\lambda(1-\lambda)^9e^{-9.5r_{9.5}}$
Total					$0.5s\lambda\sum_{i=1}^{10}(1-\lambda)^{i-1}e^{-(i-0.5)r_{i-0.5}}$	(1 - RR) $\lambda\sum_{i=1}^{10}(1-\lambda)^{i-1}e^{-(i-0.5)r_{i-0.5}}$

Table 4.2: Calculation of the expected present value of the accrual payment and the CDS payoff in case of default of the reference entity. $\lambda\in[0,1]$ is the default probability in one year conditional on no earlier default, $s>0$ is the CDS spread as a percentage of the notional amount, RR $\in[0,1]$ is the recovery rate, and $r_i\in\mathbb{R}$ is the discount rate for cash flows taking place in i years. The notional amount is 1.

sible for one of the two instruments to be paid back in full. This is a difference in the LGDs, whereas the PDs are equal if there is only one type of default event. The modelling of LGD is outside the scope of this thesis.

Having determined that the bond PD is used, the method of obtaining it from CDS spreads is now detailed. Let $s>0$ be the CDS spread as a percentage of the notional amount; this is the amount that is paid annually from the protection buyer to the protection seller. Let $\lambda\in[0,1]$ be the default probability during one year conditional on no earlier default.[2] The discount rate at time $t>0$ is denoted by $r_t\in\mathbb{R}$. It is assumed that payments are made annually in arrears and that default can only occur halfway through a year. When a default occurs, an accrual payment is made by the protection buyer to the protection seller to reflect the periodic payment over the half year between the last periodic payment and the moment of default. Then the contract is terminated, i.e. no more periodic payments take place. The tenor is 10 years, since the data consists of 10-year CDS spreads.

Unconditional default probabilities and survival probabilities are calculated and used to compute the expected present value of the periodic spread payments in Table 4.1. Note that the payment occurs only if the reference entity survives until the payment date. If the reference entity defaults between two payment dates, an accrual payment is made. The expected present value of this accrual payment is calculated in Table 4.2. In the same table, the default probabilities are used to calculate the expected present value of payoff due to default of the reference entity. The expected payoff is equal to the default probability multiplied by the LGD (which is equal to $1-$RR) and the notional amount, but since the notional amount is assumed to be equal to 1, the expected payoff is equal to the default probability multiplied by the LGD in this case.

[2] The assumption is that this probability is the same for every year within the CDS tenor ('running period' of the CDS), since a single CDS spread does not give information on how the default probability is distributed over the years. It would be possible to obtain part of this information by considering CDSs with different tenors. However, this would add too much complexity to be used for converting all of the CDS spread data to PD data.

The no-arbitrage CDS spread is obtained by equating the net present value of the CDS to zero. The periodic and accrual payments are paid by the protection buyer to the protection seller, while the payoff in case of default is paid by the seller to the buyer. This yields the equation

$$s\sum_{i=1}^{10}(1-\lambda)^i e^{-ir_i} + 0.5s\lambda\sum_{i=1}^{10}(1-\lambda)^{i-1}e^{-(i-0.5)r_{i-0.5}} = (1-\text{RR})\lambda\sum_{i=1}^{10}(1-\lambda)^{i-1}e^{-(i-0.5)r_{i-0.5}}, \tag{4.1}$$

from which one can obtain the closed-form expression

$$s = \frac{(1-\text{RR})\lambda\sum_{i=1}^{10}(1-\lambda)^{i-1}e^{-(i-0.5)r_{i-0.5}}}{\sum_{i=1}^{10}(1-\lambda)^i e^{-ir_i} + 0.5\lambda\sum_{i=1}^{10}(1-\lambda)^{i-1}e^{-(i-0.5)r_{i-0.5}}} \tag{4.2}$$

for the no-arbitrage CDS spread s in terms of the discount rates r_t, $t = 0.5, 1, \ldots, 10$ and the conditional default probability λ. Under the simplifying assumption that $-(i-0.5)r_{i-0.5} = -(ir_i - 0.5r_{0.5})$, the above expression can be simplified to

$$s = \frac{(1-\text{RR})\lambda e^{0.5r_{0.5}}}{1-\lambda+0.5\lambda e^{0.5r_{0.5}}}, \tag{4.3}$$

or rewritten to

$$\lambda = \frac{s}{(1-0.5e^{0.5r_{0.5}})s + (1-\text{RR})e^{0.5r_{0.5}}} \tag{4.4}$$

as a closed-form expression for λ in terms of the CDS spread s. Since $s \ll 1$, the term $(1-0.5e^{0.5r_{0.5}})s$ is relatively small compared to the term $(1-\text{RR})e^{0.5r_{0.5}}$. This means that λ is approximately equal to s up to a multiplicative term depending on RR and $r_{0.5}$:

$$\lambda \approx \frac{s}{(1-\text{RR})e^{0.5r_{0.5}}}. \tag{4.5}$$

If a different assumption would be made for possible moments a company can default, the above approximation would correspond to the common approximation

$$\lambda \approx \frac{s}{(1-\text{RR})}. \tag{4.6}$$

However, for the remainder of this thesis, the expression in (4.4) is used.

The only discount rate used in the calculations is the 6 month discount rate $r_{0.5}$, which is specified as the yield on 6 month US treasury bonds. For each observation date of a CDS spread, the observed yield at that date is used. Yield data is obtained from the US department of the treasury. [3]

4.2. CDS sector curve data

The sources for market data do not offer historical data for single-name CDS spreads. Instead, the *CDS sector curves* from Bloomberg are used. A CDS sector curve is obtained using five factors: region, industry, debt type, rating (high yield or investment grade) and tenor.[4] The exact methodology used to calculate the sector curves is property of Bloomberg and is therefore not publicly available. The method for obtaining market-implied PD described in Section 4.1 cannot be applied directly to a sector curve to obtain information about the PD of a single company in that sector. Instead, i is assumed that there are fictitious companies whose CDS spreads are given by the sector curves. Then the market-implied PDs for these companies can be extracted from the CDS sector curves.

Since the sector curves are calculated using the CDS spreads of all companies in the sector, the CDS spread levels of the fictitious companies are realistic. However, the volatilities and other statistical properties of the

[3] https://www.treasury.gov/resource-center/data-chart-center/interest-rates/pages/TextView.aspx?data=yieldAll, accessed on 17 May 2020.

[4] Going forward, a 'sector' in the context of sector curves or CDS spreads refers to a combination of these five factors.

Reference company	Region	Industry	Debt type	Rating	Tenor
Alibaba	Asia ex-Japan	Consumer discretionary	Senior	IG	10 years
American Airlines	America	Consumer discretionary	Senior	HY	10 years
Apple	America	Technology	Senior	IG	10 years
AT&T	America	Communications	Senior	IG	10 years
Barrick Gold	America	Materials	Senior	IG	10 years
Coca Cola	America	Consumer staples	Senior	IG	10 years
Diamond Offshore Drilling	America	Energy	Senior	HY	10 years
Boeing	America	Industrials	Senior	IG	10 years
Exxon Mobil	America	Energy	Senior	IG	10 years
Ford	America	Consumer discretionary	Senior	IG	10 years
JP Morgan senior	America	Financials	Senior	IG	10 years
JP Morgan subordinate	America	Financials	Subordinate	IG	10 years
Volkswagen	Europe	Consumer discretionary	Senior	IG	10 years

Table 4.3: Specification of the sectors for which CDS sector curve data has been obtained from Bloomberg. The sector curves are mostly from 10 year senior CDSs in America, from a variety of industries. Under Rating, IG stands for investment grade and HY for high yield. The ratings are those observed on March 2, 2020, which is the day the data was collected.

time series of CDS spreads are different from those properties for CDS spreads of real companies in the corresponding sectors. Specifically, each of the fictitious companies has less volatile CDS spreads, since these spreads are averages. However, this effect is reduced by the high correlation between CDS spreads of companies in the same sector. Economically, this can be interpreted as a fictitious company being immune to events that would only affect that company, such as a public scandal. The fictitious company is still affected by macroeconomic events that impact the entire sector, e.g. a change in the oil price for the energy sector.

Daily data on CDS sector curves between September 18, 2018 and February 28, 2020 are obtained from Bloomberg. The sectors are specified in Table 4.3; the reference companies are used to refer to their respective sectors going forward. In Figure 4.1a, implied PDs conditional on no earlier default are shown. The first observation that stands out is that the Diamond Offshore Drilling and American Airlines sectors are considered significantly more risky by the market. Additionally, the Diamond Offshore Drilling sector is extremely volatile compared to the other sectors. To give a clearer view of the remaining companies' implied PDs, the same data for all companies except Diamond Offshore Drilling and American Airlines is shown in Figure 4.1b. The safest sectors are those of Alibaba and Boeing. The general movement of all sectors is similar, although the movement is larger for some sectors, such as Exxon Mobil, than for others. Especially the steep rises and falls can be seen across all sectors. From the start of the dataset until January 2019, PDs are increasing, while they are decreasing from January until May 2019. A short but steep rise in PDs is seen between May and June 2019, after which the long-term movement of PDs becomes quite stable, albeit with some spikes and drops in between. In the last six days of the data, peaks in all implied PDs can be seen. This is due to the economic consequences of the outbreak of the corona virus. These last six days are disregarded in the analyses, in order to obtain the best possible view on normal market conditions. The data from during the corona crisis and other downturn periods is analysed in Section 4.5. A numerical description of the dataset can be found in Appendix C.

4.3. Interest rate data

For the interest rate data, 10 year interest rate swap data is used. One of the reasons to consider 10 year swaps is that they are very liquid products, which means their market price accurately reflects the true value of the swaps. Additionally, the 10 year swap rate has always been well above zero, while swap rates for lower maturities are closer to zero. This allows one to make the assumption that the 10 year swap rate continues to remain strictly positive, which simplifies the modelling. Daily data until January 3, 2020 is used, obtained from Bloomberg. The dataset goes back to 2007, but since the focus of this thesis is on the joint behaviour of PDs and swap rates, only the dataset starting on September 18, 2018 is considered, containing 317 observations. The time series of swap rate data is shown in Figure 4.2. The swap rate can be seen to fall for the first two thirds of the duration, before slightly increasing again in the last part of the dataset. To draw more meaningful conclusions from this data, it is compared to the implied PD data in the next section.

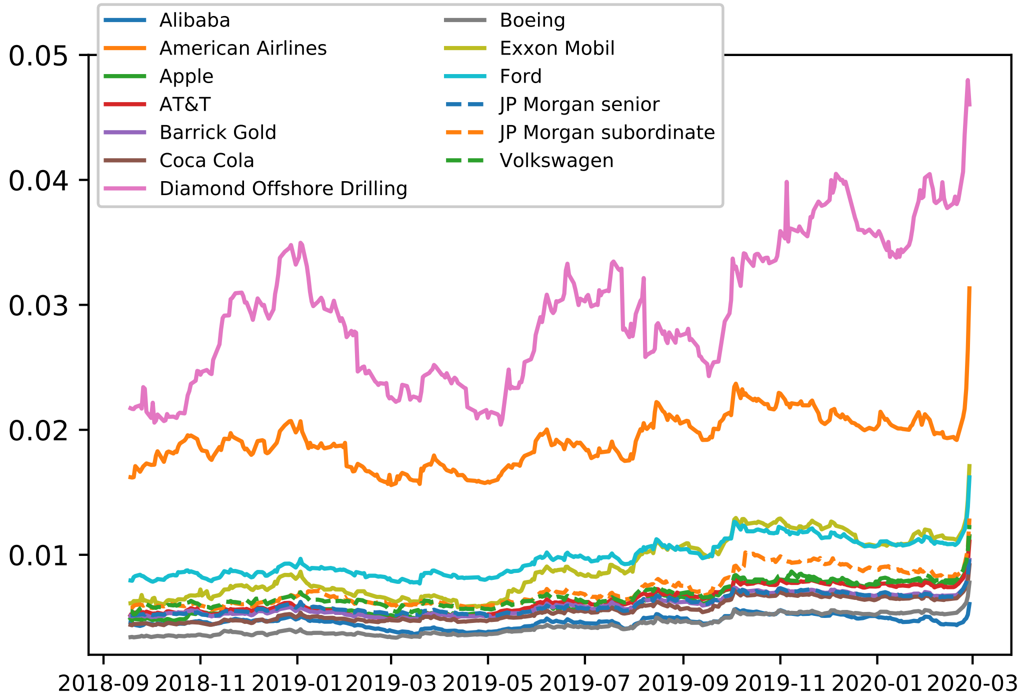

(a) All sectors

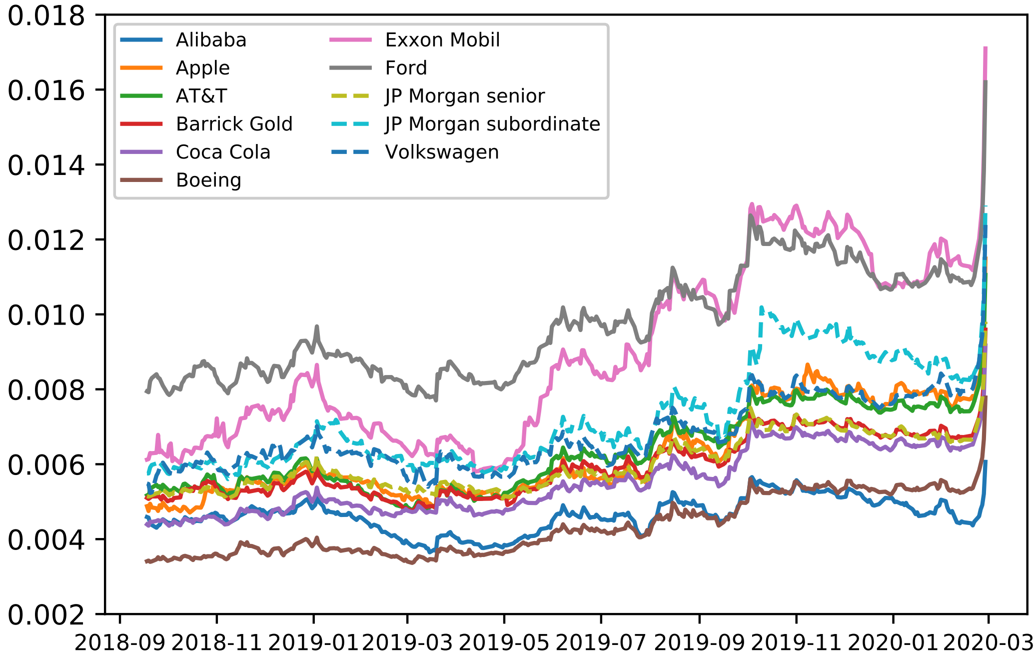

(b) Without the sectors of Diamond Offshore Drilling and American Airlines

Figure 4.1: PDs conditional on no earlier default as implied by CDS sector curves for the listed companies. Senior CDS sector curves are used for all non-financial sectors. The peak during the final 5 days is due to the start of the corona crisis. Two of the main observations are that the sectors of Diamond Offshore Drilling and American Airlines have significantly higher spreads than the other sectors and that the spreads tend to move in the same direction.

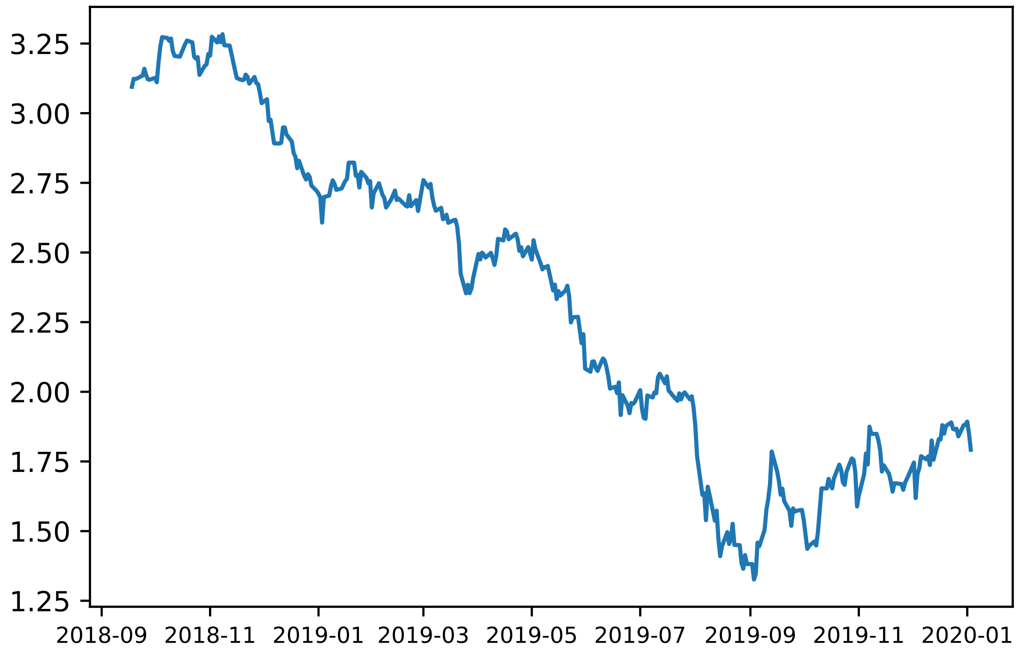

Figure 4.2: The evolution of the 10 year interest rate swap fixed rate in the dataset. A steady decline in interest rates is visible. This decline started in 2014 and caused the current low interest rate environment.

4.4. Dependence analysis

In this section, several methods are applied to the data to quantify and analyse the dependence between the swap rate log-returns and the implied PD log-returns. First, the observations of the time series plots of the swap rate and the implied PDs are mentioned. Then, scatterplots are shown to visualise the dependence, after which rank correlations are shown and tests for the statistical significance of the correlations are performed. Next, tail dependence is explored through joint quantile exceedances, and the presence of correlation in the main body of the data is tested. Finally, tests for exchangeability and radial symmetry are performed. Results useful for the fitting of copulas are reported throughout.

A comparison can be made between the swap rate in Figure 4.2 and the implied PDs in Figure 4.1. The expectation is that implied PDs rise when the swap rate falls, as a negative historical correlation between the two variables has been shown to exist by Ben-Abdallah et al. (2019) and Harris et al. (2015). This joint movement is seen when the swap rate and the implied PDs move heavily, while there does not seem to be much dependence in more stable times. Between September 2018 and November 2018, the interest rate is stable, while PDs increase slightly. However, as the swap rate declines rapidly between November 2018 and January 2019, the implied PDs can be seen to rise. The same phenomenon occurs between May 2019 and June 2019. A short drop of swap rates in April 2019, followed by a quick rise, corresponds to a rise and then a drop of PDs. A similar situation can be seen in September 2019. Furthermore, the rapid decline of the swap rate in August 2019 is mirrored by an upward jump in implied PDs. In the stable periods, e.g. between November 2019 and January 2020, there does not seem to be any meaningful dependence between the swap rate and the implied PDs.

From this point forward, only the CDS spread data until January 3, 2020 is considered, so that for every day in the dataset there are observations of both the swap rate and the CDS spreads. Log-returns are used for

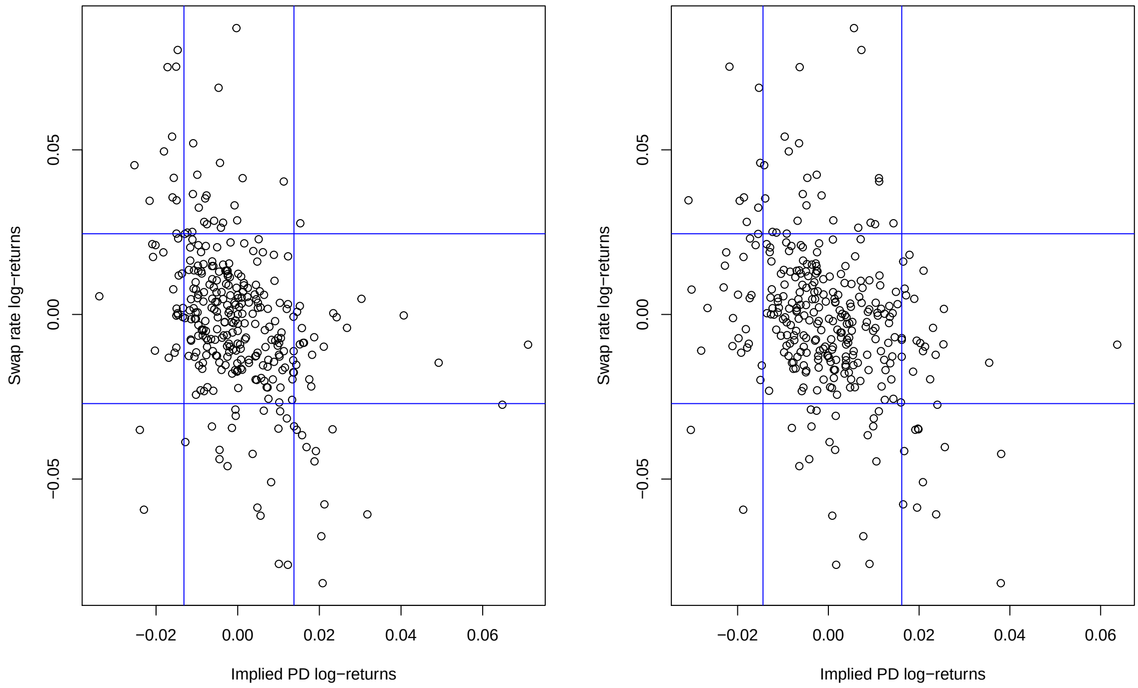

(a) Ford (b) Boeing

Figure 4.3: Scatterplot of the log-returns on implied PDs of Ford and Boeing against the log-returns on 10 year swap rates. 0.1 and 0.9 quantiles of both datasets are shown by the blue lines. The plots show some degree of negative dependence, as well as tail dependence in the top left and bottom right corners through the joint quantile exceedances.

normalisation and time-additivity reasons, as described in Section 3.2. The log-returns on implied PDs and swap rates are given by

$$\log\left(\frac{\lambda_{t_{i+1}}}{\lambda_{t_i}}\right) \quad \text{and} \quad \log\left(\frac{\mathrm{sr}_{t_{i+1}}}{\mathrm{sr}_{t_i}}\right) \tag{4.7}$$

respectively, where λ_{t_i} is the implied PD on day $i \in \mathbb{N}$ and sr_{t_i} is the swap rate on day i. The size of the dataset on log-returns is 316 observations.

The dependence structure observed in the time series plots is also visible in scatterplots of the log-returns on the implied PDs and the log-returns on the swap rates. The scatterplots for Ford and Boeing are shown in Figure 4.3, more scatterplots are shown in Figure C.1 in the appendix. These scatterplots also show that the dependence is mostly present in the tails, since the outlying points are mostly to the top left and bottom right of the main cluster in both scatterplots. The main body of the datapoints shows little dependence; the main clusters only slightly exhibit the ellipse shape that is typical for correlated random variables. The shapes of these clusters are closer to circles, which indicate independence.

A numerical description of dependence between the swap rate log-returns and the implied PD log-returns for different sectors is given by Kendall's τ correlation $\rho_\tau \in [-1,1]$ and Spearman's ρ correlation $\rho_S \in [-1,1]$. For random variables X_1 and X_2, Kendall's τ is defined as

$$\rho_\tau(X_1, X_2) = \mathbb{E}[\mathrm{sign}((X_1 - \tilde{X}_1)(X_2 - \tilde{X}_2))], \tag{4.8}$$

where $(\tilde{X}_1, \tilde{X}_2)$ is an independent copy of (X_1, X_2). It can be estimated by Kendall's rank correlation coefficient of a sample $(X_{1,1}, X_{1,2}), \ldots, (X_{n,1}, X_{n,2})$, given by

$$\binom{n}{2}^{-1} \sum_{1 \leqslant t < s \leqslant n} \mathrm{sign}((X_{t,1} - X_{s,1})(X_{t,2} - X_{s,2})). \tag{4.9}$$

Sector	Kendall's τ Sample value	p-value	Std. dev.	Spearman's ρ Sample value	p-value	Std. dev.
Alibaba	-0.15	0.0001	0.038	-0.21	0.0002	0.056
American Airlines	-0.23	0.0000	0.038	-0.34	0.0000	0.056
Apple	-0.12	0.0010	0.038	-0.18	0.0010	0.056
AT&T	-0.18	0.0000	0.038	-0.26	0.0000	0.056
Barrick Gold	-0.28	0.0000	0.038	-0.41	0.0000	0.056
Coca Cola	-0.23	0.0000	0.038	-0.34	0.0000	0.056
Diamond Offshore Drilling	-0.09	0.0172	0.038	-0.13	0.0198	0.056
Boeing	-0.23	0.0000	0.038	-0.33	0.0000	0.056
Exxon Mobil	-0.19	0.0000	0.038	-0.28	0.0000	0.056
Ford	-0.30	0.0000	0.038	-0.43	0.0000	0.056
JP Morgan senior	-0.30	0.0000	0.038	-0.43	0.0000	0.056
JP Morgan subordinate	-0.00	0.9088	0.038	-0.01	0.9226	0.056
Volkswagen	-0.24	0.0000	0.038	-0.36	0.0000	0.056

Table 4.4: Sample values of Kendall's τ correlation and Spearman's ρ correlation between implied PDs and swap rates, along with upper tail p-values of the hypothesis test between the null hypothesis of independence (zero correlation) and the alternative hypothesis of non-zero correlation. Finally, standard deviations of the sampling distribution under the null hypothesis are shown. Most companies show statistically significant negative correlation, implying negative dependence.

Spearman's ρ is defined as

$$\rho_S(X_1, X_2) = \rho(F_1(X_1), F_2(X_2)), \tag{4.10}$$

where F_1 and F_2 are the marginals of X_1 and X_2 respectively, and ρ denotes Pearson's linear correlation. Spearman's ρ can be estimated by Spearman's rank correlation coefficient of a sample $(X_{1,1}, X_{1,2}), \ldots, (X_{n,1}, X_{n,2})$:

$$\frac{12}{n(n^2-1)} \sum_{i=1}^{n} \left(\text{rank}(X_{i,1}) - \frac{1}{2}(n+1)\right)\left(\text{rank}(X_{i,2}) - \frac{1}{2}(n+1)\right), \tag{4.11}$$

where rank$(X_{i,j})$ denotes the position of $X_{i,j}$ in the ordered sample of the random variable X_j. Both estimators are measures of rank correlation, which makes them distribution-free. This is an attractive property, since the (joint and marginal) distributions of the PD log-returns and the swap rate log-returns are not yet known. This makes them preferable over Pearson's correlation, which is less meaningful for distributions other than a multivariate normal distribution. In addition, both rank correlations depend only on the copula of a bivariate distribution, while linear correlation depends on both the copula and the marginals (McNeil et al.; 2005). Of the two rank correlations, Kendall's τ is preferred here because of its smaller standard deviation. It is more time-consuming to compute for large samples, because in both sets of observations, every single pair of observations must be considered; for this dataset however, computations are still fast. An additional benefit of Kendall's τ is that confidence intervals for it are more reliable than those for Spearman's ρ (Newson; 2002).

Sample values of both rank correlation coefficients are shown in Table 4.4. Both Kendall's τ and Spearman's ρ indicate statistically significant dependence[5] between the swap rate log-returns and the implied PD log-returns for almost all sectors, since the p-values do not exceed 0.001. The only exceptions are Diamond Offshore Drilling, for which there may or may not be statistically significant dependence, depending on the level of significance chosen, and JP Morgan subordinate, for which the null hypothesis cannot be rejected. All correlation values are below zero, indicating negative dependence between the implied PD log-returns and the swap rate log-returns. Note that the standard deviations for both correlation measures are constant over the different sector curves; both standard deviations depend only on the size of the dataset.

In the scatterplots in Figure 4.3, there seems to be dependence in the tails. Tail dependence between two datasets can be measured by the amount of joint quantile exceedances. Since the implied PDs exhibit negative dependence with the swap rates, an analysis is performed on joint exceedances of the lower quantile of

[5] For most levels of significance. 'Statistically significant dependence' here means that the null hypothesis of no correlation can be rejected; non-zero correlation implies dependence between two random variables.

the implied PDs and the upper quantile of the swap rates (which are called *type 1 exceedances* going forward), as well as exceedances of the upper quantile of the implied PDs and the lower quantile of the swap rates (*type 2 exceedances*). The 0.1 and 0.9 quantiles are used in order to obtain a sizeable number of observations exceeding the quantiles, which allows more meaningful conclusions to be drawn, while still making sure the tail behaviour is isolated. The amount of joint tail exceedances for both types is shown in Table 4.5. A hypothesis test is performed for tail dependence of both types in the data. The test for type 1 tail dependence uses the null hypothesis of independence between the implied PD exceeding its lower quantile and the swap rate exceeding its upper quantile, and an alternative hypothesis of no independence:

$$\begin{aligned} H_0: &\quad \log\left(\frac{\lambda_{t_i}}{\lambda_{t_{i-1}}}\right) \le Q_\lambda(0.1) \quad \perp\!\!\!\perp \quad \log\left(\frac{\mathrm{sr}_{t_i}}{\mathrm{sr}_{t_{i-1}}}\right) \ge Q_{\mathrm{sr}}(0.9), \\ H_1: &\quad \log\left(\frac{\lambda_{t_i}}{\lambda_{t_{i-1}}}\right) \le Q_\lambda(0.1) \quad \not\perp\!\!\!\perp \quad \log\left(\frac{\mathrm{sr}_{t_i}}{\mathrm{sr}_{t_{i-1}}}\right) \ge Q_{\mathrm{sr}}(0.9), \end{aligned} \tag{4.12}$$

where $Q_\lambda : [0,1] \to \mathbb{R}$ and $Q_{\mathrm{sr}} : [0,1] \to \mathbb{R}$ are the quantile functions of the log-returns of the implied PD λ and the swap rate sr respectively. The test for dependence of type 2 is similar:

$$\begin{aligned} H_0: &\quad \log\left(\frac{\lambda_{t_i}}{\lambda_{t_{i-1}}}\right) \ge Q_\lambda(0.9) \quad \perp\!\!\!\perp \quad \log\left(\frac{\mathrm{sr}_{t_i}}{\mathrm{sr}_{t_{i-1}}}\right) \le Q_{\mathrm{sr}}(0.1), \\ H_1: &\quad \log\left(\frac{\lambda_{t_i}}{\lambda_{t_{i-1}}}\right) \ge Q_\lambda(0.9) \quad \not\perp\!\!\!\perp \quad \log\left(\frac{\mathrm{sr}_{t_i}}{\mathrm{sr}_{t_{i-1}}}\right) \le Q_{\mathrm{sr}}(0.1). \end{aligned} \tag{4.13}$$

The test statistic S_j for dependence of type j is the number of joint quantile exceedances, given by

$$S_j = \begin{cases} \#\left\{i : \log\left(\frac{\lambda_{t_i}}{\lambda_{t_{i-1}}}\right) \le Q_\lambda(0.1),\ \log\left(\frac{\mathrm{sr}_{t_i}}{\mathrm{sr}_{t_{i-1}}}\right) \ge Q_{\mathrm{sr}}(0.9)\right\}, & \text{for } j = 1, \\ \#\left\{i : \log\left(\frac{\lambda_{t_i}}{\lambda_{t_{i-1}}}\right) \ge Q_\lambda(0.9),\ \log\left(\frac{\mathrm{sr}_{t_i}}{\mathrm{sr}_{t_{i-1}}}\right) \le Q_{\mathrm{sr}}(0.1)\right\}, & \text{for } j = 2. \end{cases} \tag{4.14}$$

Under the null hypothesis, S_j, $j = 1,2$ is binomially distributed with size variable $n = 316$ equal to the number of observations and success chance $p = 0.01$, the product of the individual events of the variables exceeding their 0.1 or 0.9 quantile. For a significance level of $\alpha = 0.02$, the critical value c is obtained as

$$c = \min\{c : P(S_j \ge c | H_0) \le 0.02\} = Q_{\mathrm{binom}}(0.98) + 1 = 8, \quad j = 1,2, \tag{4.15}$$

where $Q_{\mathrm{binom}} : [0,1] \to \mathbb{N}$ is the quantile function of the binomial distribution with $n = 316$ and $p = 0.01$. Whenever the sample value of S_j is greater than or equal to c, H_0 can be rejected. A lower critical value is given by

$$c^* := \max\{c^* : P(S_j \le c^* | H_0) \le 0.02\} = Q_{\mathrm{binom}}(0.02) = 0, \quad j = 1,2. \tag{4.16}$$

This means that H_0 is also rejected whenever $S_j = 0$; this corresponds to statistically significant negative dependence between the two events in (4.12) for type 1 and in (4.13) for type 2. This does not occur in the dataset, however. The distribution of S_j is used to obtain upper tail p-values and the standard deviation of the test statistic under the null hypothesis, which is the same for both tails. Under the null hypothesis, $\mathbb{E}[S_j] = 3.16$, $j = 1,2$. The sample values of S_1 and S_2 are shown for each sector in Table 4.5, along with the p-values and the standard deviation.

One observes that for each sector, most joint exceedances are of type 2 rather than type 1. This is also reflected in the p-values, which are lower for type 2 than for type 1. The p-values for type 2 exceedances indicate that the tail dependence in this tail is statistically significant for most sectors. Instead, the tail dependence corresponding to type 1 cannot be claimed to be statistically significant, except for Boeing and Ford. Note that since the test is quantile-based, the results also apply to the pseudo-observations obtained from the data. Therefore conclusions for the copula fitting can be drawn from this test. The results in Table 4.5 imply that the copula with the best fit should have tail dependence in the tail of type 2; while independence in the type 1 tail cannot be rejected, it is not confirmed either.

The tail dependence is visualised in the scatterplots in Figure 4.3; the observations jointly exceeding the quantiles are those in the top left (type 1) and bottom right (type 2) areas. Note that there are virtually no observations in the top right and bottom left areas, i.e. observations jointly exceeding both upper quantiles or both lower quantiles. This is also indicative of negative tail dependence.

	Lower quantile PDs, upper quantile swap rate (type 1)			Upper quantile PDs, lower quantile swap rate (type 2)			
Sector	S_1	p-value	Test result	S_2	p-value	Test result	Std. dev.
Alibaba	3	0.6129	H_0 not rejected	10	0.0015	H_0 rejected	1.7687
American Airlines	3	0.6129	H_0 not rejected	9	0.0050	H_0 rejected	1.7687
Apple	6	0.0999	H_0 not rejected	8	0.0152	H_0 rejected	1.7687
AT&T	7	0.0414	H_0 not rejected	10	0.0015	H_0 rejected	1.7687
Barrick Gold	5	0.2116	H_0 not rejected	9	0.0050	H_0 rejected	1.7687
Coca Cola	6	0.0999	H_0 not rejected	8	0.0152	H_0 rejected	1.7687
Diamond Offshore Drilling	4	0.3887	H_0 not rejected	4	0.3887	H_0 not rejected	1.7687
Boeing	8	0.0152	H_0 rejected	12	0.0001	H_0 rejected	1.7687
Exxon Mobil	4	0.3887	H_0 not rejected	7	0.0414	H_0 not rejected	1.7687
Ford	11	0.0004	H_0 rejected	12	0.0001	H_0 rejected	1.7687
JP Morgan senior	6	0.0999	H_0 not rejected	11	0.0004	H_0 rejected	1.7687
JP Morgan subordinate	6	0.0999	H_0 not rejected	7	0.0414	H_0 not rejected	1.7687
Volkswagen	4	0.3887	H_0 not rejected	10	0.0015	H_0 rejected	1.7687

Table 4.5: Joint quantile exceedance ratios of the log-returns on the swap rate and the log-returns on the implied PDs for different sectors. Lower and upper quantile indicate the 0.1 and 0.9 quantile respectively. A joint quantile exceedance means the implied PD return is below (above) the lower (upper) quantile on the same day the swap rate return is above (below) the upper (lower) quantile. A null hypothesis of independence in the tails is tested, for which the p-values are shown. The significance level is $\alpha = 0.02$. The standard deviation of the joint quantile exceedance ratios under the null hypothesis is the same for both tails. For most companies, independence in the tail can be rejected only for type 2 tail dependence.

After looking at tail dependence, a logical next step is to look at dependence in the main body of the dataset, i.e. the dataset that remains if the tails are removed. To construct the main body, one starts with the thirteen pairs of datasets of one of the sectors' PD log-returns data and the swap rate log-returns data. From each of these pairs, all observations are excluded for which either the swap rate log-return or the PD log-return (or both) are below the respective 0.1 quantile or above the 0.9 quantile. The resulting set of observations is referred to as the *main body* of the dataset of swap rate log-returns and PD log-returns of that particular sector. The sample rank correlation of the main body for each sector is shown in Table 4.6. The p-values of both correlation values are much higher than those for the entire dataset (see Table 4.4), meaning the correlation is statistically much less significant, and in many cases (for many levels of significance) the null hypothesis of no correlation cannot be rejected. And even where the correlation is statistically significant, it is in every case absolutely lower than the correlation when considering the full dataset. This confirms that most of the dependence in the dataset is accounted for by the tail dependence.

Two final properties of the data that may help in choosing which copula to fit are exchangeability and radial symmetry. Hypothesis tests are performed for the presence of these properties in the dataset of pseudo-observations, as these represent the dataset without any influence from the marginals, which is the dataset to which the copula is fitted. For both tests, the null hypothesis is the presence of the property (exchangeability or radial symmetry), while the alternative hypothesis is the absence of the property. In mathematical terms, the null and alternative hypotheses are given by

$$\begin{aligned} H_0: &\quad \forall (u_1,u_2)\in[0,1]^2: \quad C(u_1,u_2)=C(u_2,u_1), \\ H_1: &\quad \exists (u_1,u_2)\in[0,1]^2: \quad C(u_1,u_2)\neq C(u_2,u_1), \end{aligned} \tag{4.17}$$

for the test for exchangeability, where C is the copula underlying the data, and by

$$\begin{aligned} H_0: &\quad \forall (u_1,u_2)\in[0,1]^2: \quad C(u_1,u_2)=\hat{C}(u_1,u_2), \\ H_1: &\quad \exists (u_1,u_2)\in[0,1]^2: \quad C(u_1,u_2)\neq \hat{C}(u_1,u_2), \end{aligned} \tag{4.18}$$

for the test for radial symmetry, where $\hat{C}$ denotes the survival copula of C.[6]

[6]The tests provided by the 'copula' package in R are used; in the package documentation (https://cran.r-project.org/web/packages/copula/copula.pdf), it is mentioned that the test statistics calculated are based on those by Genest et al. (2011) for exchangeability, and those by Genest and Nešlehová (2014) for radial symmetry. However, manually calculating the test statistics described in these papers yields different results than those in Table 4.7. It follows that unspecified adjustments are made by the 'copula' package when calculating the test statistics, therefore the expressions for the test statistics cannot be provided.

Sector	#obs.	Kendall's τ Sample value	p-value	Std. dev.	Spearman's ρ Sample value	p-value	Std. dev.
Alibaba	206	-0.0826	0.0779	0.0468	-0.1190	0.0885	0.0697
American Airlines	200	-0.0837	0.0785	0.0476	-0.1259	0.0756	0.0707
Apple	207	-0.0413	0.3771	0.0467	-0.0684	0.3269	0.0695
AT&T	209	-0.0747	0.1083	0.0465	-0.1122	0.1057	0.0692
Barrick Gold	204	-0.1627	0.0006	0.0471	-0.2433	0.0005	0.0700
Coca Cola	205	-0.1363	0.0037	0.0470	-0.1999	0.0041	0.0698
Diamond Offshore Drilling	204	-0.0392	0.4054	0.0471	-0.0575	0.4137	0.0700
Boeing	210	-0.1741	0.0002	0.0464	-0.2604	0.0001	0.0690
Exxon	203	-0.0663	0.1605	0.0472	-0.1040	0.1398	0.0702
Ford	214	-0.1886	0.0000	0.0459	-0.2728	0.0001	0.0684
JP Morgan senior	207	-0.1635	0.0005	0.0467	-0.2423	0.0005	0.0695
JP Morgan subordinate	208	-0.0245	0.5995	0.0466	-0.0344	0.6217	0.0693
Volkswagen	206	-0.1256	0.0074	0.0468	-0.1849	0.0079	0.0697

Table 4.6: Sample correlation values for the observations in the main body of the dataset. The main body for each sector consists only of those observations where neither the swap rate log-returns nor the implied PD log-returns are below the 0.1 quantile or above the 0.9 quantile. #obs. indicates the number of observations in the main body. Upper tail p-values are shown for the hypothesis test with the null hypothesis of independence (zero correlation) in the main body. Standard deviations of the sampling distribution under the null hypothesis are shown. The correlation is weaker than in the full dataset, indicating that the correlation in the full dataset is mostly caused by tail dependence.

The test statistics for exchangeability (Genest et al.; 2011) and radial symmetry (Genest and Nešlehová; 2014) do not have known distributions, since these depend on the underlying copulas, which are not yet known. Therefore, the standard deviations of the test statistics are not reported. However, p-values can be computed using bootstrap replicates of the test statistics. The results are shown in Table 4.7. The p-values indicate that the pseudo-observations of almost all sectors' implied PD log-returns combined with the swap rate log-return data are exchangeable and radially symmetric. The only exceptions are American Airlines for exchangeability and Apple for radial symmetry, with p-values of 0.048 and 0.040 respectively. Depending on the significance level one chooses for the tests, these p-values may be low enough to reject the null hypotheses (such as the common significance level $\alpha = 0.05$). Besides these two exceptions, the similarity in the results for all sectors is according to expectations, because the datasets for log-returns of implied PDs have a very similar structure (see Figure 4.1).

On first sight, these results may seem to contradict tail dependence in only one tail, which is observed for several sectors in Table 4.5. However, one must keep in mind that a failure to reject the null hypothesis generally does not allow one to accept the null hypothesis. The results of the test for radial symmetry only tell us that radial symmetry cannot be disproved; the alternative hypothesis might still be true, even though there is insufficient evidence to reject the null hypothesis based on this data. For e.g. the Alibaba sector, the p-value is equal to 0.962, which means that if H_0 were true, then

$$P(T_n \geq \hat{T}_n) = 0.962, \tag{4.19}$$

where T_n is the test statistic and $\hat{T}_n$ is its sample value. However, this does not give any information about the value of $P(T_n \geq \hat{T}_n)$ in the case where H_0 does not hold. The results for the tests for tail dependence should be interpreted similarly. For many sectors, the results could reject H_0 (independence in the tail) for type 2 tails, but not for type 1 tails. If H_0 were false for type 1 tails as well, radial symmetry would not imply a contradiction. In conclusion: for the sectors where independence in the type 2 tail was rejected based on the test, but independence in the type 1 tail and radial symmetry were not, one or both of the latter two properties must not hold, since a contradiction would arise otherwise. This is visualised in Figure 4.4.

4.5. Downturn analysis

In Section 4.4 it became clear that the dependence between PDs and swap rates is mostly present in the tails (i.e. there is significant tail dependence while the correlation in the main body is weaker); especially in the

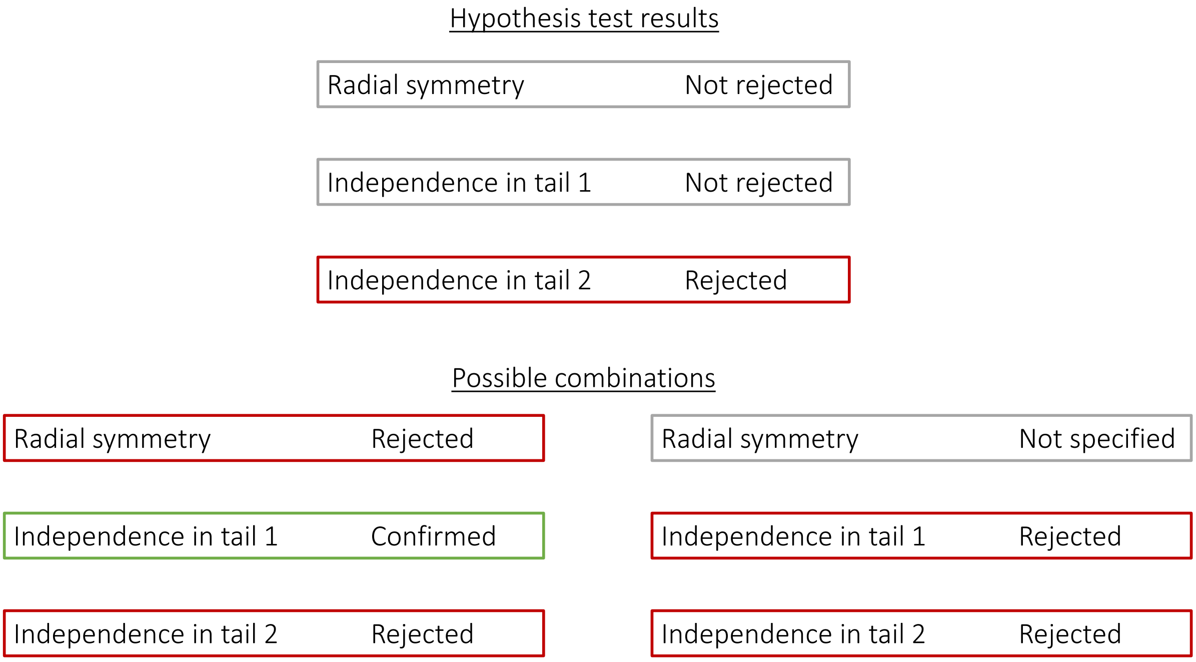

Figure 4.4: Visualisation of the results of the hypothesis tests for radial symmetry and independence in the tails. These results were found for most companies. 'Tail 1' and 'Tail 2' indicate the tails of types 1 and 2. If the data is independent in tail 1, the data cannot be radially symmetric. Otherwise, the data may or may not be radially symmetric.

	Exchangeability		Radial symmetry	
Sector	Test statistic	p-value	Test statistic	p-value
Alibaba	0.032	0.513	0.020	0.962
American Airlines	0.087	0.041	0.027	0.765
Apple	0.049	0.207	0.085	0.049
AT&T	0.019	0.911	0.043	0.372
Barrick Gold	0.021	0.789	0.030	0.653
Coca Cola	0.024	0.751	0.035	0.533
Diamond Offshore Drilling	0.018	0.941	0.023	0.929
Boeing	0.027	0.686	0.023	0.891
Exxon Mobil	0.022	0.790	0.031	0.634
Ford	0.015	0.968	0.032	0.607
JP Morgan senior	0.026	0.661	0.040	0.402
JP Morgan subordinate	0.017	0.944	0.033	0.660
Volkswagen	0.019	0.888	0.025	0.811

Table 4.7: Test statistics for tests of the null hypotheses of exchangeability and radial symmetry in the dataset of pseudo-observations, against the alternative hypotheses of the absence of these properties. The p-values are calculated from bootstrap replicates of the test statistics. The results indicate that the null hypotheses of exchangeability and radial symmetry cannot be rejected.

tail of high PD log-returns and low swap rate log-returns. This corresponds to rising PDs and declining interest rates. This section analyses and quantifies the dependence during times of economic stress. One would expect that the dependence observed in the previous section is even more present in these periods, when defaults are generally more common.

This section starts by detailing the choice of which data is used and why in Section 4.5.1. Then an analysis of the dependence in the data is given in Section 4.5.2. Quantitative results are given for the dependence in the full dataset, as well as tail dependence and dependence in the main body, along with results of hypothesis tests to determine whether the dependence is statistically significant. The results are analysed and compared to the results in Section 4.4, obtained using data from regular market conditions.

4.5.1. Choice of data

Several choices must be made on which data is used. The period to be observed, the companies on which the CDSs are written, the CDS tenor, the interest rate swap maturity and the floating rate are all among variables to be set before the collection of data can take place. These choices and the reasoning behind them are explained in this section.

The data to be analysed is obtained from multiple downturn periods. The first is from August 28, 2008 until June 4, 2009, a period which is part of the credit crisis of 2008, one of the most impactful periods of economic stress in recent history. The downturn period from April 2, 2010 until December 17, 2010, during the economic crisis following the credit crisis, is considered as well. Finally, data from during the crisis caused by the outbreak of the coronavirus in 2020 is used, during the period from February 20, 2020 until April 15, 2020. The consequences of the outbreak are still ongoing at the time of writing and therefore only data from the first part of the crisis is available. These periods are visualised for the swap rate in Figure 4.5.

The periods would ideally be as long as possible to maximise the size of the dataset. However, since this section concerns an analysis of markets under economic stress, the influence of data from stable periods on the results is undesirable. Therefore the dates are chosen such that the entire downturn periods are contained, but no data from outside the downturn periods is used.

There are two main advantages to considering multiple downturn periods. First of all, more data is available this way, which reduces the impact of outliers on the results. This means there is less variance in the results and more meaningful conclusions can be drawn. Secondly, by using data from multiple periods, the effect of the characteristics of a single downturn period is reduced. There are many possible causes for periods of economic stress, and the impact on financial markets may be different for different downturn periods as a result of this. For example, the 2008 credit crisis and the 2020 corona crisis have vastly different causes and the PDs, the interest rates and the dependence between them may react differently to these causes. Futhermore, some sectors are hit harder than others depending on the nature of the crisis, which is reflected in the PDs. Observing multiple downturn periods generalises the conclusions to apply better to other periods of economic stress. It should be noted that the inherent differences between economic crises also mean that the behaviour of financial markets will always vary (at least slightly) from the results obtained in this chapter. All models are approximations of reality, but the approximation is less accurate for periods that are as inherently volatile as economic crises.

The data used in this section is obtained through Datastream. The swap data concerns 10 year United States dollar interest rate swaps with the 3 month LIBOR as the floating rate. Data on 10 year CDS spreads is obtained for 7 large US-based, but globally operating corporates, among which are three banks, one airline, one manufacturer, one telecom and IT provider and one retailer. Senior CDS spreads are obtained for JP Morgan, Goldman Sachs, Citigroup, Southwest airlines, Ford, AT&T and Walmart, while for JP Morgan and Goldman Sachs, data on subordinate CDS spreads is obtained as well. These companies are among the biggest in their respective sectors and their stocks are all included in the S&P500 index. They are chosen because they are representative for their respective industries.

The liquidity of a CDS is an important aspect of the product. If a CDS is not traded for an entire day, the reported CDS spread in the dataset is the same for two consecutive days, corresponding to a log-return of zero. In a statistical analysis, many occurrences of zero implies a low volatility in the dataset. In reality however,

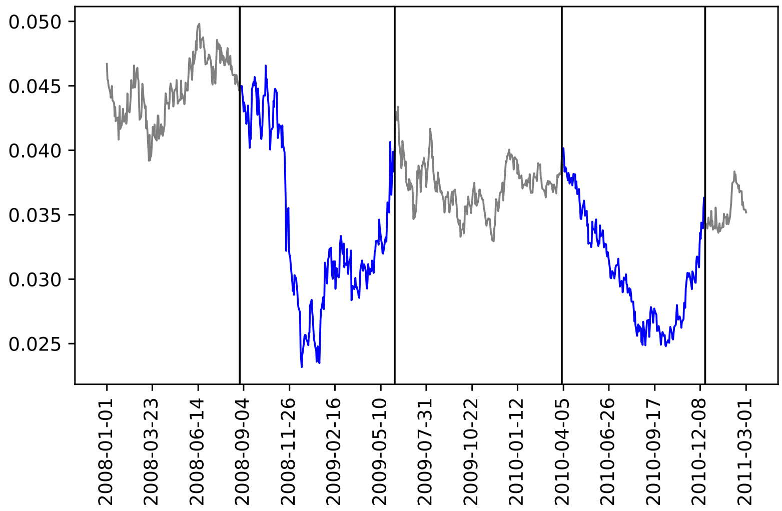

(a) Credit crisis (from August 28, 2008 until June 4, 2009) and 2010 downturn (from April 2, 2010 until December 17, 2010)

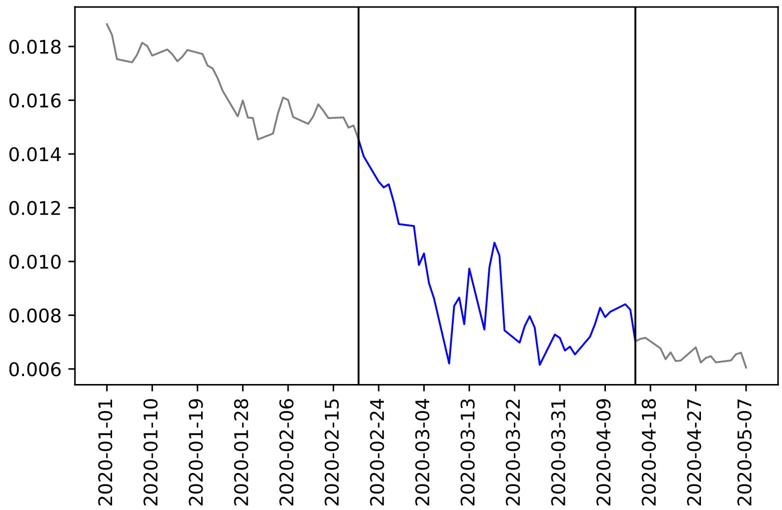

(b) Corona crisis (from February 20, 2020 until April 15, 2020)

Figure 4.5: Daily values of the 10 year swap rate during the downturn periods in blue. The vertical black lines represent the start and end dates of the downturn periods.

	One day		Two days		One week	
Company	Amount	Ratio	Amount	Ratio	Amount	Ratio
JP Morgan senior	72	0.17	13	0.06	0	0.00
JP Morgan subordinate	68	0.16	14	0.07	0	0.00
Southwest airlines	77	0.18	14	0.07	1	0.01
Ford	39	0.09	7	0.03	1	0.01
AT&T	86	0.20	23	0.11	4	0.05
Walmart	90	0.21	18	0.09	3	0.04
Goldman Sachs senior	51	0.12	7	0.03	0	0.00
Goldman Sachs subordinate	63	0.15	12	0.06	0	0.00
Citigroup	50	0.12	6	0.03	0	0.00
Total observations	424		211		82	

Table 4.8: Occurrences of log-returns equal to zero in the CDS spreads for different companies and different periods over which log-returns are calculated. Both flat amounts and ratios with respect to the total number of observations of log-returns are shown. The log-returns over one day are illiquid, but the dataset of log-returns over one week is small; the log-returns over two days provide a good middle ground.

illiquid products may also be highly volatile, especially during downturn periods. Therefore, the occurrence of days when the CDS is not traded at all distorts the results. Hence, data from liquid CDSs is preferable.

For several companies, the obtained CDS spread data contains log-returns equal to zero, implying illiquidity. This is quantified in Table 4.8. The ratio of zero log-returns is lower for longer periods over which returns are calculated, since a log-return over two days (one week) is zero only if a CDS is not traded for two (five) consecutive days. However, taking log-returns over a longer period also reduces the sample size, so a trade-off has to be made. Unfortunately, there is no quantitative method for making this trade-off, since the impact of illiquidity on the results cannot be assessed without knowing the intrinsic values that would be observed in the case of perfect liquidity. The impact of the sample size on the variance of many of the results can be quantified, but it cannot be quantitatively compared to the effect of illiquidity. Therefore, the choice of over which period to take returns has to be made based on a qualitative assessment of the information in Table 4.8.

The daily log-returns have too many occurrences of zero log-returns; the ratio of zero log-returns against total log-returns is above 0.10 for all companies except one. On the other hand, while there are virtually no weekly log-returns equal to zero, there are only 82 observations of weekly log-returns in total. This is too few to obtain meaningful results, especially for a volatile dataset. The dataset of log-returns over two days has few zero log-returns, while the size of the dataset is large enough to perform a good analysis. This is the dataset that is used for the downturn analysis.

For the discount rate, the yield on 6 month US treasury bonds is used in this section. This is the same as in the earlier parts of this chapter. After removing days without data on this yield from the dataset, the remaining dataset consists of 204 observations.

4.5.2. Dependence analysis

In this section, an analysis is performed similar to the analysis in Section 4.4 of the data from periods of regular market conditions. The differences and similarities between the results for downturn and non-downturn data are explored.

A first impression is obtained from visualisation of the data through scatterplots of the log-returns on the implied PDs of a certain company against the log-returns on the swap rates. Scatterplots for Ford and AT&T are shown in Figure 4.6, more scatterplots are shown in Figure C.2 in Appendix C. In the main body, the log-returns of the implied PDs seem to be mostly independent from the log-returns of the swap rates. This was also observed under regular market conditions in Figure 4.3. However, the negative tail dependence that was seen for regular market conditions appears to be weaker during the downturn periods.

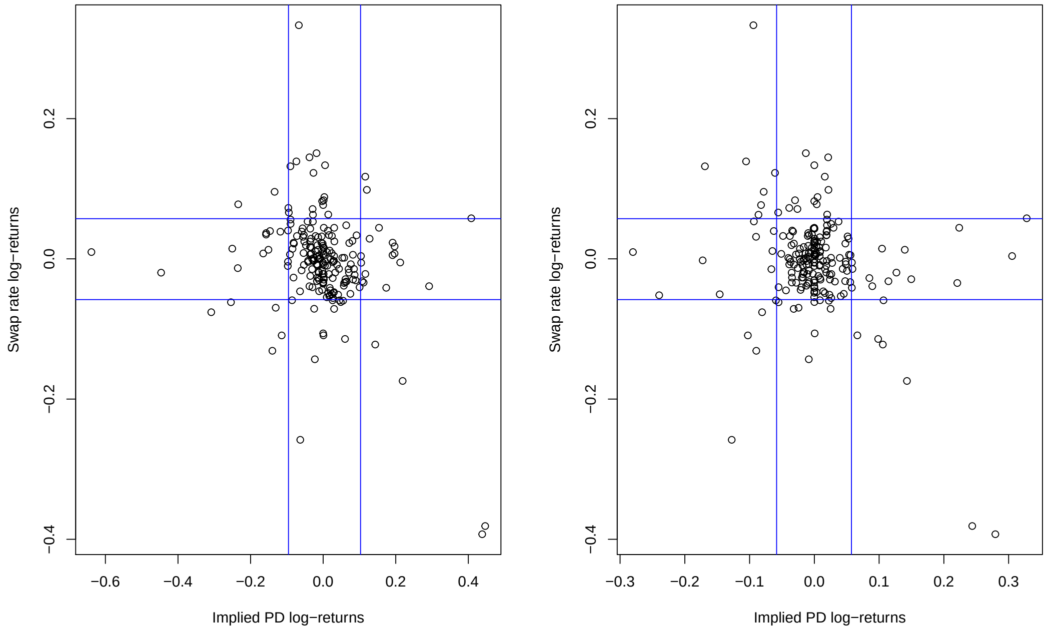

(a) Ford (b) AT&T

Figure 4.6: Scatterplot of the log-returns on implied PDs of Ford and AT&T against the log-returns on 10 year swap rates during the downturn periods. 0.1 and 0.9 quantiles of both datasets are shown by the blue lines. The plots show weaker dependence than those for the non-downturn data.

The dependence is again quantified using rank correlation coefficients. The sample values of Kendall's τ correlation and Spearman's ρ correlation are shown in Table 4.9; they are in the same range as those for the dataset during regular market conditions. On the basis of the p-values reported in the table, the null hypothesis of zero correlation can be rejected for virtually any confidence level for each company, with the exception of AT&T and Walmart. The standard deviations of both rank correlations is slightly higher than for the dataset of regular market conditions, since the size of the downturn dataset is smaller.

To analyse the tail dependence, the joint quantile exceedances are again considered. The observed amounts of joint quantile exceedances of the 0.1 quantile of implied PD log-returns and the 0.9 quantile of swap rate log-returns (type 1), as well as the number of joint exceedances of the 0.9 quantile of implied PD log-returns and the 0.1 quantile of swap rate log-returns (type 2) are shown in Table 4.10. Recall that a joint quantile exceedance is a day where both the log-return of the implied PD and the log-return of the swap rate exceed their corresponding quantiles. The test for tail dependence as detailed in Section 4.4 is performed and the results are shown in the table.

The null hypothesis of independence in the tail and the alternative hypothesis of no independence are as defined in (4.12) and (4.13) for type 1 and type 2 tail dependence respectively. The upper critical value for both types is

$$c = \min\{c : P(S_j \geq c | H_0) \leq 0.02\} = Q_{\text{binom}}(0.98) + 1 = 6, \quad j = 1, 2, \tag{4.20}$$

where $Q_{\text{binom}} : [0,1] \to \mathbb{N}$ is the quantile function of the binomial distribution with $n = 204$ and $p = 0.01$. The lower critical value is given by

$$c^* := \max\{c^* : P(S_j \leq c^* | H_0) \leq 0.02\} = Q_{\text{binom}}(0.02) = 0, \quad j = 1, 2. \tag{4.21}$$

The lower critical value is not attained, hence only the upper p-values are shown.

The null hypothesis of independence in the tails can only be rejected for four companies for both types of tail dependence. Therefore it cannot be reliably claimed that there is a tendency for tail dependence to be

Company	Kendall's τ Sample value	p-value	Std. dev.	Spearman's ρ Sample value	p-value	Std. dev.
JP Morgan senior	-0.23	0.0000	0.047	-0.34	0.0000	0.070
JP Morgan subordinate	-0.22	0.0000	0.047	-0.33	0.0000	0.070
Southwest airlines	-0.18	0.0001	0.047	-0.25	0.0003	0.070
Ford	-0.18	0.0001	0.047	-0.26	0.0002	0.070
AT&T	-0.08	0.0813	0.047	-0.12	0.0802	0.070
Walmart	-0.08	0.1095	0.047	-0.11	0.1329	0.070
Goldman Sachs senior	-0.22	0.0000	0.047	-0.32	0.0000	0.070
Goldman Sachs subordinate	-0.20	0.0000	0.047	-0.29	0.0000	0.070
Citigroup	-0.21	0.0000	0.047	-0.32	0.0000	0.070

Table 4.9: Sample values of Kendall's τ correlation and Spearman's ρ correlation between log-returns of implied PDs and log-returns of swap rates during the downturn periods, along with upper tail p-values of the hypothesis test for the null hypothesis of zero correlation. Standard deviations of the sampling distribution under the null hypothesis are shown; these are equal for all companies, since they only depend on the sample size. Significant negative dependence is present, although the correlation is weaker than for the non-downturn dataset.

	Lower quantile PDs, upper quantile swap rate (type 1)			Upper quantile PDs, lower quantile swap rate (type 2)			
Sector	S_1	p-value	Test result	S_2	p-value	Test result	Std. dev.
JP Morgan senior	3	0.3342	H_0 not rejected	5	0.0554	H_0 not rejected	1.4211
JP Morgan subordinate	4	0.1493	H_0 not rejected	7	0.0048	H_0 rejected	1.4211
Southwest airlines	5	0.0554	H_0 not rejected	6	0.0175	H_0 rejected	1.4211
Ford	3	0.3342	H_0 not rejected	4	0.1493	H_0 not rejected	1.4211
AT&T	7	0.0048	H_0 rejected	7	0.0048	H_0 rejected	1.4211
Walmart	3	0.3342	H_0 not rejected	4	0.1493	H_0 not rejected	1.4211
Goldman Sachs senior	6	0.0175	H_0 rejected	4	0.1493	H_0 not rejected	1.4211
Goldman Sachs subordinate	7	0.0048	H_0 rejected	5	0.0554	H_0 not rejected	1.4211
Citigroup	6	0.0175	H_0 rejected	6	0.0175	H_0 rejected	1.4211

Table 4.10: Amounts of joint quantile exceedances of the log-returns on the swap rate and the log-returns on the implied PDs during the downturn periods. 'Lower quantile' and 'upper quantile' indicate the 0.1 and 0.9 quantile respectively. A joint quantile exceedance means the implied PD log-return is below (above) the lower (upper) quantile on the same day the swap rate log-return is above (below) the upper (lower) quantile. A null hypothesis of independence in the tails is tested, for which the upper p-values are shown. The significance level is $\alpha = 0.02$. The standard deviation of the joint quantile exceedance ratios under the null hypothesis is the same for both tails. Tail dependence seems to be weaker than for the non-downturn dataset.

present between the log-returns of PDs and the log-returns of swap rates in times of economic crisis. This is in contrast to the results for regular market conditions, where tail dependence of type 2 is present for most sectors.

This is not surprising, however, since the cases in the tails under regular market conditions are regular cases in the volatile crisis conditions. In that regard, it would make more sense to compare the presence of tail dependence under regular market conditions to the presence of dependence in the entire dataset in economic stress. This dependence is indeed present for most companies as shown by the p-values in Table 4.9 (recall that nonzero correlation implies nonzero dependence). However, the correlation is absolutely lower than the correlation in the non-downturn data, even though it was shown that most of the correlation in the non-downturn data was due to tail dependence. This goes against the expectation that the dependence in the full datasets of downturn data should be in line with the tail dependence in the non-downturn data. This is discussed further in Section 4.7.

When removing the tails from the dataset, the dependence in the main body may be observed. The main body of the dataset is constructed as described in Section 4.4. The rank correlation values are shown in Table 4.11, as well as the standard deviations and the p-values for the test of the null hypothesis of zero correlation against the alternative hypothesis of nonzero correlation.

Company	#obs.	Kendall's τ Sample value	p-value	Std. dev.	Spearman's ρ Sample value	p-value	Std. dev.
JP Morgan senior	131	-0.10	0.1049	0.0590	-0.15	0.0848	0.0874
JP Morgan subordinate	134	-0.04	0.4899	0.0583	-0.07	0.4243	0.0864
Southwest airlines	135	-0.13	0.0309	0.0581	-0.18	0.0319	0.0861
Ford	135	-0.24	0.0000	0.0581	-0.34	0.0000	0.0861
AT&T	140	0.03	0.5852	0.0571	0.04	0.6266	0.0845
Walmart	132	-0.01	0.9138	0.0588	-0.01	0.9516	0.0870
Goldman Sachs senior	132	-0.15	0.0089	0.0588	-0.23	0.0088	0.0870
Goldman Sachs subordinate	134	-0.11	0.0721	0.0583	-0.16	0.0639	0.0864
Citigroup	134	-0.16	0.0048	0.0583	-0.26	0.0024	0.0864

Table 4.11: Sample correlation values for the observations in the main body of the dataset. The main body for each company consists only of those observations where neither the swap rate log-returns nor the implied PD log-returns are below the 0.1 quantile or above the 0.9 quantile. #obs. indicates the number of observations in the main body. Upper tail p-values are shown for the hypothesis test of the null hypothesis of independence (zero correlation) in the main body. Standard deviations of the sampling distribution under the null hypothesis are shown. As for the non-downturn dataset, the correlation in the main body is weaker than in the full dataset, although the difference is smaller here.

Company	Exchangeability Test statistic	p-value	Radial symmetry Test statistic	p-value
JP Morgan senior	0.033	0.542	0.040	0.509
JP Morgan subordinate	0.044	0.267	0.042	0.456
Southwest airlines	0.013	0.999	0.026	0.849
Ford	0.024	0.793	0.030	0.784
AT&T	0.044	0.279	0.054	0.312
Walmart	0.029	0.617	0.032	0.725
Goldman Sachs senior	0.073	0.071	0.059	0.209
Goldman Sachs subordinate	0.056	0.179	0.043	0.457
Citigroup	0.048	0.277	0.050	0.313

Table 4.12: Test statistics for tests of the null hypotheses of exchangeability and radial symmetry in the pseudo-observations during the downturn periods, against the alternative hypotheses of the absence of these properties. The p-values are calculated from bootstrap replicates of the test statistics. The null hypotheses of exchangeability and radial symmetry cannot be rejected.

When comparing the rank correlation in the main body to the rank correlation in the full dataset shown in Table 4.9, the values are closer than they are for the dataset under regular economic conditions. This is as expected, since the dependence in the tails is lower for the downturn data and therefore represents a smaller part of the dependence in the full dataset. Interestingly, the implied PD log-returns of AT&T actually show positive correlation with the swap rate log-returns in the main body. This is not unexpected, since the correlation over the whole dataset is small as well and AT&T is one of the few companies whose PDs have statistically significant negative tail dependence with the swap rates in both tails (see Table 4.10). The economical implication of this is that AT&T is assumed by market participants to be less affected by economic crises. This is understandable, since it is a telecommunications company, and their customers are likely to keep using telephones and the internet during periods of crisis.

Finally, tests for exchangeability (Genest et al.; 2011) and radial symmetry (Genest and Nešlehová; 2014) are performed on the dataset. The results are shown in Table 4.12. The test is between the null hypothesis of exchangeability or radial symmetry being present and the alternative hypothesis of absence of these properties. The results show that the null hypotheses cannot be rejected for any company for any reasonable significance level α (i.e. $0 < \alpha \leq 0.1$). This is the same result as for the dataset under normal market conditions.

4.6. Copula fitting

A choice for which copula to fit can now be made, using the analysis of the dependence in the data performed in the previous sections. The focus is on those copulas that are the most likely to be a good fit for the datasets; ideally, a copula is found which is a good fit for the datasets from both regular economic situations and downturn periods. Since almost all of the datasets exhibit exchangeability and radial symmetry (see Table 4.7 and Table 4.12), a copula that fits the data well likely has these properties. However, tail dependence is also present in the data, and there is only one well-known copula that exhibits both radial symmetry and tail dependence: the t copula. Several other copulas are also fitted, although the expectation is that the t copula performs best.

The other copulas used are the Gaussian and Frank copulas, which are radially symmetric but do not contain tail dependence, and the rotated Clayton, Gumbel, and Joe copulas, which are not radially symmetric but do show tail dependence. Recall that the rotated Clayton copula is defined as the survival copula of the Clayton copula, i.e. the copula of some bivariate random variable $(1-U_1, 1-U_2)$, when the copula of $(U_1, U_2) \in [0,1]^2$ is the Clayton copula. The reason for using the rotated Clayton copula is that the tail dependence of all copulas with one-sided tail dependence is in the same tail; the rotated Clayton, Gumbel and Joe copulas all exhibit tail dependence in the upper tail.

As the rotated Clayton, Gumbel and Joe copulas model only positive dependence, the data is transformed before fitting these copulas. Suppose that $(\hat{u}_{1,1}, \hat{u}_{1,2}), \ldots, (\hat{u}_{n,1}, \hat{u}_{n,2})$ with $n = 316$ is the dataset of pseudo-observations, where the $\hat{u}_{i,1}$ correspond to the PD log-returns and the $\hat{u}_{i,2}$ to the swap rate log-returns for $i = 1, \ldots, n$. The rotated Clayton, Gumbel and Joe copulas are fitted to $(\hat{u}_{1,1}, 1-\hat{u}_{1,2}), \ldots, (\hat{u}_{n,1}, 1-\hat{u}_{n,2})$.[7] This is still a dataset of pseudo-observations eligible for copula fitting, since the marginals are still both uniform on $[0,1]$. Transforming the pseudo-observations of the swap rate log-returns rather than the PD log-returns means that the tail dependence in these copulas is in the tail of high PD log-returns and low swap rate log-returns. This is the tail where most of the tail dependence in the data is present for the non-downturn data, see Table 4.5.

The results of fitting the copulas mentioned above are shown in Table 4.13 for the non-downturn data and in Table 4.14 for the downturn data. The goodness-of-fit test based on $S_N^{(B)}$ as described by Genest et al. (2009) and defined in (3.9) is performed. This test tests $H_0 : C \in \mathscr{C}_0$ against $H_1 : C \notin \mathscr{C}_0$, where C is the copula associated with the bivariate distribution underlying the data, and $\mathscr{C}_0$ is a certain parametric family of copulas. There is no explicit expression for the distribution of test statistic $S_N^{(B)}$, so the standard deviation of the test statistic cannot be obtained. The p-values, however, are obtained by means of a bootstrap procedure.

One of the observations that stand out is that the copula with the highest p-value does not always have the lowest AIC as well. For AT&T, Boeing, Exxon Mobil and JP Morgan senior in the non-downturn data and Goldman Sachs senior and subordinate in the downturn data, the t copula has the highest p-value, but not the lowest AIC. This is mostly due to the 'penalty' in the AIC for the t copula having a second parameter. This adds 2 to the AIC; if this 2 were not added, the t copula would actually have the lowest AIC for all of these cases except Exxon Mobil (non-downturn) and Goldman Sachs senior (downturn). With Apple (non-downturn), however, the AIC is the lowest for the t copula, while the Gumbel copula has the highest p-value.

As might be expected, no single copula is the best fit for all sectors. However, the t copula is the best fit in most cases. It has three 'wins' for the non-downturn data, i.e. it has both the highest p-value and the lowest AIC for three sectors, and six wins for the downturn data. There are five cases where the t copula has either the highest p-value or the lowest AIC (but not both) in the non-downturn data, and two of these cases in the downturn data. This confirms the expectations that the t copula would be the best fit.

The Frank copula performs second best in both datasets. For the non-downturn data, its performance is close to that of the t copula, also having three wins. For the downturn data, it performs significantly worse than the t copula, and less consistently; it is a poor fit in terms of AIC for AT&T and Walmart, although the other copulas (except for the t copula) do not perform well for these companies either. However, for the downturn datasets, it still has the highest p-value whenever the t copula does not and it has the lowest AIC whenever the t copula does not.

Another observation is that the Gaussian copula performs better than the t copula for the American Airlines and Volkswagen (non-downturn) sectors, in terms of both the p-value and the AIC. This is despite the higher flexibility of the t copula: it approaches the Gaussian copula when the amount of degrees of freedom

[7] This corresponds to the regular Clayton copula being fitted to $(1-\hat{u}_{1,1}, \hat{u}_{1,2}), \ldots, (1-\hat{u}_{n,1}, \hat{u}_{n,2})$.

Normal economic circumstances

Sector		Fitted copula					
		C^t	C^{Ga}	C^{Fr}	$C^{\text{R-Cl}}$	C^{Gu}	C^{Joe}
Alibaba	Parameter(s)	-0.22, 12.56	-0.21	-1.35	0.24	1.15	1.18
	LL	7.45	6.79	7.44	5.14	6.50	4.65
	$S_N^{(B)}$	0.022	0.022	0.018	0.402	0.025	0.045
	p-value	0.689	0.642	**0.829**	0.000	0.470	0.047
	AIC	-10.90	-11.57	**-12.88**	-8.27	-11.00	-7.30
American Airlines	Parameter(s)	-0.36, 1931.43	-0.36	-2.13	0.43	1.26	1.32
	LL	20.24	20.25	18.59	15.43	17.71	13.34
	$S_N^{(B)}$	0.039	0.039	0.047	1.072	0.053	0.095
	p-value	0.172	**0.177**	0.045	0.000	0.035	0.001
	AIC	-36.49	**-38.50**	-35.17	-28.86	-33.41	-24.67
Apple	Parameter(s)	-0.20, 9.51	-0.20	-1.16	0.22	1.14	1.17
	LL	7.08	5.87	5.59	4.67	5.97	4.47
	$S_N^{(B)}$	0.030	0.030	0.030	0.346	0.028	0.038
	p-value	0.228	0.254	0.195	0.000	**0.306**	0.101
	AIC	**-10.16**	-9.74	-9.18	-7.34	-9.94	-6.94
AT&T	Parameter(s)	-0.27, 12.61	-0.27	-1.65	0.35	1.20	1.26
	LL	12.16	11.25	11.26	10.76	11.74	9.64
	$S_N^{(B)}$	0.020	0.020	0.019	0.671	0.020	0.040
	p-value	**0.871**	0.846	0.803	0.000	0.787	0.096
	AIC	-20.33	-20.50	-20.52	-19.52	**-21.49**	-17.28
Barrick Gold	Parameter(s)	-0.40, 25.30	-0.39	-2.63	0.51	1.31	1.41
	LL	25.48	25.06	27.76	20.23	22.92	17.17
	$S_N^{(B)}$	0.023	0.026	0.019	1.466	0.042	0.118
	p-value	0.800	0.651	**0.887**	0.000	0.137	0.000
	AIC	-46.95	-48.11	**-53.51**	-38.46	-43.84	-32.35
Coca Cola	Parameter(s)	-0.34, 8.62	-0.32	-2.20	0.44	1.26	1.35
	LL	18.58	16.21	19.27	15.83	17.09	13.78
	$S_N^{(B)}$	0.021	0.032	0.020	0.985	0.029	0.065
	p-value	0.809	0.324	**0.846**	0.000	0.402	0.004
	AIC	-33.16	-30.42	**-36.54**	-29.66	-32.19	-25.55
Diamond Offshore Drilling	Parameter(s)	-0.14, 7.44	-0.15	-0.83	0.15	1.09	1.10
	LL	5.24	3.19	2.84	2.51	2.74	1.78
	$S_N^{(B)}$	0.016	0.017	0.019	0.160	0.018	0.025
	p-value	**0.873**	0.859	0.710	0.000	0.769	0.398
	AIC	**-6.48**	-4.38	-3.68	-3.02	-3.49	-1.55
Boeing	Parameter(s)	-0.35, 10.63	-0.35	-2.17	0.47	1.27	1.36
	LL	20.74	19.57	18.87	18.24	20.22	16.64
	$S_N^{(B)}$	0.026	0.026	0.033	0.973	0.033	0.065
	p-value	**0.614**	0.574	0.266	0.000	0.254	0.012
	AIC	-37.47	-37.14	-35.74	-34.49	**-38.45**	-31.28
Exxon Mobil	Parameter(s)	-0.28, 22.73	-0.28	-1.75	0.32	1.19	1.23
	LL	12.27	11.97	12.80	8.46	10.16	6.81
	$S_N^{(B)}$	0.014	0.016	0.016	0.716	0.034	0.077
	p-value	**0.992**	0.967	0.948	0.000	0.182	0.004
	AIC	-20.54	-21.94	**-23.60**	-14.92	-18.31	-11.62

Table 4.13: Results of fitting the t, Gaussian, Frank, rotated Clayton, Gumbel and Joe copulas to the the swap rate log-returns and the implied PD log-returns. Parameter(s) denotes the fitted estimates of ρ and the degrees of freedom respectively for the t copula, ρ for the Gaussian copula, and θ for the Frank, rotated Clayton, Gumbel and Joe copulas. The highest p-values and the lowest AIC values are highlighted in bold. The t copula and the Frank copula perform best for most sectors. For a description of the test generating the p-values and further interpretation of the results see Section 4.6.

Sector		Fitted copula C^t	C^{Ga}	C^{Fr}	$C^{\text{R-Cl}}$	C^{Gu}	C^{Joe}
Ford	Parameter(s)	-0.45, 7.28	-0.44	-2.93	0.60	1.39	1.50
	LL	35.67	32.54	32.64	26.26	31.52	24.00
	$S_N^{(B)}$	0.043	0.047	0.056	1.561	0.055	0.099
	p-value	**0.179**	0.096	0.033	0.000	0.041	0.000
	AIC	**-67.33**	-63.09	-63.28	-50.52	-61.03	-46.00
JP Morgan senior	Parameter(s)	-0.44, 9.70	-0.43	-2.89	0.62	1.37	1.50
	LL	32.51	30.34	32.34	28.36	31.04	25.39
	$S_N^{(B)}$	0.036	0.039	0.038	1.651	0.046	0.102
	p-value	**0.284**	0.202	0.209	0.000	0.083	0.000
	AIC	-61.02	-58.67	**-62.68**	-54.71	-60.08	-48.78
JP Morgan subordinate	Parameter(s)	-0.01, 4.05	-0.03	-0.04	0.04	1.04	1.05
	LL	6.54	0.10	0.01	0.23	0.71	0.73
	$S_N^{(B)}$	0.012	0.017	0.015	0.021	0.023	0.020
	p-value	**0.976**	0.677	0.758	0.671	0.429	0.577
	AIC	**-9.08**	1.79	1.99	1.55	0.58	0.54
Volkswagen	Parameter(s)	-0.36, 9674.54	-0.36	-2.26	0.46	1.27	1.35
	LL	20.73	20.73	21.44	16.80	18.97	14.64
	$S_N^{(B)}$	0.024	0.024	0.030	1.181	0.035	0.093
	p-value	0.717	**0.731**	0.403	0.000	0.198	0.001
	AIC	-37.46	-39.46	**-40.89**	-31.60	-35.94	-27.27

Table 4.13: Results of fitting the t, Gaussian, Frank, rotated Clayton, Gumbel and Joe copulas to the the swap rate log-returns and the implied PD log-returns. Parameter(s) denotes the fitted estimates of ρ and the degrees of freedom respectively for the t copula, ρ for the Gaussian copula, and θ for the Frank, rotated Clayton, Gumbel and Joe copulas. The highest p-values and the lowest AIC values are highlighted in bold. The t copula and the Frank copula perform best for most sectors. For a description of the test generating the p-values and further interpretation of the results see Section 4.6.

tends to infinity, so one would expect it to always perform at least as good as the Gaussian copula (at least in terms of the p-value, where the t copula is not penalised for having one more parameter than the Gaussian copula). The fitted amounts of degrees of freedom for the t copula are indeed large in these two cases, so that the t copula approaches the Gaussian copula. As a consequence, the results for the two copulas are close, as the p-value and the log-likelihood are almost equal for the two copulas.

Something else that stands out is that the rotated Clayton copula is not a good fit for any non-downturn dataset except JP Morgan subordinate. This is the only non-downturn dataset that does not show statistically significant dependence, see Table 4.4. For all other sectors, the rotated Clayton copula has a p-value of 0.000. It also has a higher AIC than all the other copulas except the Joe copula, which consistently has an even higher AIC than the rotated Clayton copula. The Joe copula does have slightly higher p-values, however. The similarity between results from the rotated Clayton and Joe copulas (i.e. both being a poor fit for most sectors) is in line with the observations in Section 3.2.2. In the dataset from downturn periods however, the results for these copulas differ a bit more. They also perform better here, in some cases being a better fit than the Gaussian, Frank or Gumbel copulas. In general however, the Gumbel copula outperforms the rotated Clayton and Joe copulas, making it the best performing non-radially symmetric copula.

Comparing the radially symmetric copulas with the non-radially symmetric copulas, the former are the better fit in most cases. They outperform the non-radially symmetric copulas in the datasets from both types of market conditions, even though the tail dependence is asymmetric for the non-downturn periods (it is stronger in the type 2 tail than in the type 1 tail). This implies that the data comes from a radially symmetric copula, which was suggested but not confirmed by hypothesis tests (see Table 4.7 and Table 4.12). As discussed at the end of Section 4.4, this would contradict tail dependence in only one of the two tails; therefore independence in the type 1 tail, which could not be rejected through hypothesis tests for many sectors where independence in the type 2 tail could be rejected, must not hold. Another argument for this statement is the poor performance of the copulas with tail dependence in one tail and independence in the other, being the

Downturn periods

Company		Fitted copula					
		C^t	C^{Ga}	C^{Fr}	$C^{\text{R-Cl}}$	C^{Gu}	C^{Joe}
JP Morgan senior	Parameter(s)	-0.34, 11.12	-0.33	-2.17	0.40	1.24	1.28
	LL	12.01	10.81	12.36	8.01	9.38	6.17
	$S_N^{(B)}$	0.025	0.024	0.018	0.056	0.040	0.092
	p-value	0.835	0.842	**0.981**	0.146	0.312	0.010
	AIC	-20.03	-19.62	**-22.71**	-14.02	-16.76	-10.34
JP Morgan subordinate	Parameter(s)	-0.35, 7.15	-0.34	-2.15	0.42	1.26	1.31
	LL	13.68	11.41	11.93	8.76	11.00	7.79
	$S_N^{(B)}$	0.020	0.021	0.023	0.053	0.033	0.073
	p-value	**0.941**	0.930	0.890	0.171	0.488	0.036
	AIC	**-23.36**	-20.82	-21.85	-15.52	-20.00	-13.59
Southwest airlines	Parameter(s)	-0.28, 2.09	-0.27	-1.78	0.47	1.26	1.38
	LL	20.91	7.27	7.48	10.94	13.22	12.77
	$S_N^{(B)}$	0.017	0.034	0.028	0.034	0.026	0.031
	p-value	**0.993**	0.443	0.693	0.528	0.717	0.457
	AIC	**-37.83**	-12.54	-12.97	-19.88	-24.45	-23.53
Ford	Parameter(s)	-0.29, 3.37	-0.25	-1.76	0.38	1.22	1.29
	LL	11.52	5.85	7.60	7.34	9.72	8.64
	$S_N^{(B)}$	0.024	0.046	0.033	0.055	0.037	0.055
	p-value	**0.871**	0.191	0.510	0.144	0.366	0.082
	AIC	**-19.05**	-9.70	-13.21	-12.67	-17.44	-15.28
AT&T	Parameter(s)	-0.14, 2.28	-0.16	-0.84	0.25	1.15	1.21
	LL	12.34	2.44	1.74	3.93	5.78	5.90
	$S_N^{(B)}$	0.028	0.029	0.029	0.031	0.032	0.029
	p-value	**0.667**	0.505	0.519	0.471	0.420	0.494
	AIC	**-20.67**	-2.88	-1.48	-5.86	-9.56	-9.81
Walmart	Parameter(s)	-0.13, 2.55	-0.10	-0.72	0.11	1.09	1.11
	LL	10.00	0.87	1.28	0.71	1.94	1.45
	$S_N^{(B)}$	0.022	0.027	0.026	0.033	0.025	0.025
	p-value	**0.842**	0.548	0.582	0.317	0.646	0.555
	AIC	**-15.99**	0.26	-0.56	0.58	-1.88	-0.91
Goldman Sachs senior	Parameter(s)	-0.32, 13.65	-0.31	-2.03	0.31	1.21	1.22
	LL	10.17	9.56	10.78	4.97	7.00	3.59
	$S_N^{(B)}$	0.029	0.034	0.031	0.079	0.057	0.108
	p-value	**0.671**	0.503	0.590	0.033	0.097	0.005
	AIC	-16.34	-17.12	**-19.56**	-7.94	-11.99	-5.17
Goldman Sachs subordinate	Parameter(s)	-0.31, 8.41	-0.30	-1.87	0.31	1.21	1.22
	LL	10.18	8.70	9.23	5.06	7.02	4.05
	$S_N^{(B)}$	0.024	0.027	0.029	0.060	0.042	0.078
	p-value	**0.798**	0.687	0.654	0.100	0.249	0.027
	AIC	-16.35	-15.39	**-16.45**	-8.12	-12.05	-6.10
Citigroup	Parameter(s)	-0.33, 7.01	-0.32	-2.09	0.38	1.24	1.27
	LL	12.29	10.29	11.12	7.46	9.48	6.31
	$S_N^{(B)}$	0.024	0.030	0.026	0.072	0.044	0.082
	p-value	**0.870**	0.653	0.766	0.043	0.252	0.024
	AIC	**-20.58**	-18.57	-20.23	-12.92	-16.96	-10.61

Table 4.14: Results of fitting the t, Gaussian, Frank, rotated Clayton, Gumbel and Joe copulas to the data from the downturn periods of the swap rate log-returns and the implied PD log-returns. Parameter(s) denotes the fitted estimates of ρ and the degrees of freedom respectively for the t copula, ρ for the Gaussian copula, and θ for the Frank, rotated Clayton, Gumbel and Joe copulas. The highest p-values and the lowest AIC values are highlighted in bold. The t copula performs best for most sectors. For a description of the test generating the p-values and further interpretation of the results see Section 3.1.

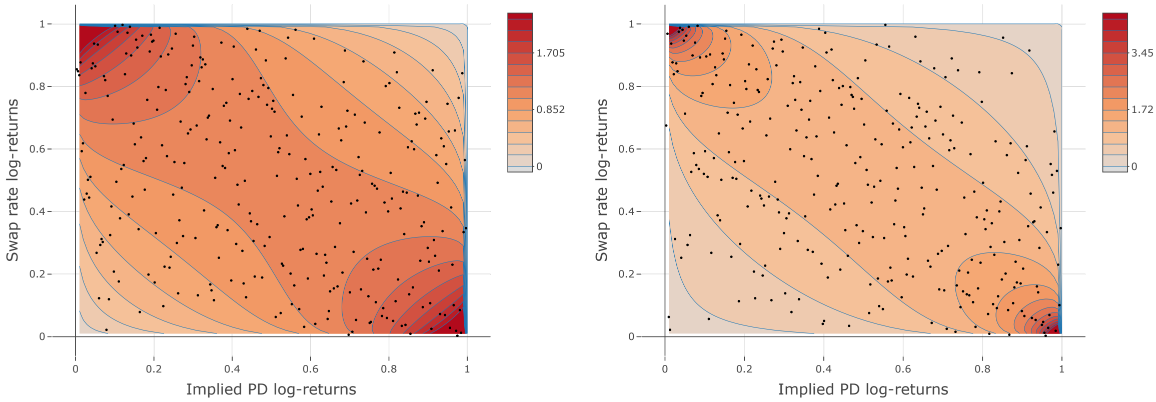

(a) American Airlines (b) Ford

Figure 4.7: Contour plots of the *t* copula density, superimposed with scatterplots of the pseudo-observations of the implied PD log-returns and the swap rate log-returns. Data is from the periods of normal economic circumstances. Note that the scales for the contour plots are different for each copula. The parameters for the *t* copula are those obtained in the fitting process, i.e. the parameters in Table 4.13. As shown by the densities, the tail dependence is stronger for a small (Ford) number of degrees of freedom. The scatterplots seem to correspond to the contour plots, indicating a good fit.

rotated Clayton and Joe copulas, and to a lesser extent the Gumbel copula.[8] It should be noted that although the radially symmetric copulas are the best fit, the tail dependence of the true underlying distribution could still be slightly different between the two tails. In this case, the true underlying copula would be 'close' to radially symmetric.

To sum up, the *t* copula is the best fit for most of the datasets, especially for those obtained from periods of financial crisis. The other radially symmetric copulas outperform the non-radially symmetric copulas, although both of them lack the consistent performance of the *t* copula. Although the Gaussian copula can be approximated by the *t* copula with a high number of degrees of freedom, it still outperforms the *t* copula in a few cases. Of the non-radially symmetric copulas, the Gumbel copula is the best fit. The rotated Clayton and Joe copulas are a poor fit for the non-downturn data, while their performance compared to the other copulas is better during downturn periods. Since the *t* copula is the best performing copula for both the dataset from downturn periods and the dataset from normal economic situations, it is the recommended copula for use in models of the joint behaviour of the swap rate and the PDs of US companies.

In Figure D.2 and Figure D.3 in the appendix, scatterplots of the pseudo-observations of the datasets of log-returns of implied PDs and log-returns of swap rates are shown for non-downturn and downturn data respectively. These scatterplots are superimposed on contour plots of the *t* copula densities, with the parameters being those fitted to the data shown in the scatterplots, as shown in Table 4.13 and Table 4.14. As an example, these plots are shown in Figure 4.7 for the non-downturn implied PD data from American Airlines and Ford, and in Figure 4.8 for the downturn data from JP Morgan subordinate and Walmart CDS spreads. The flexibility of the *t* copula is well visible in the density; the *t* copula for American Airlines has many degrees of freedom, leading to little tail dependence, while the tail dependence is more severe in the *t* copula fitted to data from the Ford sector, which has far fewer degrees of freedom. Similarly, the *t* copula fitted to JP Morgan subordinate data has an absolutely higher correlation parameter than the *t* copula fitted to Walmart data, which also shows in the plots. It can be seen that for all sectors and companies, for both the non-downturn and the downturn data, the shapes of the copula densities appear to match the shapes of the scatterplots, although the scatterplots for downturn data are less informative because of the smaller size of the dataset. This is a visual confirmation of the assessment that the *t* copula is a good modelling choice for the purpose of this thesis.

[8] Although the lower tail dependence coefficient of the Gumbel copula is zero, this is an asymptotic property. As visualised in Figure 3.1, the Gumbel copula density is higher and shows slightly more dependence in the lower tail than the densities of the Joe and rotated Clayton copulas.

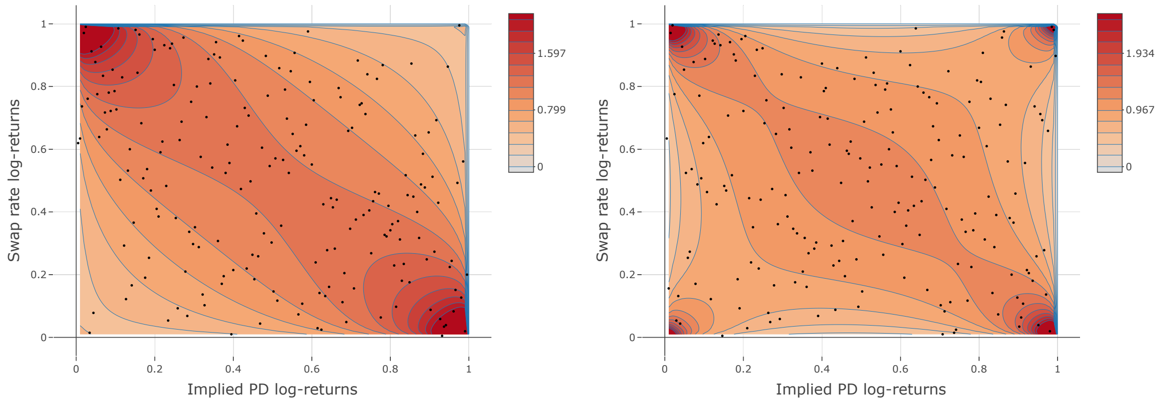

(a) JP Morgan subordinate

(b) Walmart

Figure 4.8: Contour plots of the t copula density, superimposed with scatterplots of the pseudo-observations of the implied PD log-returns and the swap rate log-returns. Data is from the crisis periods. Note that the scales for the contour plots are different for each copula. The parameters for the t copula are those obtained in the fitting process, i.e. the parameters in Table 4.14. The densities show the difference in correlation between an absolutely high (JP Morgan subordinate) and low (Walmart) parameter ρ. The scatterplots seem to correspond to the contour plots, indicating a good fit.

4.7. Financial interpretation

Many financial conclusions can be drawn from the fitted copulas for both the non-downturn and downturn datasets, and from the other analyses that have been performed. The results are most informative if they are combined before drawing conclusions, so that the differences and similarities between results of various analyses can be explored. Therefore the financial interpretation of all results is collected in this section.

The most obvious result concerning the dependence structure is the observation of statistically significant negative dependence between the log-returns of implied PDs and swap rate. This is implied by all fitted copulas, as well as by the results of statistically significant negative rank correlation coefficients. This shows that WWR is present for the receiver position of interest rate swaps, which is in line with the findings by Ben-Abdallah et al. (2019) and Harris et al. (2015) for a set of mostly financial companies.

Tail dependence was shown to be present in the non-downturn dataset, as evidenced by the t copula being the best performing copula in terms of goodness of fit. The t copula contains tail dependence in both tails, but when considering observations below the 0.1 quantile of swap rate log-returns and above the 0.9 quantile of PD log-returns and vice versa, it was shown that there is strong tail dependence of type 2, i.e. the tail of high PD log-returns and low swap rate log-returns. Tail dependence of type 1 (low PD log-returns and high swap rate log-returns) and dependence in the main body of the data is much weaker. This implies that the dependence is strongest when PDs rise and swap rates fall. This situation corresponds to periods of economic decline, as companies are more likely to default. One of the possible causes of this is the tendency of companies to borrow less when the economy is in decline. They are less willing to take risks by taking out large loans to pay for new investments, since if an investment does not work out, a company has to pay back the loan using its financial reserves, which it might need. The demand for fewer loans increases interest rates.

On the other hand, in times of a neutral or good economic situation, there is less dependence between PD log-returns and swap rate log-returns. However, the tail dependence in the tail corresponding to a good economy (i.e. the type 1 tail of low PD log-returns and high swap rate log-returns) is still strong enough for the radially symmetric copulas to outperform the copulas with tail dependence in only one tail. A possible financial reason for the weaker dependence in the main body and the type 1 tail is the difference in company strategies. While one company might look to aggressively take out loans and expand its business, another company could be content to continue its operations as they currently stand and use only their profits to finance their expenses. Companies have many good paths to take in a good economy, while in a bad economy, the best option for most companies may be to sit on their reserves and not take out any loans. This contrast might be the reason for the difference in dependence observed for different economic situations.

The main observation from the downturn analysis is that the correlation in the full dataset during the downturn periods is lower than expected, given the tail dependence observed in the dataset of regular market conditions. The expectation would be that the observed behaviour in the extreme cases (i.e. tails) during regular market conditions would carry over to general cases during the downturn periods, since all movements are more extreme in times of crisis. However, this is not the case.

To understand possible reasons for this discrepancy, first consider the economic reasons behind the dependence structure between PDs and interest rates. One of the possible causes of this dependence is the tendency of companies to borrow less when the economy is in decline, instead holding on to its financial reserves as described above. However, during a crisis, many companies are in worse situations than simply not borrowing and sitting on their reserves. Some companies will have to take out loans to be able to survive. National governments and central banks may act as guarantors for loans taken out for this reason, which would cause more loans to be taken out. The demand for loans by these struggling companies is an upward push to interest rates. Another upward driver for the interest rates is the increased risk banks face in these periods when writing out loans that are not guaranteed by governments or central banks. These two upward drivers counteract the general tendency of interest rates to move down in periods of a weaker economy and higher PDs. This could explain why a lower correlation between PDs and swap rates is observed during crisis periods.

To summarise, the analyses performed in this chapter show that WWR in IRSs is strongest when the economy is worsening, observed through rising PDs. In such situations, companies are more careful and borrow less, driving interest rates down. When the economy is stable or growing, the dependence between movements in the PDs and the swap rate is weaker because of diverging company strategies. In periods of crisis, the demand for loans needed for the survival of companies as well as guarantees on loans by central banks and governments are upward drivers for the swap rate. This reduces WWR in IRSs in these periods, although the high PDs mean that credit risk as a whole is high.

5

Interest Rate Swap Partial Insurance Contracts

After determining that WWR is present in interest rate swaps and how to model it, a logical next question is: what to do about it? An institution exposed to WWR might of course choose to simply accept the risk, but many institutions prefer to hedge their risks.

This chapter introduces a new financial product called the interest rate swap partial insurance contract (IPI). Its goal is to introduce an upper bound on the credit losses that may be suffered on an interest rate swap, thus partially hedging the position. The IPI pays out if the counterparty of the IRS goes into default (the default event) and the credit losses suffered by the IPI buyer due to the default event exceed a threshold value K. In this case, the IPI pays out the difference between the losses and K.

First, Section 5.1 explains why a different model for WWR than those used in previous chapters is necessary, and the WWR model used in this chapter is described. Then, Section 5.2 details the possible goals of a hedging product in terms of the impact on the credit losses, and describes why the goal of bounding the credit losses is chosen for the IPI. In Section 5.3, the IPI is introduced through the definition of its cash flows, which are then used to obtain an exact expression for the no-arbitrage price of the product. Finally, a sensitivity analysis on the price of an IPI is performed in Section 5.4.

5.1. Model for WWR

In this chapter, a different model for WWR is used than in the previous chapters of this thesis. As shown in this section, the method of modelling WWR used in earlier chapters does not lead to a convenient expression for the default event.[1] This is a major disadvantage when deriving an exact expression for the no-arbitrage price of the IPI.

Recall that the previous chapters estimated which copula could best be used to describe the swap rate and the probability of default of a certain company, assuming that both the distribution of the swap rate and the distribution of the probability of default (PD) were constant over time. In other words, the copula in the expression

$$P(\lambda \leq \tilde{\lambda}, \mathrm{sr} \leq \tilde{\mathrm{sr}}) = C(H(\tilde{\lambda}), G(\tilde{\mathrm{sr}})), \tag{5.1}$$

was estimated, where P is the real-world probability measure, $H : \mathbb{R} \to [0,1]$ is the CDF of the PD λ, $G : \mathbb{R} \to [0,1]$ is the CDF of the swap rate sr, and $C : [0,1]^2 \to [0,1]$ is the copula of λ and sr.

[1] One possible approach to stay within the method of the previous chapters would be to assume a company goes into default when its implied PD exceeds a certain threshold value. However, this is counter-intuitive; if the implied PD were a good approximation for true PD, it would be equal to 1 when the company defaults. Additionally, there would be two ways to describe PD (the probability of the implied PD exceeding the threshold, and the implied PD itself), leading to inconsistencies.

The WWR model used in this chapter is the copula model described by e.g. Cherubini (2013), Černý and Witzany (2018), and Böcker and Brunnbauer (2014). Rather than coupling the swap rate with the PD, this model uses copulas to describe the swap rate and the time of default. The model is defined below.

Definition 5.1 (Copula model for swap rate and time of default)**.** The copula model consists of three parts:

1. Take a set of points in time $T_0, \ldots, T_n = T$, with $0 \leq T_0 < \cdots < T_n$. The swap rate $\mathrm{fsr}(T_i) \in \mathbb{R}$ at some future time T_i for an IRS starting at T_i and with payment dates $T_{i+1}, \ldots, T_n$ and maturity $T_n \geq T_i$ is random and has CDF $G_i : \mathbb{R} \to [0,1]$. All interest rate swaps considered in this chapter have the same floating payments; as shown later, the choice of floating payments is irrelevant.

2. There is one defaultable counterparty C, which defaults at a random time $\tau \in [0, \infty]$. The CDF of τ is $F : \mathbb{R} \to [0,1]$.

3. The joint distribution of $\mathrm{fsr}(T_i)$ and τ with respect to the risk-neutral probability measure $\mathbb{Q}$ is given by

$$\mathbb{Q}(\mathrm{fsr}(T_i) \leq s, \tau \leq t) = C(G_i(s), F(t)), \tag{5.2}$$

   where $C : [0,1]^2 \to [0,1]$ is a bivariate copula.

This model may be used to describe the default event and its dependence with the swap rate $\mathrm{fsr}(T_i)$. This is essential in the analytical pricing of the IPI, whose payoff depends on the default event taking place at some time $\tau > 0$ and the level of the swap rate at that time.

5.2. Hedging methods

Reducing or eliminating the effect of market variables on credit losses can be done in many ways. Several approaches are listed below, characterised by the possible credit losses of the hedged portfolio.

1. The credit losses are equal to zero.
   In this approach, the portfolio or product is completely immune to any counterparty credit risk, including the credit risk not caused by WWR. This is achieved by an insurance contract on the portfolio, such as a contingent CDS (C-CDS). A C-CDS is similar to a CDS, but at the credit event, the protection seller is ready to pay an exposure on a derivative contract rather than a fixed amount. As there are already existing methodologies to reach an EL of zero (Brigo and Pallavicini; 2006), this approach is not explored further.

2. The credit losses are bounded.
   This goal can be realised using a contract similar to an option or swaption, effectively 'activating' only when the market variable of interest is above or below a certain threshold value. This approach is an example of partial hedging.

3. The credit losses are equal to the hypothetical credit losses in the case of no WWR, i.e. independence between PD and exposure.
   This is a method that isolates and hedges the effect of WWR on the total credit risk, but leaves the remaining credit risk, to be accepted by the institution or hedged in a different way.

4. The credit losses are equal to the hypothetical credit losses in the case of constant WWR.
   This protects the institution against changes in the dependence structure between the counterparty's PD and the exposure, but leaves it exposed to the initial WWR and the credit risk not caused by WWR. Since the dependence structure cannot be directly observed, this approach may be realised as a swap on the value of an observed dependence measure between the counterparty's PD and the exposure or the value of the portfolio or product.

The third and fourth approach both require a hypothetical scenario to be created not only for the pricing, but also for determining the payoff. This means the counterparties entering into an IPI must agree on how to model this scenario, since there cannot be any discrepancies about the payoff. Hence, a hedging product aiming to have the third or fourth of the listed effects on the total credit losses is unlikely to be traded in practice.

The goal of the IPI is therefore to bound the credit losses, which is the second approach listed above. The bound may be determined by the counterparties, to be customised to different levels of risk aversion. A high bound means the product only covers losses caused by occurrences of high WWR, while with a low bound, the product may also cover a part of the losses that would have been suffered without WWR.

5.3. Defining and pricing the product

The product can be seen as a partial insurance on an IRS; therefore the product is referred to as an interest rate swap partial insurance contract, or IPI. This section defines the cash flows of an IPI and determines its no-arbitrage value.[2]

The cash flows of the product are defined as follows. Say counterparty A has some IRS contract with reference entity C, which is called IRS_1 for the remainder of this chapter. Suppose A wants to buy protection against particularly high losses due to default of C and the occurrence of WWR. It enters into an IPI with protection seller B. Initially, A pays B the price of the IPI. If C does not default during the lifetime of IRS_1, no more IPI cash flows occur. Now suppose C does default within the lifetime of IRS_1, and denote by τ the time of its default. Then A suffers losses equal to the default-free value of IRS_1 (if positive) multiplied by the LGD. If these losses exceed a predefined barrier value $K > 0$, the difference is paid by B to A. If the losses do not exceed the barrier value, no payment is made. In mathematical terms,

$$\text{Payoff}_{\text{IPI}}(\tau) = \text{LGD}\left(V^{+}_{\text{IRS}_1}(\tau) - K^*\right)^+ = \text{LGD}\left(V_{\text{IRS}_1}(\tau) - K^*\right)^+, \tag{5.3}$$

where $K^* = K/\text{LGD}$, $V_{\text{IRS}_1}(\tau) \in \mathbb{R}$ denotes the default-free value of IRS_1 at time τ, and LGD is loss given default, which is assumed to be a deterministic constant for simplicity. The second equality above holds by definition if $V_{\text{IRS}_1}(\tau) \geq 0$, and if $V_{\text{IRS}_1}(\tau) < 0$, then

$$\text{LGD}\left(V^{+}_{\text{IRS}_1}(\tau) - K^*\right)^+ = \text{LGD}\left(V_{\text{IRS}_1}(\tau) - K^*\right)^+ = 0. \tag{5.4}$$

The cash flows of an IPI are also shown schematically in Figure 5.1, and the timing of the cash flows of an IPI and the cash flows and credit loss of IRS_1 are shown in Table 5.1.

Now suppose the payment dates of IRS_1 are $T_0, \ldots, T_n = T$, where $T_0 < \cdots < T_n$ and T is the maturity of IRS_1. Then the price $V_{\text{IPI}}(t, T_n)$ at time $t \geq 0$ for an IPI with IRS_1 being the underlying IRS can be split up as

$$V_{\text{IPI}}(t, T_n) = \sum_{i=0}^{n-1} V_{\text{IPI}}(t, T_i, T_{i+1}), \tag{5.5}$$

where $V_{\text{IPI}}(t, T_i, T_{i+1}) \geq 0$ is the value of the possible payoff due to default of reference entity C between times T_i and T_{i+1}. This value is given by

$$V_{\text{IPI}}(t, T_i, T_{i+1}) = P(t, T_{i+1})\text{LGD}\,\mathbb{E}_t\left[\left(V_{\text{IRS}_1}(\tau) - K^*\right)^+ \mathbb{1}\{T_i < \tau \leq T_{i+1}\}\right], \quad i = 1, \ldots, n-1, \tag{5.6}$$

where $\mathbb{1}\{T_i < \tau \leq T_{i+1}\}$ is the indicator function, which is equal to 1 if $T_i < \tau \leq T_{i+1}$ and zero otherwise, $P(t, T_{i+1}) > 0$ is the price at time t of a unit nominal zero-coupon bond maturing at time T_{i+1} (used as the discounting factor), and $\mathbb{E}_t$ is the conditional expected value conditional on the natural filtration $\mathscr{F} = (\mathscr{F}_t)_{t\geq 0}$ of the stochastic process $\text{fsr}(t)$ and a jump process for the default of C. This filtration contains all information up to time t of the swap rates $\text{fsr}(t)$ and the default time τ (i.e. whether $\tau \leq t$ or not). Now define an auxiliary function

$$VV(t, \tilde{T}, T_{i+1}, T_n) := P(t, T_{i+1})\text{LGD}\,\mathbb{E}_t\left[\left(V_{\text{IRS}_1}(T_{i+1}, T_n) - K^*\right)^+ \mathbb{1}\{\tau \leq \tilde{T}\}\right], \quad i = 1, \ldots, n-1 \tag{5.7}$$

for $\tilde{T} \in (T_i, T_{i+1}]$. The assumption[3] is made that whenever the default event occurs between T_i and T_{i+1}, IRS_1 is terminated from T_{i+1} onward and the losses are incurred at T_{i+1}. If the default event occurs at T_{i+1},

[2] The price for which a financial product is traded is governed by supply and demand; but here the terms price and pricing refer to the intrinsic, no-arbitrage value of an IPI.

[3] This is not an assumption but reality for many definitions of the default event that are common for CDS contracts, such as the reference entity being 90 days late on its IRS payment. In that case, the time of default is only known 90 days after the missed payment, but for the sake of losses and IPI payoff, the time of the default event is the moment the missed payment would have taken place.

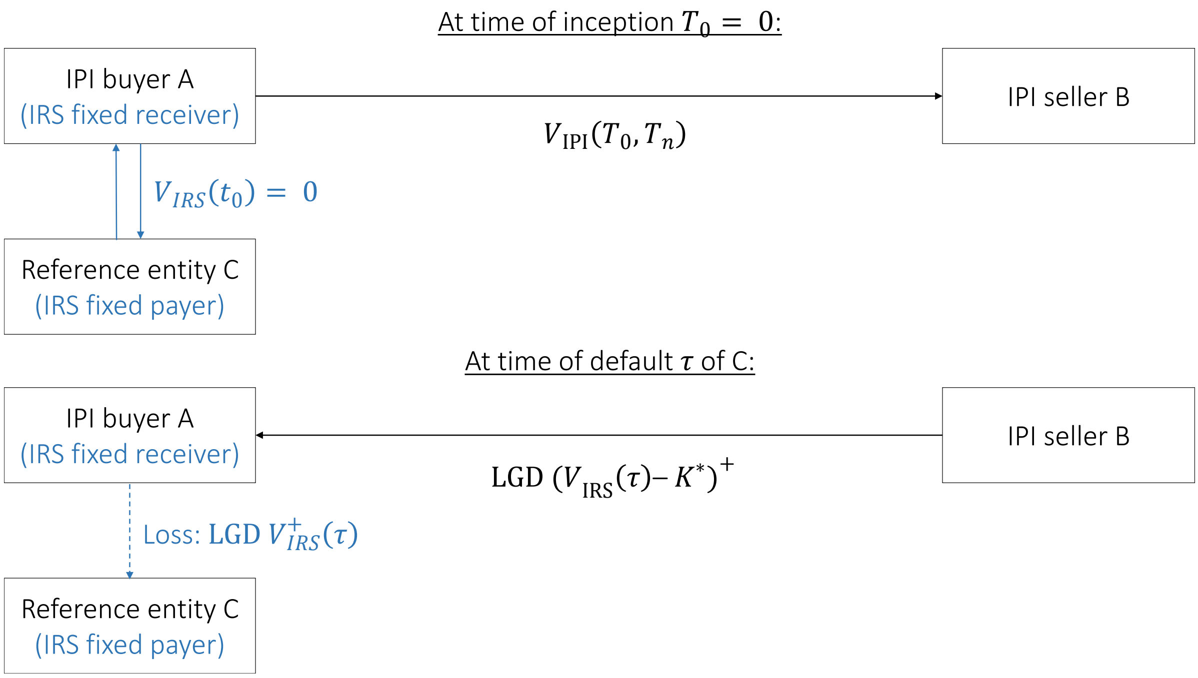

Figure 5.1: The cash flows between the relevant counterparties of an IPI in the case where $\tau < T$. The cash flows of IRS_1 are shown in blue. Note that the IRS position is not part of the IPI and it is not necessary for A and C to enter into an IRS. It is also possible for A to be the fixed payer and C the fixed receiver.

the IRS_1 cash flow that would take place at T_{i+1} does not occur by convention. Under the above assumption, $V_{\text{IRS}_1}(T_{i+1})$ is equal to $V_{\text{IRS}_1}(\tau)$ if $T_i < \tau \le T_{i+1}$. One may write

$$V_{\text{IPI}}(t, T_i, T_{i+1}) = VV(t, T_{i+1}, T_{i+1}, T_n) - VV(t, T_i, T_{i+1}, T_n), \tag{5.8}$$

such that the task of pricing of the IPI is reduced to finding an expression for the conditional expectation in (5.7).

From here on, the focus is on the case where counterparty A has a receiver position in IRS_1, since the earlier chapters of this thesis show that WWR is present in the receiver end of interest rate swaps. The pricing of the IPI in the case where A has a payer position is analogous, however.

To calculate $V_{\text{IRS}_1}(T_{i+1}, T_n)$, note that its no-arbitrage value stays the same if a position in a different IRS starting at T_{i+1} is added, since the swap rate of the latter swap is such that the value of the swap is zero at time T_{i+1}. Specifically, suppose a payer position is added in an interest rate swap IRS_2 starting at time T_{i+1} with maturity T_n and with the same floating payments as IRS_1. Denote by $\text{fsr}(T_{i+1})$ the swap rate of IRS_2. Since opposite positions are taken in the two swaps, the floating payments cancel out, and only the fixed payments remain (see also Table 5.1). This means that

$$V_{\text{IRS}_1}(T_{i+1}, T_n) = X(T_{i+1}, T_{i+1}, T_n)(\text{sr} - \text{fsr}(T_{i+1})), \tag{5.9}$$

where sr is the swap rate of IRS_1, and

$$X(t, T_i, T_n) = \sum_{j=i}^{n} \delta_j P(t, T_j) \tag{5.10}$$

is the value of an annuity, with δ_i being the year fraction between payment dates T_{i-1} and T_i, depending on the calendar convention. Only the case where $\delta_i = \delta$ is independent of the payment date is considered, since this holds in most IRS contracts. Note that IRS_2 is only used to obtain (5.9), and no position in it is entered for the purposes of hedging IRS_1 using the IPI.

Time	Default-free IRS_1	Credit loss on IRS_1	IRS_2	Default-free $\text{IRS}_1 + \text{IRS}_2$	IPI
$T_0 = 0$					$-V_{\text{IPI}}(T_0, T_n)$
T_1	$\delta(\text{sr} - \text{fl}(T_1))$			$\delta(\text{sr} - \text{fl}(T_1))$	
$\vdots$	$\vdots$			$\vdots$	
T_i	$\delta(\text{sr} - \text{fl}(T_i))$			$\delta(\text{sr} - \text{fl}(T_i))$	
$\tau = T_{i+1}$	$\delta(\text{sr} - \text{fl}(T_{i+1}))$	$-V^+_{\text{IRS}_1}(T_{i+1})$	$\delta(\text{fl}(T_{i+1}) - \text{fsr}(T_{i+1}))$	$\delta(\text{sr} - \text{fsr}(T_{i+1}))$	$\text{LGD}\left(V_{\text{IRS}_1}(T_{i+1}) - K^*\right)^+$
T_{i+2}	$\delta(\text{sr} - \text{fl}(T_{i+2}))$		$\delta(\text{fl}(T_{i+2}) - \text{fsr}(T_{i+1}))$	$\delta(\text{sr} - \text{fsr}(T_{i+1}))$	
$\vdots$	$\vdots$		$\vdots$	$\vdots$	
T_{N-1}	$\delta(\text{sr} - \text{fl}(T_{N-1}))$		$\delta(\text{fl}(T_{N-1}) - \text{fsr}(T_{i+1}))$	$\delta(\text{sr} - \text{fsr}(T_{i+1}))$	
T_N	$\delta(\text{sr} - \text{fl}(T_N))$		$\delta(\text{fl}(T_N) - \text{fsr}(T_{i+1}))$	$\delta(\text{sr} - \text{fsr}(T_{i+1}))$	

Table 5.1: Timing of the cash flows and credit losses of the underlying swap IRS_1, the swap IRS_2 starting at T_{i+1}, and the IPI, with default of the reference entity taking place at T_{i+1}. The credit loss is indicated by a negative amount. $\text{fl}(t)$ denotes the floating rate at time t used in both IRS_1 and IRS_2.

Using this, one can write

$$VV(t, \tilde{T}, T_{i+1}, T_n) \approx \text{LGD}\ X(t, T_{i+1}, T_n)\mathbb{E}_t[(\text{sr} - \text{fsr}(T_{i+1}) - \tilde{K}_{i+1})^+ \mathbb{1}\{\tau \leq \tilde{T}\}], \tag{5.11}$$

where $\tilde{K}_{i+1} = K^*/X(T_{i+1}, T_{i+1}, T_n) = (\text{LGD}\ X(T_{i+1}, T_{i+1}, T_n))^{-1}K$. The approximation sign is due to the assumption that $X(T_{i+1}, T_{i+1}, T_n)$ is $\mathscr{F}_t$-measurable for all $t \geq T_0$ and the approximation

$$P(t, T_{i+1})X(T_{i+1}, T_{i+1}, T_n) \approx X(t, T_{i+1}, T_n). \tag{5.12}$$

Going forward, an approach similar to the one by Černý and Witzany (2018) is used. As shown in Appendix B.1, one may write

$$\mathbb{E}_t[(\text{sr} - \text{fsr}(T_{i+1}) - \tilde{K}_{i+1})^+ \mathbb{1}\{\tau \leq \tilde{T}\}] = \int_0^{(\text{sr}-\tilde{K}_{i+1})^+} \mathbb{Q}(\text{fsr}(T_{i+1}) \leq s, \tau \leq \tilde{T})ds, \tag{5.13}$$

where $\mathbb{Q}$ is the risk-neutral probability measure. Whenever $\tilde{K}_{i+1} \geq \text{sr}$, the integral on the right hand side is zero. This situation corresponds to no losses being insured by the IPI, since the losses cannot exceed K.[4] This is more likely for higher i as $\tilde{K}_{i+1}$ is increasing in i, since it is decreasing in $X(T_{i+1}, T_{i+1}, T_n)$ which is decreasing in i. The financial explanation for this is that the exposure of an IRS decreases as it approaches maturity, since there are fewer future cash flows left. Therefore the losses can no longer exceed K.

Now (5.13) can be rewritten as

$$\mathbb{E}_t[(\text{sr} - \text{fsr}(T_{i+1}) - \tilde{K}_{i+1})^+ \mathbb{1}\{\tau \leq \tilde{T}\}] = \int_0^{(\text{sr}-\tilde{K}_{i+1})^+} C(G_{i+1}(s), F(\tilde{T}))ds, \tag{5.14}$$

where $G_{i+1} : \mathbb{R} \to [0,1]$ is the CDF of $\text{fsr}(T_{i+1})$, $F : \mathbb{R} \to [0,1]$ is the CDF of τ, and $C : [0,1]^2 \to [0,1]$ is the bivariate copula of $\text{fsr}(T_{i+1})$ and τ, as described in Definition 5.1. If C is the independence copula or the comonotonicity copula (the upper Fréchet bound),[5] analytical expressions may be found for $V_{\text{IPI}}(t, T_i, T_{i+1})$, giving the value of the IPI in terms of swaptions and credit default swaps. The derivations are shown in Appendix B.2. For the comonotonicity copula $C^{\text{COMON}}(u_1, u_2) = \min\{u_1, u_2\}$, $(u_1, u_2) \in [0,1]^2$, the value of an IPI on a receiver interest rate swap with notional amount 1 is given by

$$\begin{aligned} V_{\text{IPI}}^{\text{COMON}}(t, T) \approx \text{LGD} \sum_{i=0}^{n-1} \Big[& X(t, T_{i+1}, T_n) \\ & \times \left[(\text{sr} - \tilde{K}_{i+1} - b_{i+1})^+ F(T_{i+1}) - (\text{sr} - \tilde{K}_{i+1} - a_i)^+ F(T_i) \right] \\ & + V_{\text{RSwaption}}\left(t, T_{i+1}, T, \min\left\{b_{i+1}, (\text{sr} - \tilde{K}_{i+1})^+\right\}\right) \\ & - V_{\text{RSwaption}}\left(t, T_{i+1}, T, \min\left\{a_i, (\text{sr} - \tilde{K}_{i+1})^+\right\}\right)\Big], \end{aligned} \tag{5.15}$$

[4] Note that the value and therefore the losses of a receiver position in an IRS are bounded, as can be seen by considering the case $\text{fsr}(T_{i+1}) = 0$ in (5.9).

[5] Positive dependence between $\text{fsr}(T_{i+1})$ and τ corresponds to negative dependence between $\text{fsr}(T_{i+1})$ and the PD of C, which is the direction of the dependence observed earlier in this thesis.

where

$$a_i = G_{i+1}^{-1}(F(T_i)), \quad b_{i+1} = G_{i+1}^{-1}(F(T_{i+1})), \tag{5.16}$$

and $V_{\text{RSwaption}}(t, T_{i+1}, T, s_K) \geq 0$ denotes the value at time t of a default-free[6] receiver swaption exercised at time T_{i+1} (such that the first payment takes place at T_{i+2}) and maturing at time T, with strike rate s_K. In this case, the IPI may be replicated by long positions default-free CDSs on the reference entity C, long positions in default-free receiver swaptions with strikes $\min\{b_{i+1}, \text{sr} - \tilde{K}_{i+1}\}$, and short positions in default-free receiver swaptions with strikes $\min\{a_i, \text{sr} - \tilde{K}_{i+1}\}$. This also constitutes a super-replicating strategy for the IPI. The value of the IPI under the independence copula $C^{\text{IND}}(u_1, u_2) = u_1 u_2$, $(u_1, u_2) \in [0,1]^2$, corresponding to the case of no WWR, is given by

$$V_{\text{IPI}}^{\text{IND}}(t, T) \approx \text{LGD} \sum_{i=0}^{n-1} (F(T_{i+1}) - F(T_i)) V_{\text{RSwapion}}\left(t, T_{i+1}, T_n, (\text{sr} - \tilde{K}_{i+1})^+\right), \tag{5.17}$$

so that the IPI may be hedged with long positions in CDSs on reference entity C and long positions in receiver swaptions with strikes $\text{sr} - \tilde{K}_{i+1}$.

Other levels of dependence may be modelled by using a mixture copula which linearly interpolates between the comonotonicity and independence copulas, given by

$$C^{\text{MIX}}(u_1, u_2) = \hat{\rho} C^{\text{COMON}}(u_1, u_2) + (1 - \hat{\rho}) C^{\text{IND}}(u_1, u_2), \quad (u_1, u_2) \in [0,1]^2, \tag{5.18}$$

where $C^{\text{COMON}}(u_1, u_2) = \min(u_1, u_2)$ and $C^{\text{IND}}(u_1, u_2) = u_1 u_2$ denote the comonotonicity and independence copulas respectively, and $\hat{\rho} \in [0,1]$. This way one can model any level of positive dependence by means of a flat dependence parameter. When using this copula, the value of an IPI is interpolated in the same way, i.e.

$$V_{\text{IPI}}^{\text{MIX}}(t, T) = \hat{\rho} V_{\text{IPI}}^{\text{COMON}}(t, T) + (1 - \hat{\rho}) V_{\text{IPI}}^{\text{IND}}(t, T). \tag{5.19}$$

If there are pricing methods in place for CDS and swaption contracts, the above expressions allow for an exact computation of the no-arbitrage price of an IPI contract for any level of dependence.

An estimate for $\hat{\rho}$ is given by the Spearman's correlation coefficient of the data, which is theoretically equal to $\hat{\rho}$. To see why this holds, consider the expression

$$\rho_S(X_1, X_2) = 12 \int_0^1 \int_0^1 (C(u_1, u_2) - u_1 u_2) \, \mathrm{d}u_1 \mathrm{d}u_2 \tag{5.20}$$

for any two random variables X_1, X_2 with copula C, which is proved by McNeil et al. (2005). Since all operations applied to the copula in this expression are linear, one has

$$\rho_S\left(C^{\text{MIX}}\right) = \hat{\rho} \rho_S\left(C^{\text{COMON}}\right) + (1 - \hat{\rho}) \rho_S\left(C^{\text{IND}}\right), \tag{5.21}$$

where $\rho_S(C)$ denotes Spearman's rank correlation of a copula C. Since Spearman's rank correlation of the comonotonicity and independence copulas is equal to 1 and 0 respectively, this yields $\rho_S\left(C^{\text{MIX}}\right) = \hat{\rho}$. Being a measure of rank correlation, Spearman's correlation coefficient is well-suited as an estimator, since it is independent of the marginals and can be easily calculated from a dataset. [7]

A numerical test is performed to compare Spearman's correlation coefficient to the fitted value of $\hat{\rho}$. Several bivariate datasets on $[0,1]^2$ are generated by simulating from different copulas, and the mixture copula in (5.18) is fitted to the datasets. The fitting is done by using ordinary least squares (OLS)[8] on the equation

$$\hat{C}^{\text{MIX}}(u_1, u_2) = \hat{\rho} C^{\text{COMON}}(u_1, u_2) + (1 - \hat{\rho}) C^{\text{IND}}(u_1, u_2), \tag{5.22}$$

[6] Default-free products do not exist in practice, but one can minimise the counterparty default risk e.g. by requiring collateral.

[7] As $\hat{\rho}$ can be estimated by Spearman's correlation coefficient, which is the linear correlation coefficient of a copula, one may wonder if $C_*^{\text{MIX}}(u_1, u_2) = \hat{\rho} C^{\text{COMON}}(u_1, u_2) + \sqrt{1 - \hat{\rho}^2} C^{\text{COMON}}(u_1, u_2)$ for $(u_1, u_2) \in [0,1]^2$ could work as a mixture copula. However, the function C_*^{MIX} is not a distribution function, since $C_*^{\text{MIX}}(1,1) \neq 1$ in general, and therefore it is not a copula.

[8] Maximum likelihood estimation is not available, since the density of the comonotonicity copula does not exist everywhere.

Sampling copula	Parameters	Fitted $\hat{\rho}$	Spearman
Independence copula		0.0176	0.0256
Mixture copula	$\hat{\rho} = 0.25$	0.2723	0.2464
Mixture copula	$\hat{\rho} = 0.5$	0.5356	0.4950
Mixture copula	$\hat{\rho} = 0.75$	0.7379	0.7496
Comonotonicity copula		0.9566	1
Gaussian copula	$\rho = 0.5$	0.4660	0.4876
t copula	$\rho = 0.5$, df = 4	0.4525	0.4818
Frank copula	$\theta = 2$	0.2447	0.3219
Gumbel copula	$\theta = 2$	0.6248	0.6831

Table 5.2: Comparison of Spearman's correlation coefficient and fitted values of $\hat{\rho}$. Fitted values are obtained by fitting the mixture copula in (5.18) to a dataset. Samples are obtained from several different copulas; 'Mixture copula' indicates the copula in (5.18). df is degrees of freedom. As expected, Spearman's correlation coefficient seems to be a good estimate for $\hat{\rho}$.

where $\hat{C}^{\text{MIX}}$ is the empirical distribution function based on the sample. The set $[0,1]^2$ is discretised to a grid and the observed dependent variable $\hat{C}^{\text{MIX}}(u_1,u_2)$ and the explanatory variables $C^{\text{COMON}}(u_1,u_2)$ and $C^{\text{IND}}(u_1,u_2)$ are calculated for each grid point (u_1,u_2). The resulting estimates for $\hat{\rho}$ and Spearman's correlation coefficients for the samples are shown in Table 5.2.

The results show that Spearman's correlation coefficient is a good estimate for $\hat{\rho}$, confirming the theoretical findings. When the sampling copula is the mixture copula itself, Spearman's correlation coefficient is actually a better estimate for $\hat{\rho}$ than the value found with OLS fitting.

5.4. Sensitivity analysis

In this section, a numerical analysis of the sensitivity of the value of an IPI to its underlying variables is performed. The effect of changing one of the parameters is analysed, while the other parameters are constant. The maturity of the swap is 10 years, with quarterly payments, such that $\delta = 0.25$. For the swaption values, a standard Black model is used, which assumes that the future swap rate follows a lognormal distribution with volatility parameter σ, i.e.

$$\text{fsr}(T_{i+1}) = \text{sr} \, \exp\left(-\frac{\sigma^2}{2} T_{i+1} + \sigma W(T_{i+1})\right), \tag{5.23}$$

where $W(T_{i+1}) \sim N(0, T_{i+1})$ is normally distributed. The time of default is assumed to follow an exponential distribution with default intensity h. This means that a_i and b_{i+1} can be expressed explicitly as

$$\begin{aligned} a_i &= \text{sr} \, \exp\left\{-\frac{\sigma^2}{2}(T_{i+1}-t) + \Phi^{-1}(1-\exp\{-h(T_i-t)\})\sigma\sqrt{T_{i+1}-t}\right\}, \\ b_{i+1} &= \text{sr} \, \exp\left\{-\frac{\sigma^2}{2}(T_{i+1}-t) + \Phi^{-1}(1-\exp\{-h(T_{i+1}-t)\})\sigma\sqrt{T_{i+1}-t}\right\}. \end{aligned} \tag{5.24}$$

The constant values of the parameters are as follows. LGD = 0.6, corresponding to the common assumption that the recovery rate is equal to 0.4. The swap rate sr of IRS_1 is equal to 0.006051, which was the 10 year US swap rate on May 7, 2020. A realistic estimate that $\hat{\rho} = 0.25$ is used. The volatility of the future swap rate is assumed to be constant at $\sigma = 0.4$, an estimate also made by Černý and Witzany (2018). For the parameter h of the exponential distribution for default time, $h = 0.0152$ is used, based on the calibration by Ben-Abdallah et al. (2019) for JP Morgan.

Figure 5.2 visualises the results. The value V_{IPI} is relatively stable for low K, as most losses on IRS_1 are expected to exceed the bound. V_{IPI} quickly drops to zero as K grows, however; this happens when K is close to the expected losses on IRS_1. The transition from the area where V_{IPI} is stable in K to the area where $V_{\text{IPI}} = 0$ is slower if the volatility σ is higher.

As expected, the value of the IPI is linear in $\hat{\rho}$, since the interpolation is linear. It is notable, however, that $V_{\text{IPI}} \approx 0$ for $\hat{\rho} = 0$, meaning the IPI has almost no value if the swap rate and the time of default of the reference entity (i.e. the counterparty of IRS_1) are independent. This implies that for the chosen parameters, the

IPI covers only losses caused by WWR, although there is no indication that it covers all losses caused by WWR.

The sensitivity of V_{IPI} to the fixed swap rate is reminiscent of the sensitivity of the no-arbitrage value of a European call option to the underlying stock. Recall that the IPI can indeed be interpreted as an option on the future swap rate, which can be exercised conditional on the default of the reference entity. The future swap rate at inception time of the IPI is equal to the fixed swap rate, therefore the observed sensitivity is expected.

The expectation is that V_{IPI} is increasing in the volatility σ of the future swap rate, since this would give a higher probability of a positive payoff, and the possible payoff is larger. This is indeed observed for low σ in Figure 5.2d; however, as the volatility increases further, the value of the IPI decreases. This is surprising, and no explanation for this behaviour is found.

As expected, V_{IPI} is increasing in the parameter h of the exponential distribution of the time of default of C. As h increases, a counterparty default becomes more likely to occur before maturity, therefore a sharp rise in V_{IPI} can be seen for low h. If h increases further, the probability of a default occurring earlier rises. However, the exposure of an IRS is low (if positive) close to its inception time, since the swap rate is such that the value of the IRS is zero at the inception time. Therefore such an early default does not increase the payoff of an IPI, so for higher h, V_{IPI} is almost constant in h.

The sensitivity to the LGD is not surprising either. For low LGD, the losses do not exceed the bound, so no losses are insured and the IPI has no value. For high LGD, V_{IPI} is linear in the LGD, as the losses are linear in the LGD as well. The non-linearity in the middle of the plot is due to the dependence of the augmented bounds K^* and $\tilde{K}_{i+1}$ on the LGD.

To sum up, the observations are generally according to expectation. A useful observation is that the sensitivity to the swap rate confirms the analogy between an IPI and an option. For the chosen parameters, the IPI has almost no value if the copula is the independence copula (i.e. $\hat{\rho} = 0$), implying that it only covers losses due to WWR. An unexpected observation is that V_{IPI} is decreasing in the volatility σ of the future swap rate for high σ; no explanation for this is found.

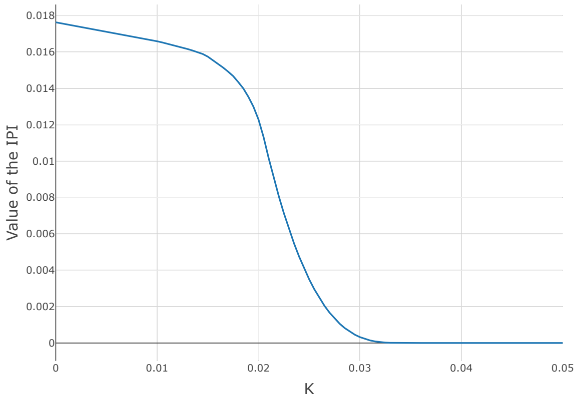

(a) Sensitivity to bound K

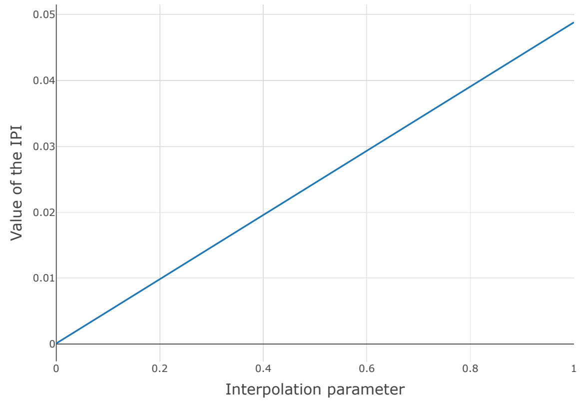

(b) Sensitivity to interpolation parameter $\hat{\rho}$

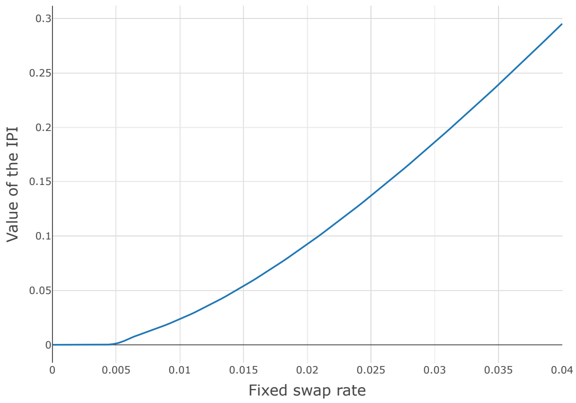

(c) Sensitivity to fixed swap rate sr

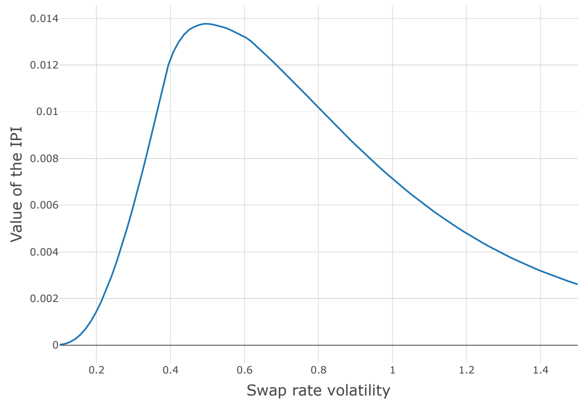

(d) Sensitivity to swap rate volatility σ

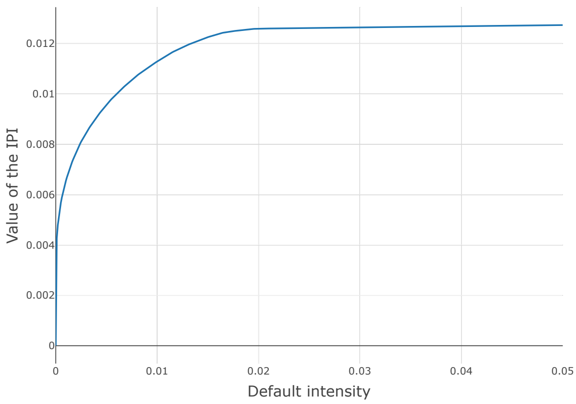

(e) Sensitivity to default intensity h

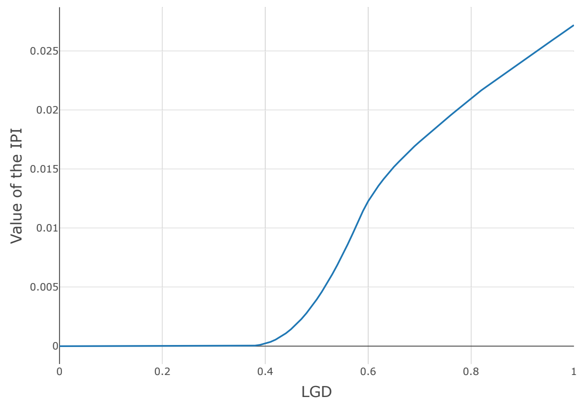

(f) Sensitivity to the LGD

Figure 5.2: Visualisation of the sensitivity of V_{IPI} to the relevant variables. One of the variables varies in each plot, while the others are fixed. The fixed variables are LGD = 0.6, sr = 0.006051, $\hat{\rho} = 0.25$, $\sigma = 0.4$, $h = 0.0152$ and $K = 0.02$. The sensitivity to σ is surprising.

6 Conclusion

The main goals of this thesis were to quantify wrong-way risk (WWR) in interest rate swaps (IRSs), and to provide a method for hedging it. These goals have been achieved. A copula model was developed to model WWR in IRSs, and the model was calibrated to historical data. The observed presence and severity of WWR gives a strong argument for the usefulness of hedging it. The goal of providing a hedging method for WWR in IRSs was achieved by developing a novel product called the IRS partial insurance contract (IPI). This is an important result, since there are no existing well-known products aimed at hedging WWR. This chapter summarises how the goals of this study are achieved. Section 6.1 lists potential subjects for future research.

For the modelling of the connection between the 10-year US dollar swap rate and the PD of a large US-based multinational company, the dependence was found to be negative, and for the non-downturn data, significant tail dependence was observed. These results were both expected, as mentioned in the introduction. The best fitting copula was found to be a t copula. For the non-downturn data, the Frank copula also performed well, but it does not model tail dependence, while the t copula does. For the downturn data, the t copula performed significantly better than the other copulas. The tail dependence observed for the non-downturn data was expected to carry over to the main body of the data during crisis periods, but it was shown that this is not applicable.

The above mathematical results were interpreted financially. One possible explanation for the tail dependence during regular economic circumstances is that during these periods, when the economic situation is deteriorating but not in a crisis, companies are more risk-averse and thus take out fewer loans, instead holding onto their financial reserves. This drop in demand for loans drives down interest rates. During financial crises however, some companies need loans to survive the crisis. Central banks and governments may act as guarantors for loans during these periods, causing even more loans to be taken out. This increase in demand for loans, coupled with the increased risk banks run on non-guaranteed loans, drives up the interest rates. This counteracts the general tendency of interest rates to move down in periods of higher PDs, which could explain the lower absolute correlation observed during downturn periods.

The second main result of this thesis is the development of a novel product named the IPI, aimed at hedging WWR in IRSs. The usefulness of such a product is shown by the earlier results, being that WWR is indeed present for IRSs and manifests itself especially in periods of economic decline outside financial crises. These periods are already challenging for financial institutions, so it can be a great benefit to limit the losses suffered. Furthermore, there are currently no well-known methods for hedging WWR available.

The IPI introduces an upper bound to the credit losses suffered on an IRS. The IPI buyer pays the seller the price of the contract up front. Then if a predefined reference entity defaults, the seller pays the buyer the difference (if positive) between the default-free value of an IRS and a predetermined barrier value. An IPI can be seen as a conditional option that can only be exercised at the moment of default of the reference entity, with the value of an IRS as the underlying variable. The barrier value plays the role of a strike price. The hypothesis was that the product would not isolate WWR, as this would require both counterparties to agree on a model for WWR; this hypothesis was confirmed.

The pricing of an IPI has been performed using the comonotonicity copula, the independence copula or a mixture copula that linearly interpolates between these two copulas to model WWR. The no-arbitrage value of an IPI can be expressed in terms of the prices of swaptions and CDSs. If ways to determine the prices of swaptions and CDSs are in place, one can easily determine the price of an IPI in this way for different levels of WWR.

In the course of finding the best fitting copula to model WWR, another useful result was obtained. It was found that the underlying copula of a dataset can be identified based on the Akaike Information Criterion (AIC) and the goodness of fit statistic $S_N^{(B)}$ described by Genest et al. (2009), whenever the true copula is the t, Gaussian, Frank or Gumbel copula. As the AIC is a well-known tool for comparing goodness of fit, and the test based on $S_N^{(B)}$ is one of the most powerful out of several tests described by Genest et al. (2009), this finding was expected. A more surprising result was the similarity of the Joe copula and the survival copula of the Clayton copula, as the model based on the AIC and $S_N^{(B)}$ could not distinguish between them.

During the writing of this thesis, several insights were afforded on how the work could have been improved, if different decisions had been made earlier. Firstly, the observation of tail dependence in the non-downturn data leads to the question of how well the data would be described by extreme value copulas, such as the Tawn, Galambos or t-EV copulas. One could go even further and use the flexibility of copulas to fit separate copulas to the tails and to the main body. Conversely, fitting both the rotated Clayton copula and the Joe copula to real data was not necessary in hindsight, as the fitting model was unable to differentiate between these two copulas.

Moreover, better estimates for the marginals could have been made during the copula fitting. The empirical marginal distributions have been used, but after observing tail dependence, it became clear that better estimates of the tails of the marginals might be useful. Parametric distributions could be fitted as marginals, or techniques from extreme value theory might be used for the tails. McNeil et al. (2005) propose a generalised Pareto distribution for the tails and an empirical distribution for the body of the marginals. More accurate estimates for the marginals also allow for a better analysis of those aspects of the dependence structure that also depend on the marginals.

Furthermore, it might have been more useful to use the same copula model for both parts of the thesis, i.e. the modelling of WWR and the development of the IPI. The WWR model used to price an IPI could have been analysed in the earlier parts of the thesis, finding which copula would be the best fit for the data. While this model contains path inconsistency, a solution for this issue might have been found if more time was spent analysing the model.

Additionally, the non-downturn data and the downturn data on CDS spreads could have been obtained for the same companies or sector curves. With this data, useful comparisons could have been made between the behaviour of a single CDS spread in different economic situations. Finally, the downturn dataset was small, especially since data from every two days was used to counteract illiquidity. Therefore data could have been collected from more downturn periods, or from more volatile markets than the US market.

6.1. Future research

During the writing of this thesis, the obtained results have sometimes given rise to more questions. Due to time constraints, not all of these questions could be answered. For the same reason, some simplifying assumptions had to be made; new studies could investigate the effect of relaxing these assumptions. Some potential topics for future research based on this study are listed below.

In Chapter 5, an analytical expression for the price of an IPI is obtained when the copula used to describe the relationship between the time of default and the swap rate is an interpolation between the comonotonicity and the independence copulas. It is likely that such a copula is not the best copula to describe this relationship. Therefore, a good extension of this study would be to determine expressions for the price of an

IPI using different copulas.

The copula model used in Chapter 5, which couples the time of default of the counterparty with the swap rate, exhibits path inconsistency. Böcker and Brunnbauer (2014) propose a method to solve this issue, although it has its drawbacks compared to the model currently used. This method could be applied to the copula model used for pricing an IPI. Furthermore, one could study a way to mitigate the drawbacks of this method.

Wrong-way risk was interpreted as the positive dependence between the PD and the EAD of a counterparty in this thesis, while the LGD was assumed to be constant. A more general definition of WWR is the dependence between the PD of the counterparty on an exposure and the possible loss generated by that exposure, which is equal to EAD × LGD. Although the current literature on WWR typically assumes either the EAD or the LGD to be constant, research could be done where both quantities are modelled stochastically. The PD, EAD and LGD could be described by a multivariate model, such as a three-dimensional copula.

In Section 5.4, it was found that the no-arbitrage value V_{IPI} is decreasing in the volatility σ of the future swap rate for high σ. This is contrary to the expectation that V_{IPI} would be increasing in σ, as a higher volatility means a higher probability of payoff and a larger potential payoff. No explanation was found for this counterintuitive behaviour in this thesis, so this could be a topic for future research.

Finally, part of the financial interpretation of the results in this thesis could be verified by a future study. On several occasions, a possible economic reason for the observed mathematical results was given, e.g. for the observation that WWR was present in the tails of the non-downturn data, but less so in the main body of the downturn data. A possible reason for this was given, being the fact that during a financial crisis, the demand for loans is greater because some institutions need loans to survive and because some loans are guaranteed by governments or central banks. While this phenomenon can generally indeed be observed, a scientific study on its effects on the swap rates and through that on WWR could provide valuable insights.

A

The copula framework

In this appendix, copulas, the main method used to model WWR in this thesis, are clarified. Only the concepts used in this thesis are described; further reading on copulas is found in Nelsen (2006). First the definition and an essential theorem are considered in Section A.1. This section is a copy of the first part of Section 2.2.1, repeated here for completeness. The most important copulas are described in Section A.2 and some possible properties of copulas are explored in Section A.3.

A.1. Defining copulas

A vector of random variables is defined by its joint distribution, while the individual random variables can be considered by looking at their marginals. An intuitive point of view is that when the effect the marginals have on the joint distribution is removed, what remains is called the *copula* of the random vector[1]. The formal definition of a copula is given below.

Definition A.1. A d-dimensional copula $C(\cdot)$ is a distribution function on $[0,1]^d$ with standard uniform marginals.

While copulas can be defined for any dimension $d \geq 2$, $d \in \mathbb{N}$, this thesis only uses two-dimensional copulas $C(u_1, u_2)$. This is because there are two random variables of interest, i.e. the swap rate and either the probability of default or the time of default.

The intuitive interpretation above is confirmed by Sklar's theorem (Sklar; 1959). This important theorem shows firstly that a copula can be obtained from all multivariate distribution functions, and secondly that copulas can be used together with univariate CDFs to construct multivariate CDFs.

Theorem A.2 (Sklar 1959)**.** Let F be a joint distribution with marginals F_1, F_2. Then there exists a copula $C : [0,1] \times [0,1] \to [0,1]$ such that, for all $x_1, x_2 \in \overline{\mathbb{R}} = [-\infty, \infty]$,

$$F(x_1, x_2) = C(F_1(x_1), F_2(x_2)). \tag{A.1}$$

If the marginals are continuous, then C is unique; otherwise C is uniquely determined on $\operatorname{Ran} F_1 \times \operatorname{Ran} F_2$, where $\operatorname{Ran} F_i = F_i(\mathbb{R})$ denotes the range of F_i. Conversely, if C is a copula and F_1, F_2 are univariate distribution functions, then the function F defined in (A.1) is a joint distribution function with marginals F_1, F_2.

Proof. See Schweizer and Sklar (1983). □

Corollary A.3. The copula C can be obtained from the multivariate CDF and the marginals as

$$C(u_1, u_2) = F(F_1^{\leftarrow}(u_1), F_2^{\leftarrow}(u_2)), \tag{A.2}$$

where $F_1^{\leftarrow}$ and $F_2^{\leftarrow}$ denote the generalised inverses of F_1 and F_2 respectively.

[1] There has been discussion about the question of whether the copula completely describes the dependence structure of a multivariate distribution. This has largely to do with one's interpretation of the term 'dependence structure'. There are many, such as Genest and Rémillard (2006), who define a dependence structure as a margin-free concept. However, some dependence concepts from extreme value theory require marginals to be known, as described in section 8.2 of the paper by Mikosch (2006). See also Section 2.3.

In the above framework, C may be referred to as the *copula of F*, or as the *copula of X* if X is a bivariate random variable with multivariate CDF F and marginals F_1, F_2.

A.2. Relevant copulas

The copula world is quite big; as shown by Definition A.1, there are infinitely many possible copulas. Some of the most relevant copulas for this thesis are explored in this section. The copulas in this section can be divided into three categories: independence and bounds, elliptical copulas and Archimedean copulas.

Independence and bounds

The first copulas considered provide the most basic of dependence structures: independence, comonotonicity and countermonotonicity. Each copula models one level of dependence, and as such they are the only copulas without parameters described in this section.

The *independence copula* is given by

$$C(u_1, u_2) = u_1 u_2. \tag{A.3}$$

This corresponds to the general notion in probability theory that two events are independent if and only if the probability of both events happening is equal to the probability of the first event happening multiplied by the probability of the second event happening.

The *comonotonicity copula* is

$$C(u_1, u_2) = \min\{u_1, u_2\}. \tag{A.4}$$

Note that this copula is the joint CDF of the clearly monotonic random vector (U, U), where $U \sim U(0, 1)$.

The *countermonotonicity copula* is given by

$$C(u_1, u_2) = \max\{u_1 + u_2 - 1, 0\}. \tag{A.5}$$

This is the joint CDF of the countermonotonic random vector $(U, 1 - U)$, where $U \sim U(0, 1)$. Unlike the independence copula and the comonotonicity copula, the countermonotonicity copula cannot be extended to dimensions higher than two, much like the concept of countermonotonicity itself.

Bounds for copulas are given by the *Fréchet bounds*. These bounds are themselves copulas, specifically the comonotonicity and countermonotonicity copulas:

$$\max\{u_1 + u_2 - 1, 0\} \leqslant C(u_1, u_2) \leqslant \min\{u_1, u_2\}. \tag{A.6}$$

Intuitively this makes sense, since these copulas represent the most extreme cases of dependence. Note that these bounds can be extended to higher dimensions, although as mentioned, the lower bound is not a copula itself for dimensions higher than 2.

In practice, the independence, comonotonicity and countermonotonicity copulas are useful for testing extreme cases, and comparing them to the base case of independence. This can yield bounds for credit-related quantities such as CVA. They can also be used in mixture copulas that interpolate between independence and comonotonicity or countermonotonicity. This is done by for example Cherubini (2013) where the copula

$$C_\rho(u_1, u_2) = \rho \min(u_1, u_2) + (1 - \rho) u_1 u_2$$

is considered, with dependence parameter ρ.

Elliptical copulas

Another class of copulas are elliptical copulas, which are the copulas of elliptical distribution, such as the normal distribution and the t distribution. An important property of all elliptical copulas is radial symmetry. The copulas considered here are the Gaussian copula and the t copula. Both of these are copulas that are implied by a multivariate distribution. This means that the copula is defined as the copula of the corresponding multivariate distribution through (A.2). As such, there is no closed form expression of these copulas.

If $Y \sim N_d(\mu, \Sigma)$ is a Gaussian random vector, then its copula is called a *Gaussian copula* or *Gauss copula*. The operation of standardizing the marginals is a strictly increasing transformation, and it can be shown that strictly increasing transformations do not affect the copula of a distribution (see for example McNeil et al.; 2005). Therefore, the copula of Y is the same as the copula of $X \sim N_2(0, P)$, where $P = \wp(\Sigma)$ is the correlation matrix of Y. Through (A.2), this copula is given by

$$C_\rho^{\mathrm{Ga}}(u_1, u_2) = \Phi_\rho(\Phi^{-1}(u_1), \Phi^{-1}(u_2)), \tag{A.7}$$

with parameter ρ. This copula does not have a simple closed form, but can be expressed as the integral over the density of X. For $|\rho| < 1$, the copula can be written as

$$C_\rho^{\mathrm{Ga}}(u_1, u_2) = \int_{-\infty}^{\Phi^{-1}(u_1)} \int_{-\infty}^{\Phi^{-1}(u_2)} \frac{1}{2\pi(1-\rho^2)^{1/2}} \exp\left\{ \frac{-\left(s_1^2 - 2\rho s_1 s_2 + s_2^2\right)}{2(1-\rho^2)} \right\} \mathrm{d}s_1 \mathrm{d}s_2. \tag{A.8}$$

Note that for $\rho = -1$, $\rho = 0$ and $\rho = 1$ one obtains the countermonotonicity, independence and comonotonicity copulas respectively.

Using the same approach as for the Gaussian copula, one can obtain a copula from the multivariate t distribution, called the *t copula*. It is given by

$$C_{\nu,\rho}^t(u_1, u_2) = t_{\nu,\rho}(t_\nu^{-1}(u_1), t_\nu^{-1}(u_2)), \tag{A.9}$$

with two parameters ν and ρ. This can be written in integral form as

$$C_{\nu,\rho}^t(u_1, u_2) = \int_{-\infty}^{t_\nu^{-1}(u_1)} \int_{-\infty}^{t_\nu^{-1}(u_2)} \frac{\Gamma\left(\frac{\nu+2}{2}\right)}{\Gamma\left(\frac{\nu}{2}\right)\nu\pi(1-\rho^2)^{1/2}} \left(1 + \frac{-\left(s_1^2 - 2\rho s_1 s_2 + s_2^2\right)}{\nu(1-\rho^2)}\right)^{-\frac{\nu+2}{2}} \mathrm{d}s_1 \mathrm{d}s_2. \tag{A.10}$$

Like for the Gaussian copula, for $\rho = 1$ the t copula is equal to the comonotonicity copula and for $\rho = -1$ one obtain the countermonotonicity copula. But for $\rho = 0$, the t copula is in general not equal to the independence copula. This is because uncorrelated multivariate t-distributed random variables are not independent. When $\nu \to \infty$, the t copula approaches the Gaussian copula.

The Gaussian copula is the copula behind the famous model by Li (2000), where the multivariate Gaussian copula was used to model dependence between default times of different companies. The estimate for the correlation parameters is done according to the CreditMetrics method developed by J.P. Morgan (1997), where assuming the same correlation ρ between each pair of companies in a large pool is one of the proposed approaches. The model has several shortcomings, about which Li himself warned in the Wall Street Journal (Whitehouse; 12 September 2005), naming misuse of the model one of the biggest dangers. Nevertheless, his model was widely used and misused in the mid-2000s, and it was one of the causes for the 2008 credit crisis (MacKenzie and Spears; 2014). Some of the reasons for this were the use of a single correlation parameter ρ for each pair of defaults of companies in a large pool and the inability of the Gaussian copula to correctly model the dependence between extreme events, such as extremely short times to default of multiple companies.

Archimedean copulas

Next Archimedean copulas are considered, a family of copulas with a specific structure. These copulas are widely used in credit risk modelling (see e.g. Hofert and Scherer; 2011; Gatfaoui; 2005; Naifar; 2011). Many Archimedean copulas are of the form

$$C(u_1, u_2) = \phi^{-1}(\phi(u_1) + \phi(u_2)), \tag{A.11}$$

where ϕ is a continuous, strictly decreasing function known as the *generator* of the copula with $\phi(1) = 0$. Not all generators have inverses with domain $[0, \infty]$, hence the official definition of Archimedean copulas uses a form of generalised inverse called the *pseudo-inverse*.

Definition A.4 (Pseudo-inverse)**.** Let $\phi : [0,1] \to [0,\infty]$ be a continuous, strictly decreasing function with $\phi(1) = 0$ and $\phi(0) \leqslant \infty$. The pseudo-inverse of ϕ with domain $[0,\infty]$ is defined as

$$\phi^{[-1]}(t) = \begin{cases} \phi^{-1}(t), & 0 \leqslant t \leqslant \phi(0), \\ 0, & \phi(0) < t \leqslant \infty. \end{cases} \tag{A.12}$$

Theorem A.5 (Archimedean copula)**.** Let ϕ and $\phi^{[-1]}$ be as in Definition A.4. Then

$$C(u_1,u_2) = \phi^{[-1]}(\phi(u_1)+\phi(u_2)) \tag{A.13}$$

is a copula if and only if ϕ is convex.

Proof. See (Nelsen; 2006), pp. 91, 92. □

If ϕ is convex, the function defined in (A.13) is known as an *Archimedean copula*.

A widely used Archimedean copula is the *Clayton copula*, defined as

$$C_\theta^{\mathrm{Cl}}(u_1,u_2) = \left(u_1^{-\theta} + u_2^{-\theta} - 1\right)^{-1/\theta}, \quad 0 < \theta < \infty. \tag{A.14}$$

Its generator is $\phi^{\mathrm{Cl}}(t) = \frac{1}{\theta}\left(t^{-\theta} - 1\right)$. For $\theta \to 0$ the Clayton copula approaches the independence copula, and for $\theta \to \infty$ it approaches the comonotonicity copula.

Another example of an Archimedean copula is the *Gumbel copula*, given by

$$C_\theta^{\mathrm{Gu}}(u_1,u_2) = \exp\left\{-\left((-\ln(u_1))^\theta + (-\ln(u_2))^\theta\right)^{1/\theta}\right\}, \quad 1 \leqslant \theta < \infty. \tag{A.15}$$

The Gumbel copula is generated by generator $\phi^{\mathrm{Gu}}(t) = (-\ln(t))^\theta$. It interpolates between the independence copula ($\theta = 1$) and the comonotonicity copula ($\theta \to \infty$).

Often considered together with the Clayton and Gumbel copulas is the *Frank copula*, which is defined as

$$C_\theta^{\mathrm{Fr}}(u_1,u_2) = -\frac{1}{\theta}\ln\left(1 + \frac{(\exp(-\theta u_1)-1)(\exp(-\theta u_2)-1)}{\exp(-\theta)-1}\right), \quad \theta \in \mathbb{R}. \tag{A.16}$$

It has generator

$$\phi^{\mathrm{Fr}}(t) = -\ln\left(\frac{\mathrm{e}^{-\theta t}-1}{\mathrm{e}^{-\theta}-1}\right).$$

For $\theta \to -\infty$ it approaches the countermonotonicity copula, for $\theta \to 0$ it approaches the independence copula, and for $\theta \to \infty$ it approaches the comonotonicity copula.

The final Archimedean copula used in this thesis is the *Joe copula*, given by

$$C_\theta^{\mathrm{Joe}}(u_1,u_2) = 1 - \left[(1-u)^\theta + (1-v)^\theta - (1-u)^\theta(1-v)^\theta\right]^{1/\theta}, \quad 1 \leqslant \theta < \infty. \tag{A.17}$$

Its generator is $\phi^{\mathrm{Joe}}(t) = -\ln\left[1-(1-t)^\theta\right]$. Like the Gumbel copula, it interpolates between the independence copula for $\theta = 1$ and the comonotonicity copula for $\theta \to \infty$.

A.3. Several properties

An *exchangeable copula* C is the CDF of an exchangeable random vector U of uniform random variables U_1, U_2 i.e. a copula C is exchangeable if

$$C(u_1,u_2) = C(u_2,u_1). \tag{A.18}$$

All copulas described in this appendix are exchangeable. Exchangeable copulas are useful for e.g. modelling default dependence for homogeneous groups of companies.

A version of (A.1) also applies to multivariate survival functions of distributions. Let X be a bivariate random variable with CDF F and marginals F_1, F_2. Then it has bivariate survival function $\bar{F} = 1 - F$ and marginal survival functions $\bar{F}_1 = 1 - F_1, \bar{F}_2 = 1 - F_2$ and one has the identity

$$\bar{F}(x_1, x_2) = \hat{C}(\bar{F}_1(x_1), \bar{F}_2(x_2)) \tag{A.19}$$

for copula $\hat{C}$. This copula is known as the *survival copula*. In general, the *survival copula* $\hat{C}$ *of a copula* C is the CDF of $1 - U$ when U has CDF C. This corresponds to the framework above for $U = (F_1(x_1), F_2(x_2))$. A copula and its survival copula are related through

$$\hat{C}(1 - u_1, 1 - u_2) = 1 - u_1 - u_2 + C(u_1, u_2). \tag{A.20}$$

Radial symmetry can be a property of any multivariate distribution. Radial symmetry can be expressed in terms of copulas and survival copulas, and since copulas are multivariate CDFs themselves, they can be radially symmetric.

Definition A.6 (Radial symmetry)**.** A random vector $X \in \mathbb{R}^{n\times 2}$ with $n \in \mathbb{N}$, or its distribution, is radially symmetric about $\mathbf{a} \in \mathbb{R}^2$ if $X - \mathbf{a} \overset{d}{=} \mathbf{a} - X$. If $\mathbf{a}$ is not specified, radial symmetry about $(0.5, 0.5)$ is meant.

If $\mathbf{U}$ has CDF C, where C is a copula, then $\mathbf{C}$ is radially symmetric if $\mathbf{U} \overset{d}{=} 1 - \mathbf{U}$, or equivalently, $\hat{C} = C$. All elliptical copulas are radially symmetric, but Archimedean copulas are generally not. The Frank copula is the only radially symmetric Archimedean copula.

An important implication is that for a radially symmetric copula, the dependence structure is the same in the lower tail as in the upper tail. This is particularly useful to keep in mind when considering which copula to fit to a dataset. If radial symmetry is detected in the data, a radially symmetric copula should be used.

Being joint distributions, many copulas have *copula densities* given by

$$c(u_1, u_2) = \frac{\partial^2 C(u_1, u_2)}{\partial u_1 \partial u_2}. \tag{A.21}$$

Not all copulas have joint densities; the comonotonicity and countermonotonicity are examples of copulas without densities. All parametric copulas described in this appendix, however, do have copula densities. For an absolutely continuous joint CDF F with strictly increasing, continuous marginals F_1, F_2 with inverses F_1^{-1}, F_2^{-1}, joint density f and marginal densities f_1, f_2, the copula density can be related to the joint density by

$$c(u_1, u_2) = \frac{f\left(F_1^{-1}(u_1), F_2^{-1}(u_2)\right)}{f_1\left(F_1^{-1}(u_1)\right) f_2\left(F_2^{-1}(u_2)\right)}. \tag{A.22}$$

Copula densities are required for e.g. fitting copulas to data by maximum likelihood, see Section 3.1.

B

Mathematical derivations

B.1. Integral representation of conditional expectation

Here the proof of the statement

$$\mathbb{E}_t[(\mathrm{sr}-\mathrm{fsr}(T_{i+1})-\tilde{K}_{i+1})^+\mathbb{1}\{\tau\le\tilde{T}\}]=\int_0^{(\mathrm{sr}-\tilde{K}_{i+1})^+}\mathbb{Q}(\mathrm{fsr}(T_{i+1})\le s,\tau\le\tilde{T})ds \tag{B.1}$$

is given. This is shown as follows:

$$\begin{aligned}\mathbb{E}_t[(\mathrm{sr}-\mathrm{fsr}(T_{i+1})-\tilde{K}_{i+1})^+\mathbb{1}\{\tau\le\tilde{T}\}] &= \mathbb{E}_t\left[\int_0^\infty \mathbb{1}\left\{x\le(\mathrm{sr}-\mathrm{fsr}(T_{i+1})-\tilde{K}_{i+1})^+\mathbb{1}\{\tau\le\tilde{T}\}\right\}dx\right]\\ &= \mathbb{E}_t\left[\int_0^\infty \mathbb{1}\left\{x\le(\mathrm{sr}-\mathrm{fsr}(T_{i+1})-\tilde{K}_{i+1})^+,\tau\le\tilde{T}\right\}dx\right]\\ &= \mathbb{E}_t\left[\int_0^{(\mathrm{sr}-\tilde{K}_{i+1})^+}\mathbb{1}\{\mathrm{fsr}(T_{i+1})\le s,\tau\le\tilde{T}\}\,ds\right]\\ &= \int_0^{(\mathrm{sr}-\tilde{K}_{i+1})^+}\mathbb{E}_t[\mathbb{1}\{\mathrm{fsr}(T_{i+1})\le s,\tau\le\tilde{T}\}]ds\\ &= \int_0^{(\mathrm{sr}-\tilde{K}_{i+1})^+}\mathbb{Q}(\mathrm{fsr}(T_{i+1})\le s,\tau\le\tilde{T})ds,\end{aligned} \tag{B.2}$$

where the last equality is due to a well-known relation between the expected value and the probability measure, and the third equality is due to the equivalence of the events

$$\begin{aligned}\{x\le(\mathrm{sr}-\mathrm{fsr}(T_{i+1})-\tilde{K}_{i+1})^+\},\quad x\in[0,\infty) &\Leftrightarrow \{x\le(\mathrm{sr}-\mathrm{fsr}(T_{i+1})-\tilde{K}_{i+1})^+\}, && x\in[0,(\mathrm{sr}-\tilde{K}_{i+1})^+]\\ &\Leftrightarrow \{x+\mathrm{fsr}(T_{i+1})\le(\mathrm{sr}-\tilde{K}_{i+1})^+\}, && x\in[0,(\mathrm{sr}-\tilde{K}_{i+1})^+]\\ &\Leftrightarrow \{\mathrm{fsr}(T_{i+1})\le(\mathrm{sr}-\tilde{K}_{i+1})^+-x\}, && x\in[0,(\mathrm{sr}-\tilde{K}_{i+1})^+]\\ &\Leftrightarrow \{\mathrm{fsr}(T_{i+1})\le s\}, && s\in[0,(\mathrm{sr}-\tilde{K}_{i+1})^+],\end{aligned} \tag{B.3}$$

with the substitution $s=(\mathrm{sr}-\tilde{K}_{i+1})^+-x$ being used in the last equivalence.

B.2. Final derivations for the expression for V_{IPI}

Under the comonotonicity copula $C^{\mathrm{COMON}}(u_1,u_2)=\min(u_1,u_2)$ for $(u_1,u_2)\in[0,1]^2$, the arbitrage-free value of an IPI is given by

$$\begin{aligned}V_{\mathrm{IPI}}^{\mathrm{COMON}}(t,T)\approx \mathrm{LGD}\sum_{i=0}^{n-1}&\Big[X(t,T_{i+1},T_n)\\ &\times\left[(\mathrm{sr}-\tilde{K}_{i+1}-b_{i+1})^+F(T_{i+1})-(\mathrm{sr}-\tilde{K}_{i+1}-a_i)^+F(T_i)\right]\\ &+V_{\mathrm{RSwaption}}\left(t,T_{i+1},T,\min\{b_{i+1},(\mathrm{sr}-\tilde{K}_{i+1})^+\}\right)\\ &-V_{\mathrm{RSwaption}}\left(t,T_{i+1},T,\min\{a_i,(\mathrm{sr}-\tilde{K}_{i+1})^+\}\right)\Big],\end{aligned} \tag{B.4}$$

where

$$a_i=G_{i+1}^{-1}(F(T_i)),\quad b_{i+1}=G_{i+1}^{-1}(F(T_{i+1})), \tag{B.5}$$

and $V_{\text{RSwaption}}\left(t, T_{i+1}, T, \min\{b_{i+1}, \text{sr} - \tilde{K}_{i+1}\}\right) > 0$ denotes the value at time t of a default-free receiver swaption exercised at time T_{i+1} and maturing at time T, with strike $\min\{b_{i+1}, \text{sr} - \tilde{K}_{i+1}\}$. The value of the IPI under the independence copula $C^{IND}(u_1, u_2) = u_1 u_2$ for $(u_1, u_2) \in [0,1]^2$, is given by

$$V_{\text{IPI}}^{\text{IND}}(t, T) \approx \text{LGD} \sum_{i=0}^{n-1} \left(F(T_{i+1}) - F(T_i)\right) V_{\text{RSwapion}}\left(t, T_{i+1}, T_n, \text{sr} - \tilde{K}_{i+1}\right). \tag{B.6}$$

Part of the derivations to arrive at these expressions are given in Section 5.3; the remainder is shown here. First recall that

$$\mathbb{E}_t[(\text{sr} - \text{fsr}(T_{i+1}) - \tilde{K}_{i+1})^+ \mathbb{1}\{\tau \leq \tilde{T}\}] = \int_0^{(\text{sr}-\tilde{K}_{i+1})^+} C(G_{i+1}(s), F(\tilde{T}))ds. \tag{B.7}$$

Substituting C^{COMON} as the copula, this can be rewritten as

$$\int_0^{(\text{sr}-\tilde{K}_{i+1})^+} C(G_{i+1}(s), F(\tilde{T}))ds = \int_0^{(\text{sr}-\tilde{K}_{i+1})^+} \min(G_{i+1}(s), F(\tilde{T}))ds. \tag{B.8}$$

Note that

$$\min(G_{i+1}(s), F(\tilde{T})) = \begin{cases} G_{i+1}(s) & \text{for } s \leq G_{i+1}^{-1}(F(\tilde{T})) \\ F(\tilde{T}) & \text{for } s > G_{i+1}^{-1}(F(\tilde{T})) \end{cases}, \tag{B.9}$$

so

$$\begin{aligned} \int_0^{(\text{sr}-\tilde{K}_{i+1})^+} \min(G_{i+1}(s), F(\tilde{T}))ds &= \int_0^{\min((\text{sr}-\tilde{K}_{i+1})^+, G_{i+1}^{-1}(F(\tilde{T})))} G_{i+1}(s)ds \\ &+ \int_{\min((\text{sr}-\tilde{K}_{i+1})^+, G_{i+1}^{-1}(F(\tilde{T})))}^{(\text{sr}-\tilde{K}_{i+1})^+} F(\tilde{T})ds \\ &= \int_0^{\min((\text{sr}-\tilde{K}_{i+1})^+, G_{i+1}^{-1}(F(\tilde{T})))} G_{i+1}(s)ds \\ &+ [\text{sr} - \tilde{K}_{i+1} - G_{i+1}^{-1}(F(\tilde{T}))]^+ F(\tilde{T}). \end{aligned} \tag{B.10}$$

Due to derivations similar to those in Appendix B.1, one has

$$\int_0^{s_K} G_{i+1}(s)ds = \mathbb{E}_t\left[(s_K - \text{fsr}(T_{i+1}))^+\right]. \tag{B.11}$$

Recall that V_{IPI} can be deconstructed as follows:

$$\begin{aligned} V_{\text{IPI}}(t, T_n) &= \sum_{i=0}^{n-1} V_{\text{IPI}}(t, T_i, T_{i+1}), \\ V_{\text{IPI}}(t, T_i, T_{i+1}) &= VV(t, T_{i+1}, T_{i+1}, T_n) - VV(t, T_i, T_{i+1}, T_n), \\ VV(t, \tilde{T}, T_{i+1}, T_n) &\approx \text{LGD } X(t, T_{i+1}, T_n)\mathbb{E}_t[(\text{sr} - \text{fsr}(T_{i+1}) - \tilde{K}_{i+1})^+ \mathbb{1}\{\tau \leq \tilde{T}\}]. \end{aligned} \tag{B.12}$$

The derivations above yield

$$\begin{aligned} VV(t, \tilde{T}, T_{i+1}, T_n) \approx\ &\text{LGD } X(t, T_{i+1}, T_n)(\text{sr} - \tilde{K}_{i+1} - G_{i+1}^{-1}(F(\tilde{T})))^+ F(\tilde{T}) \\ &+ \text{LGD } V_{\text{RSwaption}}\left(t, T_{i+1}, T, \min\left\{G_{i+1}^{-1}(F(\tilde{T})), (\text{sr} - \tilde{K}_{i+1})^+\right\}\right), \end{aligned} \tag{B.13}$$

where the presence of

$$V_{\text{RSwaption}}\left(t, T_{i+1}, T_n, s_K\right) = X(t, T_{i+1}, T_n)\mathbb{E}_t[(s_K - \text{fsr}(T_1))^+] \tag{B.14}$$

is due to (B.11). This yields the final result

$$\begin{aligned} V_{\text{IPI}}^{\text{COMON}}(t, T) \approx \text{LGD} \sum_{i=0}^{n-1} &\left[X(t, T_{i+1}, T_n)\right. \\ &\times\left[(\text{sr} - \tilde{K}_{i+1} - b_{i+1})^+ F(T_{i+1}) - (\text{sr} - \tilde{K}_{i+1} - a_i)^+ F(T_i)\right] \\ &+ V_{\text{RSwaption}}\left(t, T_{i+1}, T, \min\left\{b_{i+1}, (\text{sr} - \tilde{K}_{i+1})^+\right\}\right) \\ &\left. - V_{\text{RSwaption}}\left(t, T_{i+1}, T, \min\left\{a_i, (\text{sr} - \tilde{K}_{i+1})^+\right\}\right)\right], \end{aligned} \tag{B.15}$$

where

$$a_i = G_{i+1}^{-1}(F(T_i)), \quad b_{i+1} = G_{i+1}^{-1}(F(T_{i+1})). \tag{B.16}$$

Now consider the case of the independence copula C^{IND}. Substituting this copula into (B.7), one obtains

$$\int_0^{(\text{sr}-\tilde{K}_{i+1})^+} C(G_{i+1}(s), F(\tilde{T}))ds = F(\tilde{T})\int_0^{(\text{sr}-\tilde{K}_{i+1})^+} G_{i+1}(s)ds. \tag{B.17}$$

Using (B.11), one has

$$VV(t,\tilde{T},T_{i+1},T_n) \approx \text{LGD}F(\tilde{T})\, V_{\text{RSwapion}}\left(t,T_{i+1},T_n,(\text{sr}-\tilde{K}_{i+1})^+\right), \tag{B.18}$$

from which the final result

$$V_{\text{IPI}}^{\text{IND}}(t,T) \approx \text{LGD}\sum_{i=0}^{n-1}\left(F(T_{i+1})-F(T_i)\right) V_{\text{RSwapion}}\left(t,T_{i+1},T_n,(\text{sr}-\tilde{K}_{i+1})^+\right) \tag{B.19}$$

follows.

C
Statistical properties of the data

Here a short statistical overview of the data is given. For the non-downturn data, daily data is obtained for the period between September 18, 2018 and February 28, 2020. However, data after February 20, 2020 is disregarded, since the market conditions were extraordinary during these days due to the economic consequences of the corona virus. For each company, there is a total of 349 data points. Some properties of the data on CDS sector curve spreads is given in Table C.1. After applying the method described in Section 4.1, a dataset with conditional PD values is obtained, which is described in Table C.2. Statistical properties of the dataset of swap rates is shown in Table C.3. The swap data ranges from September 18, 2018 to January 3, 2020 and contains 317 observations. Similar statistical descriptions are given for the log-returns on the data in Table C.4 for the CDS sector curve spreads, in Table C.5 for the implied annual PDs, and in Table C.6 for the swap rates. Note that the log-returns on the CDS spreads and the implied PDs are equal up to the amount of digits displayed, since the CDS spreads and the implied PDs are approximately equal up to a multiplicative factor (see (4.5)). The same properties for the downturn data is given in Tables C.7 to C.12. The downturn data consists of data from three periods: from August 28, 2008 to June 4, 2009, from April 2, 2010 to December 17, 2010, and from February 20, 2020 until April 15, 2020. As the daily data is illiquid, data from every two days is used.

Scatterplots of the swap rate returns against the implied PD returns (only the data from before January 3, 2020 for the non-downturn data) are shown in Figure C.1 and Figure C.2. The 0.1 and 0.9 quantiles of both variables are indicated by the blue lines.

Raw data, non-downturn period

CDS sector curve spreads

	Mean	Std. dev.	Min	0.25	Quantiles Median	0.75	Max
Alibaba	0.008078	0.001172	0.005684	0.007147	0.007912	0.008858	0.010506
American Airlines	0.032968	0.004175	0.024947	0.030107	0.032605	0.035471	0.042452
Apple	0.010659	0.000718	0.009247	0.010156	0.010635	0.011047	0.012468
AT&T	0.010768	0.000662	0.009677	0.010315	0.010619	0.011078	0.012930
Barrick Gold	0.010206	0.000808	0.008786	0.009549	0.010141	0.010760	0.012085
Coca Cola	0.009457	0.000616	0.008350	0.008963	0.009436	0.009950	0.011049
Diamond Offshore Drilling	0.049869	0.006938	0.037976	0.045398	0.048781	0.052322	0.071388
Boeing	0.007377	0.000346	0.006644	0.007128	0.007291	0.007609	0.008317
Exxon	0.014935	0.001455	0.011896	0.013963	0.014993	0.016126	0.017932
Ford	0.016634	0.001271	0.014098	0.015821	0.016700	0.017469	0.019832
JPM sen	0.010364	0.000995	0.008649	0.009548	0.010281	0.011076	0.012803
JPM sub	0.012324	0.000868	0.010489	0.011720	0.012308	0.012753	0.015121
Volkswagen	0.011617	0.001092	0.010006	0.010621	0.011497	0.012460	0.014397

Table C.1: Statistical properties of the data on CDS sector curve spreads. All spreads for non-financials are senior. Data is obtained from Bloomberg.

Implied PDs

	Mean	Std. dev.	Min	0.25	Quantiles Median	0.75	Max
Alibaba	0.004625	0.000450	0.003648	0.004381	0.004650	0.004929	0.005656
American Airlines	0.019050	0.001916	0.015578	0.017541	0.018959	0.020490	0.023693
Apple	0.006226	0.001148	0.004709	0.005347	0.005691	0.007604	0.008660
AT&T	0.006271	0.001006	0.004772	0.005373	0.006106	0.007436	0.008061
Barrick Gold	0.005909	0.000760	0.004766	0.005262	0.005744	0.006721	0.007374
Coca Cola	0.005495	0.000827	0.004355	0.004754	0.005309	0.006425	0.007134
Diamond Offshore Drilling	0.029276	0.005523	0.020414	0.024406	0.029244	0.033772	0.040486
Boeing	0.004303	0.000739	0.003365	0.003645	0.004117	0.005236	0.005606
Exxon	0.008850	0.002258	0.005799	0.006732	0.008433	0.010858	0.012947
Ford	0.009661	0.001349	0.007701	0.008416	0.009411	0.010873	0.012643
JPM sen	0.005981	0.000684	0.005023	0.005383	0.005734	0.006687	0.007506
JPM sub	0.007195	0.001302	0.005602	0.006078	0.006707	0.008312	0.010188
Volkswagen	0.006717	0.000843	0.005233	0.006072	0.006408	0.007636	0.008421

Table C.2: Statistical properties of the obtained values of annual PDs conditional on no earlier default. Values are implied from the market data on CDS sector curve spreads. PD refers to the default event of a fictitious company that is assumed to have CDS spreads equal to the sector curve spreads in Table C.1.

Swap rates

	Mean	Std. dev.	Min	0.25	Quantiles Median	0.75	Max
Swap rate	2.311163	0.579147	1.3263	1.762625	2.3639	2.748725	3.2836

Table C.3: Statistical properties of the data on 10 year interest rate swap rates. Data is obtained from Bloomberg.

Log-returns, non-downturn period

CDS sector curve spreads

	Mean	Std. dev.	Min	0.25	Quantiles Median	0.75	Max
Alibaba	-0.000146	0.017571	-0.065377	-0.010692	-0.000523	0.009310	0.095258
American Airlines	0.000488	0.019550	-0.103762	-0.010386	-0.000993	0.010403	0.075710
Apple	0.001364	0.020248	-0.063763	-0.009760	-0.000178	0.012495	0.093191
AT&T	0.001101	0.017401	-0.058523	-0.008641	-0.000401	0.010496	0.091208
Barrick Gold	0.000816	0.016258	-0.052110	-0.008840	-0.000170	0.008380	0.090559
Coca Cola	0.001143	0.016242	-0.047079	-0.008672	0.000144	0.010158	0.074635
Diamond Offshore Drilling	0.001620	0.030563	-0.218763	-0.011673	0.002573	0.015152	0.127732
Boeing	0.001308	0.017688	-0.055903	-0.010695	0.000407	0.011106	0.079266
Exxon	0.001740	0.023269	-0.088405	-0.009948	-0.001341	0.012634	0.087846
Ford	0.000908	0.017453	-0.050953	-0.010313	-0.000555	0.009172	0.087554
JPM sen	0.000757	0.015411	-0.051798	-0.008318	-0.000390	0.009221	0.062879
JPM sub	0.001066	0.020031	-0.055543	-0.010885	0.000361	0.012222	0.115587
Volkswagen	0.001098	0.019835	-0.055659	-0.010897	-0.000015	0.011209	0.131276

Table C.4: Statistical properties of the log-returns on CDS sector curve spreads. All spreads for non-financials are senior. Data is obtained from Bloomberg.

Implied PDs

	Mean	Std. dev.	Min	0.25	Quantiles Median	0.75	Max
Alibaba	-0.000146	0.017571	-0.065377	-0.010692	-0.000523	0.009310	0.095258
American Airlines	0.000488	0.019550	-0.103762	-0.010386	-0.000993	0.010403	0.075710
Apple	0.001364	0.020248	-0.063763	-0.009760	-0.000178	0.012495	0.093191
AT&T	0.001101	0.017401	-0.058523	-0.008641	-0.000401	0.010496	0.091208
Barrick Gold	0.000816	0.016258	-0.052110	-0.008840	-0.000170	0.008380	0.090559
Coca Cola	0.001143	0.016242	-0.047079	-0.008672	0.000144	0.010158	0.074635
Diamond Offshore Drilling	0.001620	0.030563	-0.218763	-0.011673	0.002573	0.015152	0.127732
Boeing	0.001308	0.017688	-0.055903	-0.010695	0.000407	0.011106	0.079266
Exxon	0.001740	0.023269	-0.088405	-0.009948	-0.001341	0.012634	0.087846
Ford	0.000908	0.017453	-0.050953	-0.010313	-0.000555	0.009172	0.087554
JPM sen	0.000757	0.015411	-0.051798	-0.008318	-0.000390	0.009221	0.062879
JPM sub	0.001066	0.020031	-0.055543	-0.010885	0.000361	0.012222	0.115587
Volkswagen	0.001098	0.019835	-0.055659	-0.010897	-0.000015	0.011209	0.131276

Table C.5: Statistical properties of the returns on annual PDs conditional on no earlier default. Daily values are implied from the market data on CDS sector curve spreads. PD refers to the default event of a fictitious company that is assumed to have CDS spreads equal to the sector curve spreads in Table C.1.

Swap rates

	Mean	Std. dev.	Min	0.25	Quantiles Median	0.75	Max
Swap rate	-0.001621	0.022591	-0.081623	-0.012602	-0.001312	0.008845	0.080334

Table C.6: Statistical properties of the returns on 10 year interest rate swap rates. Data is obtained from Bloomberg.

Raw data, downturn periods

CDS spreads

	Mean	Std. dev.	Min	0.25	Quantiles Median	0.75	Max
JP Morgan senior	0.011582	0.002925	0.006043	0.009304	0.011050	0.013438	0.021500
JP Morgan subordinate	0.016057	0.005016	0.008204	0.011901	0.015000	0.019159	0.029500
Southwest airlines	0.020408	0.007292	0.007230	0.016372	0.018000	0.021975	0.042500
Ford	0.097744	0.083288	0.023726	0.036137	0.071100	0.116244	0.467500
AT&T	0.013418	0.004336	0.007950	0.011049	0.012130	0.013788	0.036212
Walmart	0.007130	0.002384	0.002522	0.005628	0.005838	0.009338	0.013750
Goldman Sachs senior	0.019717	0.007637	0.008630	0.014721	0.017103	0.023750	0.058700
Goldman Sachs subordinate	0.026273	0.008713	0.012897	0.019214	0.023300	0.033500	0.061500
Citigroup senior	0.023323	0.010532	0.007683	0.016702	0.018961	0.026787	0.055500

Table C.7: Statistical properties of the data on CDS sector curve spreads. All spreads for non-financials are senior. Data is obtained from Bloomberg.

Implied PDs

	Mean	Std. dev.	Min	0.25	Quantiles Median	0.75	Max
JP Morgan senior	0.019075	0.004731	0.010009	0.015368	0.018165	0.022299	0.034692
JP Morgan subordinate	0.026286	0.008054	0.013563	0.019612	0.024556	0.031437	0.047858
Southwest airlines	0.033016	0.011303	0.011882	0.026858	0.029246	0.035765	0.068260
Ford	0.143633	0.108616	0.038729	0.058380	0.111713	0.176929	0.555345
AT&T	0.021970	0.006991	0.013002	0.018140	0.019924	0.022531	0.058325
Walmart	0.011746	0.003887	0.004178	0.009321	0.009669	0.015284	0.022501
Goldman Sachs senior	0.032207	0.012022	0.014166	0.024311	0.027989	0.038721	0.091997
Goldman Sachs subordinate	0.042561	0.013726	0.021098	0.031389	0.038014	0.054198	0.096178
Citigroup senior	0.037819	0.016545	0.012622	0.027323	0.031030	0.043521	0.088212

Table C.8: Statistical properties of the obtained values of annual PDs conditional on no earlier default. Values are implied from the market data on CDS sector curve spreads. PD refers to the default event of a fictitious company that is assumed to have CDS spreads equal to the sector curve spreads in Table C.7.

Swap rates

	Mean	Std. dev.	Min	0.25	Quantiles Median	0.75	Max
Swap rate	0.030297	0.008643	0.006153	0.026897	0.030475	0.034652	0.04538

Table C.9: Statistical properties of the data on 10 year interest rate swap rates. Data is obtained from Bloomberg.

Log-returns, downturn periods

CDS spreads

					Quantiles		
	Mean	Std. dev.	Min	0.25	Median	0.75	Max
JP Morgan senior	0.001398	0.099486	-0.519578	-0.041944	0.000000	0.041944	0.350430
JP Morgan subordinate	0.001347	0.081296	-0.349126	-0.035290	-0.000022	0.034087	0.341214
Southwest airlines	0.001891	0.078538	-0.276316	-0.027214	-0.000383	0.019241	0.545707
Ford	-0.001794	0.122267	-0.612210	-0.039151	-0.000674	0.033871	0.521200
AT&T	0.003549	0.069784	-0.244665	-0.021226	0.000000	0.019589	0.333428
Walmart	-0.002054	0.066549	-0.492256	-0.016399	0.000000	0.019977	0.235906
Goldman Sachs senior	0.000685	0.124745	-0.745333	-0.050038	0.000000	0.050324	0.689746
Goldman Sachs subordinate	0.001381	0.109519	-0.607883	-0.038043	0.000000	0.042279	0.645519
Citigroup senior	0.004042	0.124670	-0.748063	-0.045079	0.000000	0.049506	0.565261

Table C.10: Statistical properties of the log-returns on CDS sector curve spreads. All spreads for non-financials are senior. Data is obtained from Bloomberg.

Implied PDs

					Quantiles		
	Mean	Std. dev.	Min	0.25	Median	0.75	Max
JP Morgan senior	0.001729	0.100768	-0.513701	-0.042120	0.000005	0.044078	0.347256
JP Morgan subordinate	0.001510	0.082428	-0.343260	-0.034451	-0.000168	0.034736	0.337544
Southwest airlines	0.002029	0.078862	-0.271465	-0.027171	-0.000541	0.021668	0.537538
Ford	-0.001499	0.112106	-0.638510	-0.036122	-0.000750	0.030525	0.446400
AT&T	0.003663	0.071226	-0.280101	-0.021477	0.000002	0.019604	0.327940
Walmart	-0.002075	0.076542	-0.763585	-0.016224	0.000425	0.020563	0.232911
Goldman Sachs senior	0.001103	0.124664	-0.726327	-0.049697	0.000002	0.052965	0.664377
Goldman Sachs subordinate	0.001734	0.108545	-0.590103	-0.037996	0.000011	0.042420	0.620211
Citigroup senior	0.004493	0.124459	-0.733613	-0.044556	0.000435	0.055129	0.552444

Table C.11: Statistical properties of the returns on annual PDs conditional on no earlier default. Daily values are implied from the market data on CDS sector curve spreads. PD refers to the default event of a fictitious company that is assumed to have CDS spreads equal to the sector curve spreads in Table C.7.

Swap rates

					Quantiles		
	Mean	Std. dev.	Min	0.25	Median	0.75	Max
Swap rate	-0.003936	0.069493	-0.392761	-0.03182	-0.00245	0.024758	0.333244

Table C.12: Statistical properties of the returns on 10 year interest rate swap rates. Data is obtained from Bloomberg.

Regular market conditions

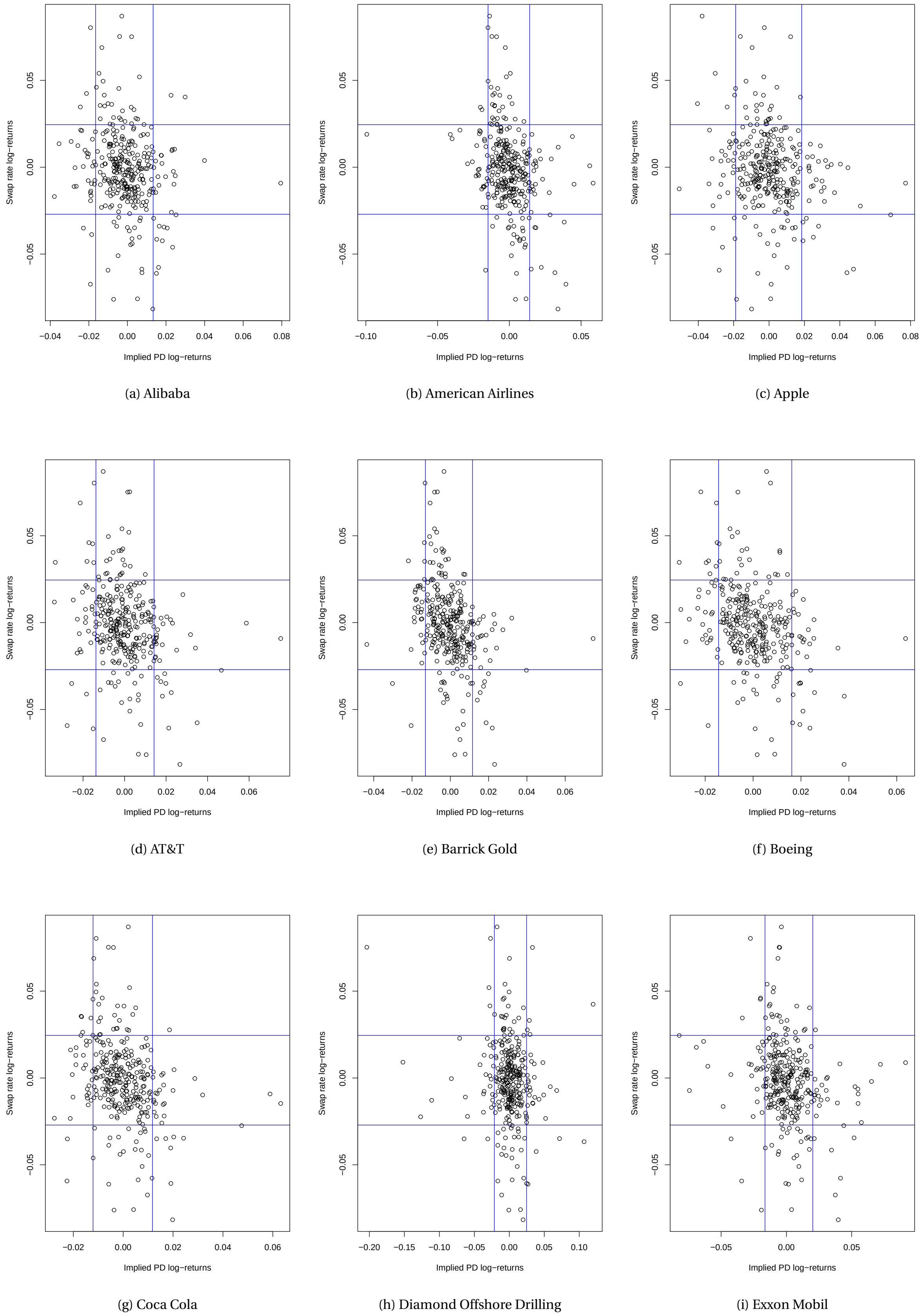

Figure C.1: Scatterplots of the log-returns on implied PDs of all sectors against the log-returns on 10 year swap rates. 0.1 and 0.9 quantiles are shown for both implied PDs and swap rates by the blue lines.

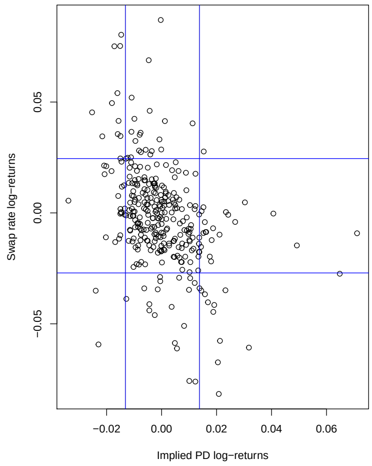

(j) Ford

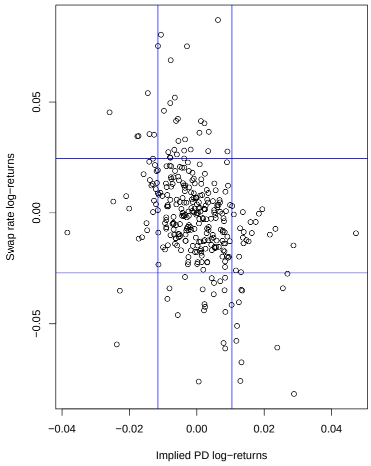

(k) JP Morgan senior

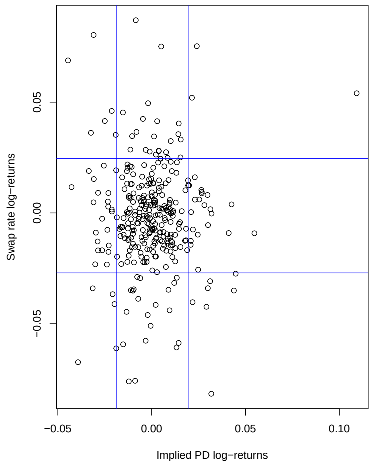

(l) JP Morgan subordinate

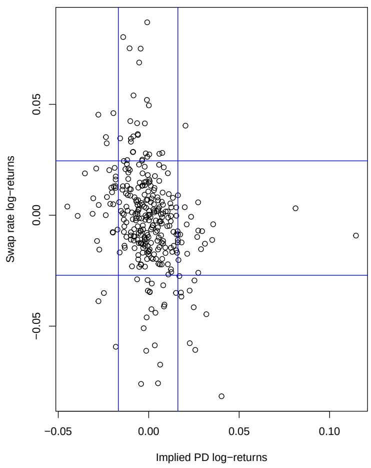

(m) Volkswagen

Figure C.1: Scatterplots of the log-returns on implied PDs of all sectors against the log-returns on 10 year swap rates. 0.1 and 0.9 quantiles are shown for both implied PDs and swap rates by the blue lines.

Downturn periods

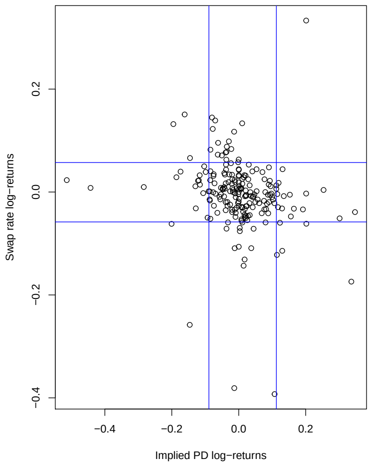

(a) JP Morgan senior

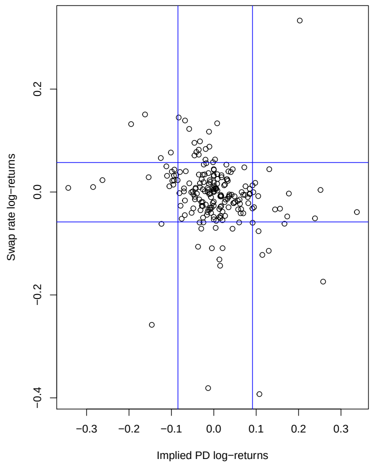

(b) JP Morgan subordinate

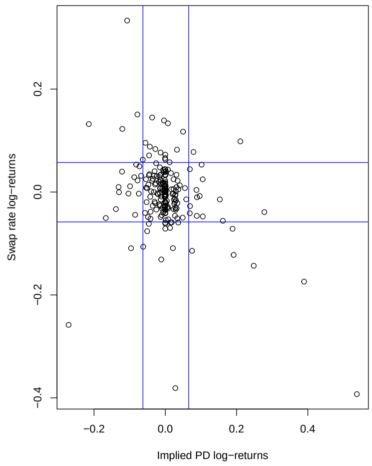

(c) Southwest airlines

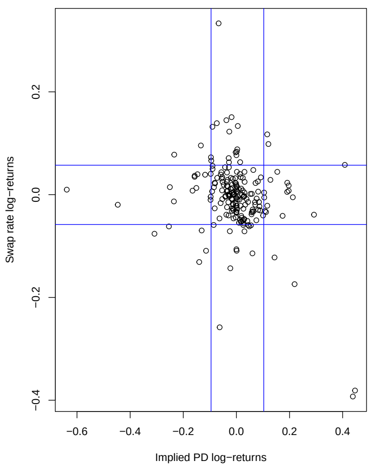

(d) Ford

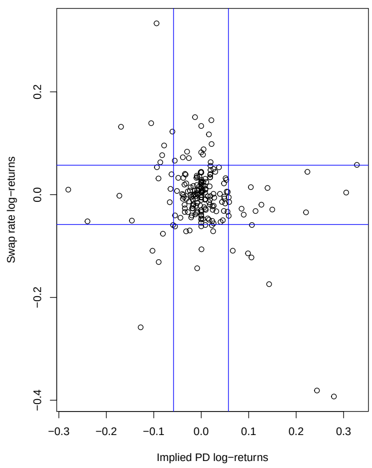

(e) AT&T

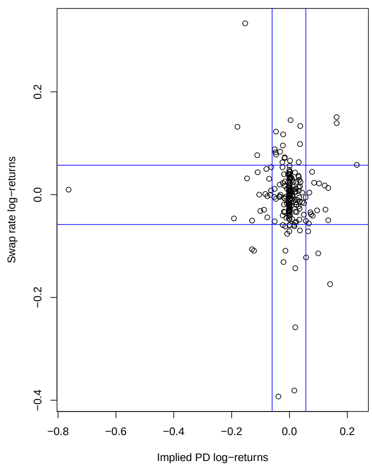

(f) Walmart

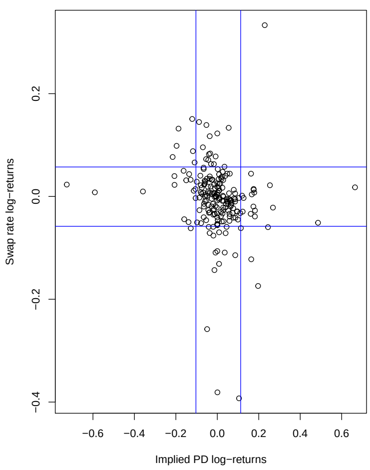

(g) Goldman Sachs senior

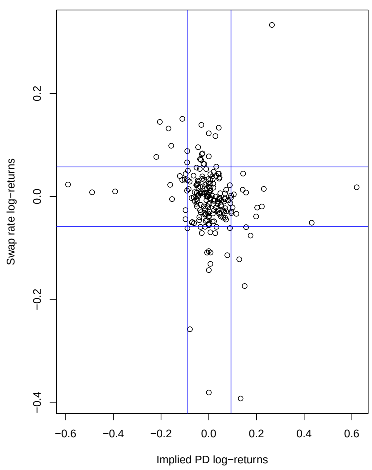

(h) Goldman Sachs subordinate

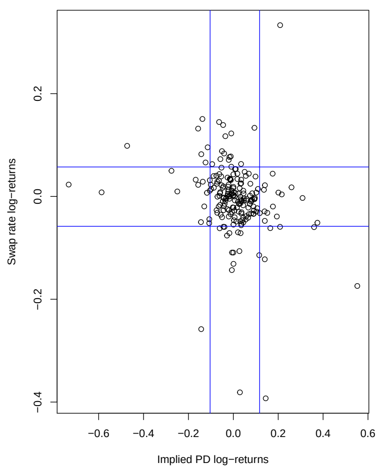

(i) Citigroup

Figure C.2: Scatterplots of the log-returns on implied PDs of all companies against the log-returns on 10 year swap rates during the downturn periods. 0.1 and 0.9 quantiles are shown for both implied PDs and swap rates by the blue lines.

D

Contour plots

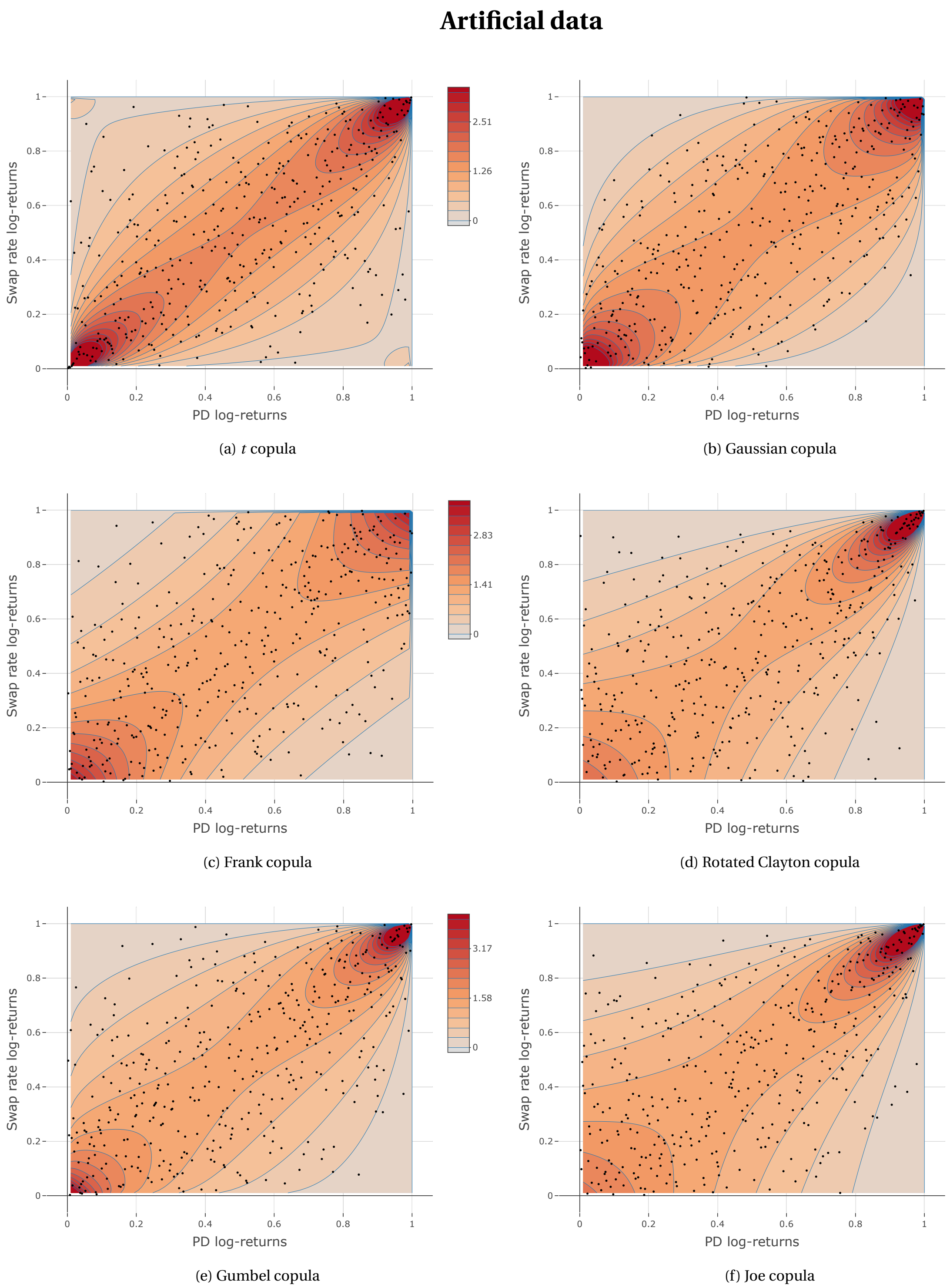

Figure D.1: Contour plots of the densities of the t, Gaussian, Frank, rotated Clayton, Gumbel and Joe copulas, superimposed with scatterplots of the artificial data generated by these respective copulas. Note that the scales for the contour plots are different for each copula.

Real data, normal economic circumstances

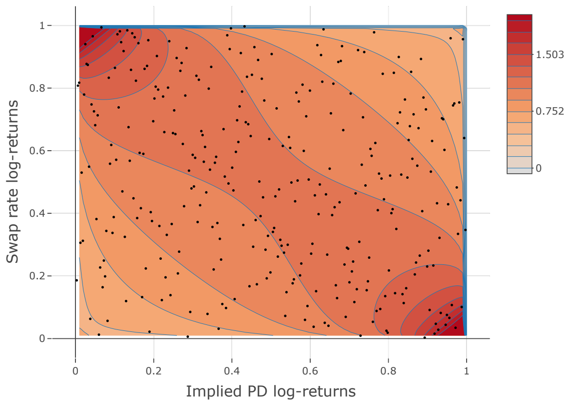

(a) Alibaba

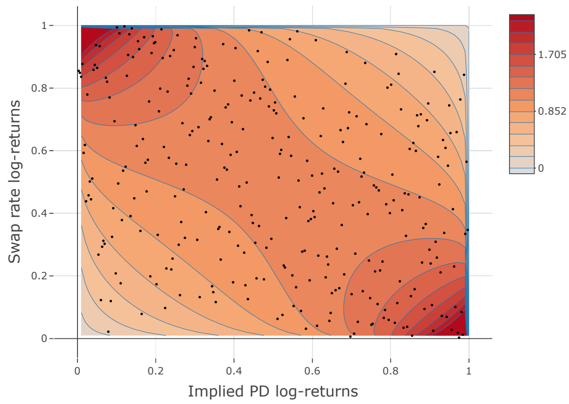

(b) American Airlines

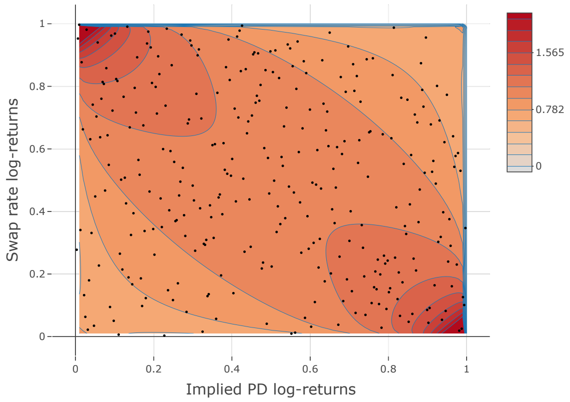

(c) Apple

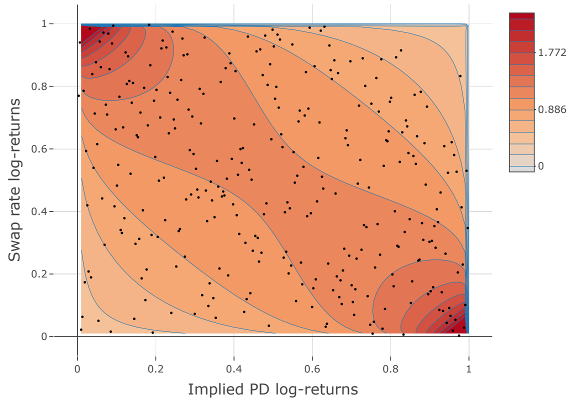

(d) AT&T

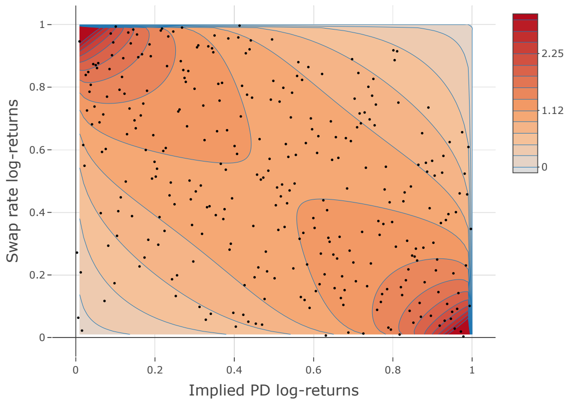

(e) Barrick Gold

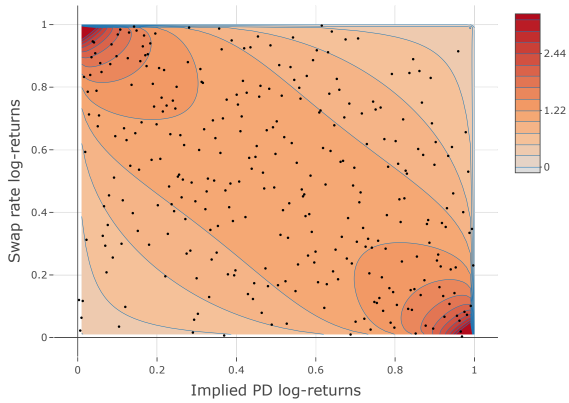

(f) Coca Cola

Figure D.2: Contour plots of the t copula density, superimposed with scatterplots of the pseudo-observations of the implied PD log-returns and the swap rate log-returns. Data is from the periods of normal economic circumstances. Note that the scales for the contour plots are different for each copula. The parameters for the t copula are those obtained in the fitting process, i.e. the parameters in Table 4.13.

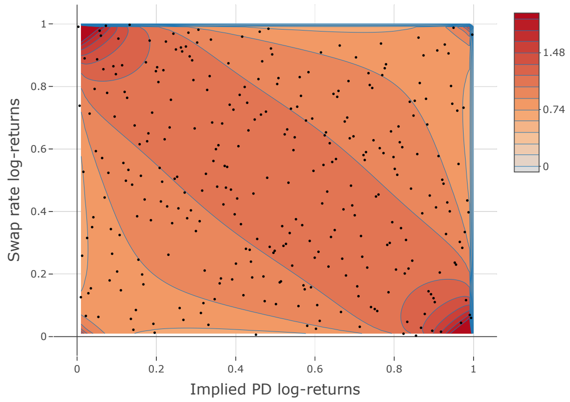

(g) Diamond Offshore Drilling

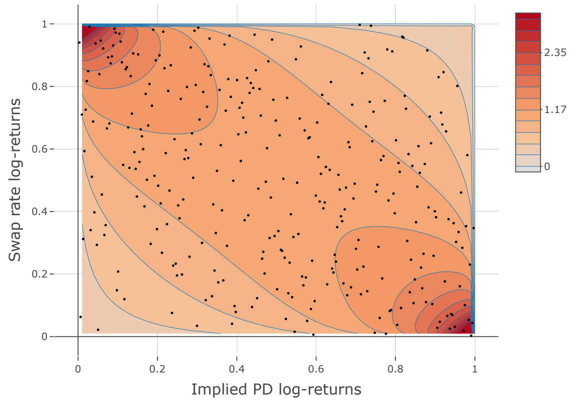

(h) Boeing

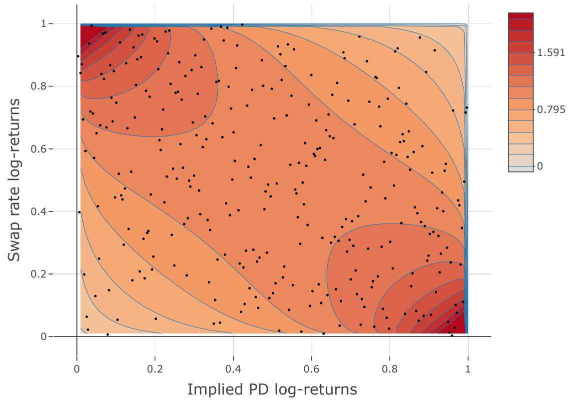

(i) Exxon Mobil

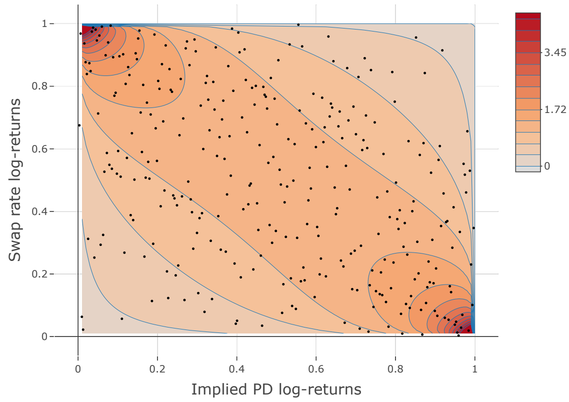

(j) Ford

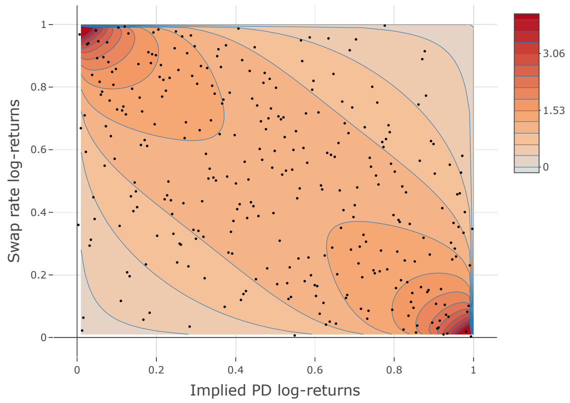

(k) JP Morgan senior

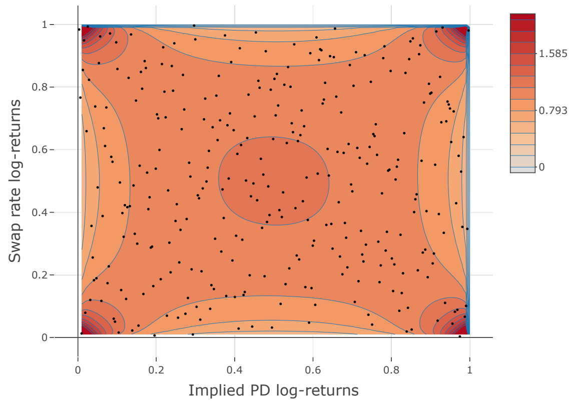

(l) JP Morgan subordinate

Figure D.2: Contour plots of the t copula density, superimposed with scatterplots of the pseudo-observations of the implied PD log-returns and the swap rate log-returns. Data is from the periods of normal economic circumstances. Note that the scales for the contour plots are different for each copula. The parameters for the t copula are those obtained in the fitting process, i.e. the parameters in Table 4.13.

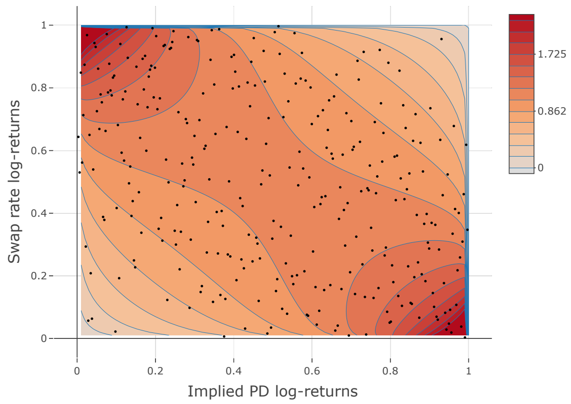

(m) Volkswagen

Figure D.2: Contour plots of the t copula density, superimposed with scatterplots of the pseudo-observations of the implied PD log-returns and the swap rate log-returns. Data is from the periods of normal economic circumstances. Note that the scales for the contour plots are different for each copula. The parameters for the t copula are those obtained in the fitting process, i.e. the parameters in Table 4.13.

Real data, crisis periods

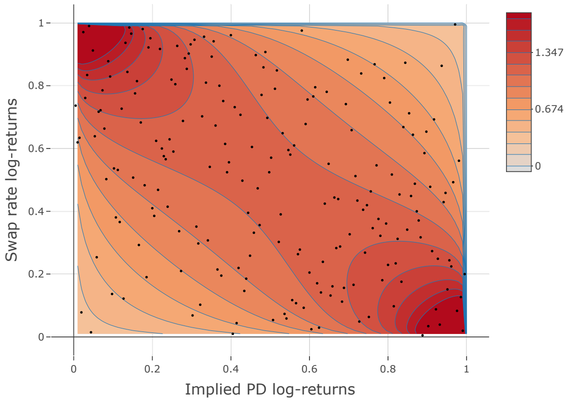

(a) JP Morgan senior

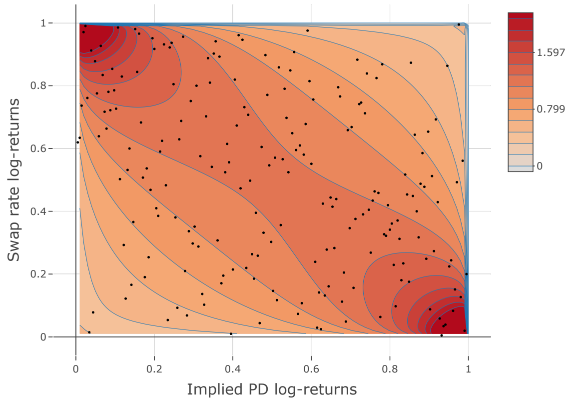

(b) JP Morgan subordinate

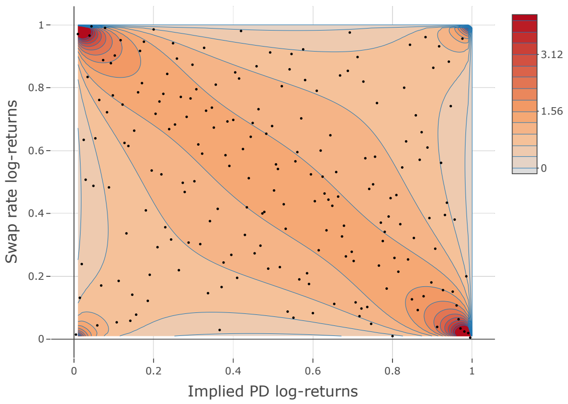

(c) Southwest Airlines

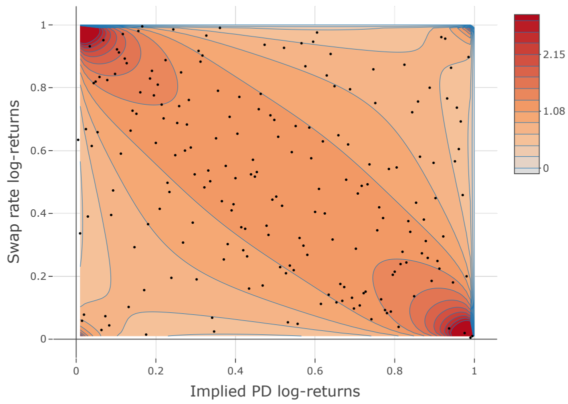

(d) Ford

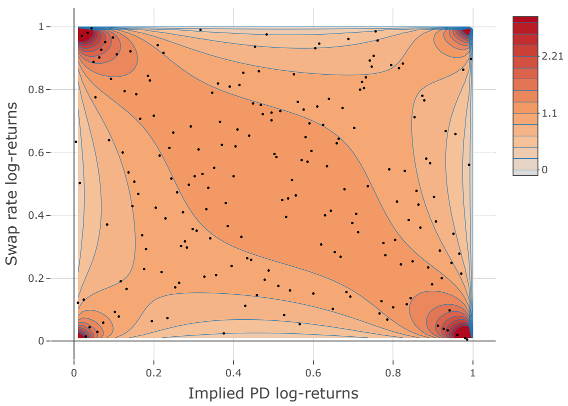

(e) AT&T

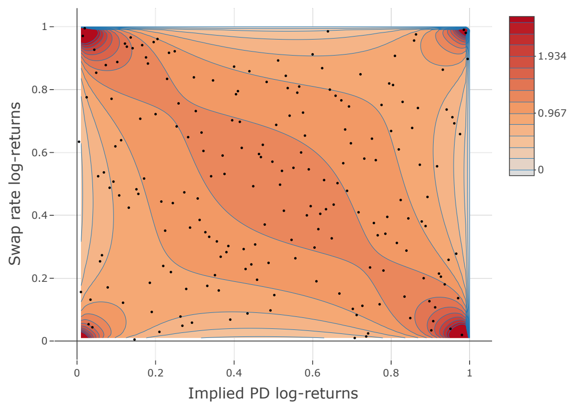

(f) Walmart

Figure D.3: Contour plots of the t copula density, superimposed with scatterplots of the pseudo-observations of the implied PD log-returns and the swap rate log-returns. Data is from the crisis periods. Note that the scales for the contour plots are different for each copula. The parameters for the t copula are those obtained in the fitting process, i.e. the parameters in Table 4.14

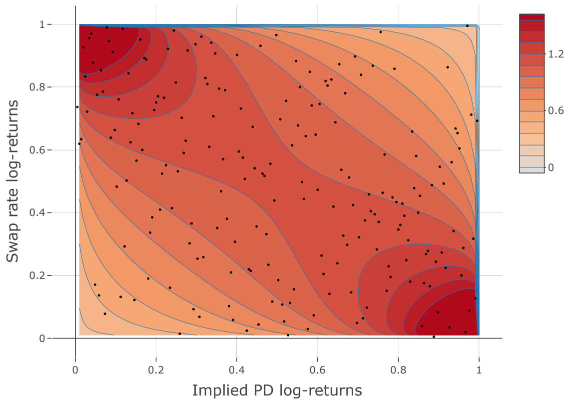

(g) Goldman Sachs senior

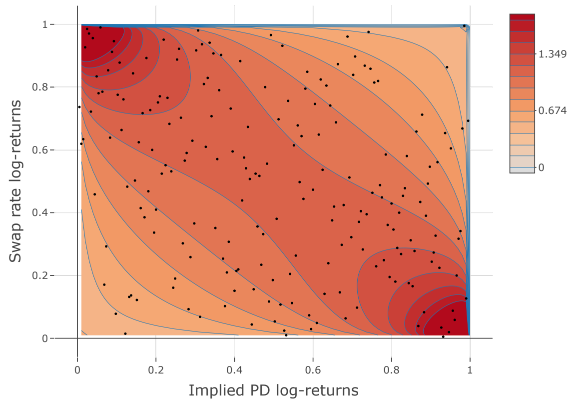

(h) Goldman Sachs subordinate

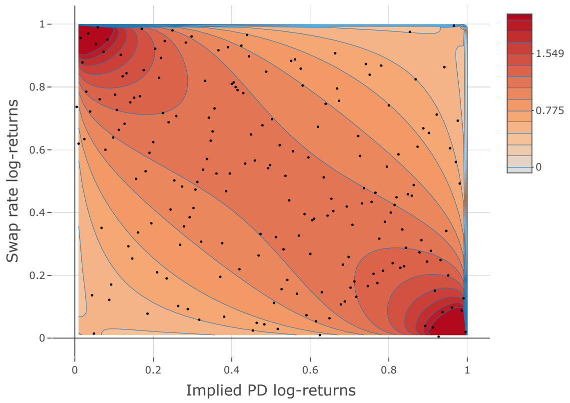

(i) Citigroup

Figure D.3: Contour plots of the t copula density, superimposed with scatterplots of the pseudo-observations of the implied PD log-returns and the swap rate log-returns. Data is from the crisis periods. Note that the scales for the contour plots are different for each copula. The parameters for the t copula are those obtained in the fitting process, i.e. the parameters in Table 4.14

Bibliography

Bank for International Settlements (2019). BIS statistical bulletin, *Technical report*. https://www.bis.org/statistics/bulletin1912.pdf, accessed 29 November 2019.

Basel Committee on Banking Supervision (2019). The Basel framework, *Technical report*. https://www.bis.org/basel_framework/index.htm, accessed 2 March 2020.

Ben-Abdallah, R., Breton, M. and Marzouk, O. (2019). Wrong-way risk of interest-rate instruments, *Journal of Credit Risk* **15**(2): 21–44.

Böcker, K. and Brunnbauer, M. (2014). Path-consistent wrong-way risk, *Risk* **27**(11): 48–53.

Bolton, P. and Oehmke, M. (2014). Should derivatives be privileged in bankruptcy?, *The Journal of Finance* **70**(6): 2353–2394.

Brigo, D., Hvolby, T. and Vrins, F. (2018). *Wrong-way risk adjusted exposure: analytical approximations for options in default intensity models*, World Scientific, pp. 27–45.

Brigo, D. and Pallavicini, A. (2006). Counterparty risk and contingent cds valuation under correlation between interest-rates and default, *Econometric eJournal* .

Casassus, J., Collin-Dufresne, P. and Goldstein, B. (2005). Unspanned stochastic volatility and fixed income derivatives pricing, *Journal of Banking & Finance* **29**: 2723–2749.

Cheng, D. and Cirillo, P. (2019). An urn-based nonparametric modeling of the dependence between PD and LGD with an application to mortgages, *Risks* **7**(3): 1–21.

Cherubini, U. (2013). Credit valuation adjustment and wrong way risk, *Quantitative Finance Letters* **1**: 9–15.

Cherubini, U. and Luciano, E. (2003). Pricing and hedging credit derivatives with copulas, *Economic Notes* **32**(2): 219–242.

Cox, J. C., Ingersoll, J. E. and Ross, S. A. (1985). A theory of the term structure of interest rates, *Econometrica* **53**(2): 305–408.

Fischer, M., Köstler, C. and Jakob, K. (2016). Modeling stochastic recovery rates and dependence between default rates and recovery rates within a generalized credit portfolio framework, *Journal of statistical theory and practice* **10**(2): 342–356.

Gatfaoui, H. (2005). How does systematic risk impact US credit spreads? A copula study, *Bankers, Markets & Investors* **77**: 5–16.

Genest, C. and Nešlehová, J. (2014). On tests of radial symmetry for bivariate copulas, *Statistical papers* **55**: 1107–1119.

Genest, C., Nešlehová, J. and Quessy, J.-F. (2011). Tests of symmetry for bivariate copulas, *The Institute of Statistical Mathematics* **64**: 811–834.

Genest, C. and Rémillard, B. (2006). Discussion of 'Copulas: Tales and facts,' by Thomas Mikosch, *Extremes* **9**(1): 27–36.

Genest, C., Rémillard, B. and Beaudoin, D. (2009). Goodness-of-fit tests for copulas: A review and a power study, *Insurance: Mathematics and Economics* **44**: 199—-213.

Harris, G., Wu, T. L. and Yang, J. (2015). The relationship between counterparty default and interest rate volatility and its impact on the credit risk of interest rate derivatives, *Journal of Credit Risk* **11**(1): 93–127.

Hofer, M. (2016). Path-consistent wrong-way risk: a structural model approach, *Journal of Risk* **19**(1): 25–42.

Hofert, M. and Scherer, M. (2011). CDO pricing with nested Archimedean copulas, *Quantitative Finance* **11**(5): 775–787.

Hull, J. C. and White, A. (2012). CVA and wrong way risk, *Financial Analysts Journal* **68**(5): 9–15.

J.P. Morgan (1997). CreditMetrics - technical document, *Technical report*. https://www.msci.com/documents/10199/93396227-d449-4229-9143-24a94dab122f, accessed 13 March 2020.

Li, D. (2000). On default correlation: A copula function approach, *The Journal of Fixed Income* **9**(4): 43–54.

MacKenzie, D. and Spears, T. (2014). 'A device for being able to book P&L': The organizational embedding of the gaussian copula, *Social Studies of Science* **44**(3): 418–440.

McNeil, A. J., Frey, R. and Embrechts, P. (2005). *Quantitative Risk Management: Concepts, Techniques and Tools*, Princeton University Press.

Mikosch, T. (2006). Copulas: Tales and facts, *Extremes* **9**(1): 3–20.

Naifar, N. (2011). Modelling dependence structure with Archimedean copulas and applications to the iTraxx CDS index, *Journal of Computational and Applied Mathematics* **235**(8): 2459–2466.

Nelsen, R. B. (2006). *An introduction to Copulas*, 2nd edn, Springer.

Newey, W. K. and McFadden, D. (1994). *Large sample estimation and hypothesis testing*, Elsevier Science, pp. 2111–2245.

Newson, R. (2002). Parameters behind "nonparametric" statistics: Kendall's tau, Somers' D and median differences, *The Stata Journal* **2**(1): 45–64.

Pan, K. (2018). CVA pricing for commodities with WWR, *Risk* .

Rosen, D. and Saunders, D. (2012). CVA the wrong way, *Journal of Risk Management in Financial Institutions* **5**(3): 252–272.

Ruiz, I., Pachón, R. and del Boca, P. (2015). Optimal right- and wrong-way risk from a practitioner standpoint, *Financial Analysts Journal* **71**(2): 47–60.

Schweizer, B. and Sklar, A. (1983). *Probabilistic Metric Spaces*, Dover Publications.

Sklar, A. (1959). Fonctions de répartition à n dimensions et leurs marges, *Publications de l'Institut de Statistique de l'Université de Paris* **8**: 229–231.

van Dijk, B. (2020). Shell boekt $400 tot $800 mln af door corona, *Het Financieele Dagblad* . https://fd.nl/ondernemen/1339900/shell-boekt-400-mln-tot-800-mln-af-door-corona (in Dutch).

Černý, J. and Witzany, J. (2018). A copula approach to credit valuation adjustment for swaps under wrong-way risk, *Journal of Credit Risk* **14**(1): 31–43.

Whitehouse, M. (12 September 2005). How a formula ignited market that burned some big investors, *The Wall Street Journal* p. A1.